VYSOKÉ UČENÍ TECHNICKÉ V BRNĚ
BRNO UNIVERSITY OF TECHNOLOGY

FAKULTA STROJNÍHO INŽENÝRSTVÍ
ENERGETICKÝ ÚSTAV

FACULTY OF MECHANICAL ENGINEERING
ENERGY INSTITUTE

VALVES TIMING OF COMPRESSOR FOR CO_2 REFRIGERANT

ČASOVÁNÍ VENTILŮ KOMPRESORU NA CO_2 CHLADIVO

DIPLOMOVÁ PRÁCE
MASTER'S THESIS

AUTOR PRÁCE — Bc. ROBIN KAMENICKÝ
AUTHOR

VEDOUCÍ PRÁCE — Ing. JIŘÍ HEJČÍK, Ph.D.
SUPERVISOR

BRNO 2015

Vysoké učení technické v Brně, Fakulta strojního inženýrství

Energetický ústav
Akademický rok: 2014/2015

ZADÁNÍ DIPLOMOVÉ PRÁCE

student(ka): Bc. Robin Kamenický

který/která studuje v **magisterském navazujícím studijním programu**

obor: **Energetické inženýrství (2301T035)**

Ředitel ústavu Vám v souladu se zákonem č.111/1998 o vysokých školách a se Studijním a zkušebním řádem VUT v Brně určuje následující téma diplomové práce:

Časování ventilů kompresoru na CO2 chladivo

v anglickém jazyce:

Valves timing of compressor for CO2 refrigerant

Stručná charakteristika problematiky úkolu:

Neustálý tlak konkurence a snižování zátěže na životní prostředí nutí výrobce kompresorů vyvíjet kompresory s vyšší účinností. V rámci diplomové práce se bude řešit optimalizace designu sacího a výtlačného ventilu pístového kompresoru na chladivo R744, přinášející zvýšení účinnosti kompresoru při zachování dlouhé životnosti jednotlivých dílů.

Cíle diplomové práce:

Cílem práce je navrhnout úpravy ventilové desky kompresoru, vedoucí ke zvýšení jeho účinnosti.

Seznam odborné literatury:

[1] KOLEKTIV AUTORŮ. Chladicí a klimatizační technika. 1. vyd. Praha: Svaz chladicí a klimatizační techniky, 2012, 181 s.
[2] DINÇER, Ibrahim. Refrigeration systems and applications. Chichester: Wiley, 2003, 584 s. ISBN 04-716-2351-2.

Vedoucí diplomové práce: Ing. Jiří Hejčík, Ph.D.

Termín odevzdání diplomové práce je stanoven časovým plánem akademického roku 2014/2015.

V Brně, dne 29.10.2014

L.S.

doc. Ing. Jiří Pospíšil, Ph.D. Ředitel ústavu	doc. Ing. Jaroslav Katolický, Ph.D. Děkan fakulty

ABSTRAKT

V posledních několika desetiletích se objevuje snaha o snížení firemních nákladů, stejně tak jako nákladů, které je nucen vynaložit zákazník, čímž se společnosti snaží získat výhodu vůči svým konkurentům na trhu. Spolu s tímto trendem jde i neustálá snaha snížit dopady na životní prostředí. Vývoj stávajících produktů se proto zdá být klíčovým prvkem.

Tento dokument se zabývá vývojem pístového kompresoru na CO_2 chladivo, který vyrábí společnost Emerson Climate Technologies. Cíl práce je zvýšit COP kompresoru při zachování stávající životnosti kompresoru. Diplomová práce je rozčleněna do několika kapitol, které se zabývají analýzou originálního designu kompresoru, návrhem a vyhodnocením designů nových. Nezbytné teoretické základy mohou být také shlédnuty v počátečních kapitolách. V poslední části dokumentu jsou sdělena možná další vylepšení a případné jiné konstrukce.

Vývoj byl zaměřen na sestavu ventilové desky. Na základě několika předpokladů a výsledků analýzy původního designu kompresoru byly navrženy nové konstrukce, které byly dále testovány statickou strukturální analýzou. Pomoci modální analýzy byly také vypočteny vlastní frekvence a vlastní tvary sacího jazýčku. Mimo modální a statické strukturální analýzy byla provedena také CFD analýza. V posledním kroku byly testovány navržené prototypy a jejich výsledky byly porovnány s původním kompresorem.

K správnému návrhu bylo zapotřebí programové podpory a to především v podobě MATLABu, ANSYSu WB a Microsoft Excelu. V práci jsou velmi často prezentovány obzvláště výsledky získané v programu ANSYS WB.

KLÍČOVÁ SLOVA

Kompresor, kompresor s vratným pístem, ventilová deska typu flapper, chladivo, oxid uhličitý, Coefficient of performance, statická strukturální analýza, modální analýza, CFD analýza.

ABSTRACT

Together with an endeavour to decrease companies' costs and costs of their customers, significant effort to decrease an impact on the environment in the last decades was made. To do so a development is the crucial step.

This paper is focused on a development of a CO_2 reciprocating compressor, which is produced by Emerson Climate Technologies. The diploma work goal is to increase the compressor COP, while maintaining its durability. The document is divided into a few chapters, which address an analysis of an original compressor design, a description of a new design proposals and an evaluation of the new designs. Necessary theoretical knowledge base is also provided. In the last document part, can be read about other design possibilities and improvements.

The main compressor part, for the development, was a valve plate assembly. Base on a few assumptions and original valve plate analyses, the new designs were suggested and subsequently tested as static structural problems. Natural shapes and frequencies of suction valve were determined by modal analysis. Apart from the modal and static structural analyses a CFD analysis was performed. In the last step, prototypes were tested and results were compared with the original compressor design.

Software support was necessary for successful designing, thus mainly MATLAB, ANSYS WB and Microsoft Excel were used. Especially results obtained in ANSYS WB are frequently presented in this work.

KEYWORDS

Compressor, reciprocating compressor, flapper valve plate, refrigerant, carbon dioxide, coefficient of performance, static structural analysis, modal analysis, CFD analysis.

BIBLIOGRAPHIC CITATION

KAMENICKÝ, R. *Valves timing of compressor for CO_2 refrigerant*. Brno: Brno University of Technology, Faculty of Mechanical Engineering, 2015. *97* p. Supervisor Ing. Jiří Hejčík Ph.D..

AFFIDAVIT

I declare that I wrote this thesis on my own without using any other sources and aids as I state in the list. I had worked independently under the direction of Ing. Jiří Hejčík, Ph.D.

Brno, date 28th May 2015 ……...…..……..

Robin Kamenický

ACKNOWLEDGEMENTS

I would like to sincerely thank to my supervisor Ing. Jiří Hejčík Ph.D. for his help and advices. Moreover, I would like to express my thanks to my family for their encouragement.

CONTENTS

INTRODUCTION

The purpose of this work is to improve current type of a reciprocating compressor for CO_2 refrigerant from Emerson Climate Technologies. The paper objective is to raise COP of the mentioned compressor, during maintaining present durability. The COP increase must be reached by adjustments of a suction and discharge mechanism, not by redefining of a compressor operating envelop, hence not by changes of thermodynamic conditions.

To be able to improve the original design knowledge are required. The COP is influenced by many things from mechanical and thermodynamic view and all of these things are closely tied together. If it is going about improving the original compressor, the first logical step is to analyze its assembly. It is necessary to check whether all parts seats preciously on others, whether clearance volume can be decreased and what defines design boundaries, thus, how much can be the particular design adjusted. It is also very important to test the original design in different working conditions, measure data and analyse them carefully.

Different software can be very convenient in data analyzing and simulation. Especially CO_2 compressor has to withstand very high pressures and so it is crucial to perform simulations and determine its durability. Apart from stress simulations, a simulation of refrigerant flow can also be made. This can provide valuable information, on its base higher efficiency can be reached.

This diploma thesis covers a little of theory as well as the compressor development procedure. The analyses of the original design together with ideas behind new suggested designs are described. A few chapters are also devoted to simulations in ANSYS WB, which was used for static structural simulation, modal analysis and CFD analysis. Further development recommendations and valve plate assembly designs, which were not observed in this work, are also included in this document.

The final part introduce manner of the compressor testing together with final results of the new designs.

1 THERMODYNAMICS

A compressor development and evaluation requires knowledge of physic particularly thermodynamic. Therefore some thermodynamic basics are described in this chapter.

IDEAL GAS

In some cases, low pressure state, compressor medium (gas) can be described as ideal gas. Its state can be sufficiently described by main three parameters. These are volume, pressure and temperature. The ideal gas equation of state is following. [5]

$$\frac{p \cdot v}{T} = constant \tag{1.1}$$

or

$$p \cdot v = R \cdot T \tag{1.2}$$

The only unknown variable is R which depends on gas molar mass M, thus the gas constant vary according individual gas. Its dependence expresses a relation with universal gas constant $\bar{R} = 8.314\ kJ \cdot kmol^{-1} \cdot K^{-1}$. [5]

$$R = \frac{\bar{R}}{M} \tag{1.3}$$

For making a decision whether gas can be treated as ideal gas or not, generalized compressibility chart (Figure 1.1) can be used. If compressibility factor Z, on vertical axes, is equal to value around 1, the gas behaviour is very similar to ideal gas. This supports the previous words, that we can consider gas as ideal gas when its pressure is low. The compressibility factor is sometime called also as correction factor. [5]

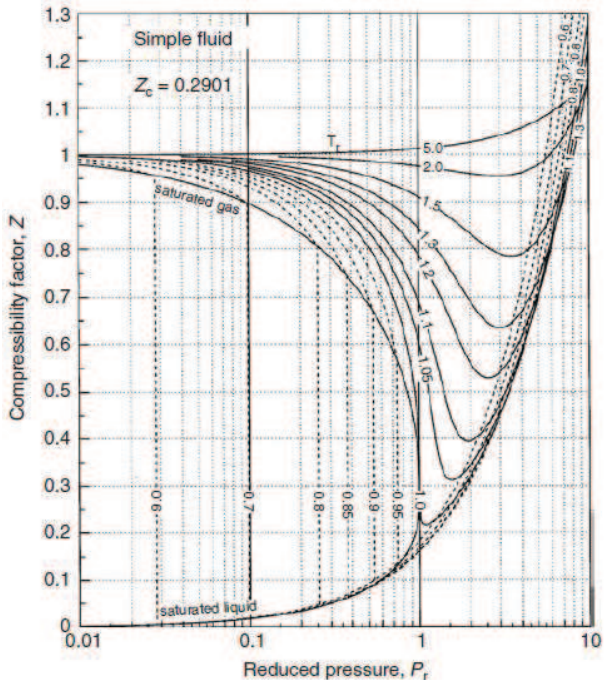

Figure 1.1 Generalized compressibility chart [5]

$$Z = \frac{p \cdot v}{R \cdot T} \tag{1.4}$$

Next three important parameters, specifically reduced pressure P_R, reduced temperatures T_R and reduced volume V_R, are required for solving problems with using the chart. These parameters are described by ratio of a system values to its critical states values. It results from knowledge, that the most of gas properties are significantly tied to its critical values. [5]

$$T_R = \frac{T}{T_C} \tag{1.5}$$

$$P_R = \frac{P}{P_C} \tag{1.6}$$

$$V_R = \frac{V}{V_C} \tag{1.7}$$

Pressure, temperature or volume can be constant in some processes. To describe these cases three gas laws were defined. These laws assume closed system with given quantity of ideal gas. The first one, Charles' law, tells that if pressure is constant, a ratio of initial volume and initial temperature is equal to a ratio of final volume to final temperature and their relation is linear.

$$\frac{V_1}{T_1} = \frac{V_2}{T_2} \tag{1.8}$$

The second law, Gay-Lussac's law, describes the process when increasing temperature causes increasing of pressure at constant volume. The relation between pressure and temperature is linear.

$$\frac{p_1}{T_1} = \frac{p_2}{T_2} \tag{1.9}$$

The third law, Boyl's law, defines behaviour of ideal gas at constant temperature. The raising pressure leads to decreasing of volume, hence the product of pressure and volume at given temperature is constant.

$$p_1 \cdot V_1 = p_2 \cdot V_2 \tag{1.10}$$

Other frequently used equations for describing thermodynamic processes are isentropic and polytrophic. Isentropic also called adiabatic process is based on ideal gas equation in following form.

$$p_1 \cdot v_1^{\kappa} = p_2 \cdot v_2^{\kappa} \tag{1.11}$$

κ is known as adiabatic exponent and is defined as ratio of specific heat capacities.

$$\kappa = \frac{c_p}{c_v} \tag{1.12}$$

Polytrophic process is described by similar equation as adiabatic process, only difference is the exponent, where the adiabatic exponent κ is replaced by polytrophic exponent n. The n depends on deviation of log P and log V diagram.

$$p_1 \cdot v_1^{n} = p_2 \cdot v_2^{n} \tag{1.13}$$

The mentioned processes are depicted in the Figure 1.2

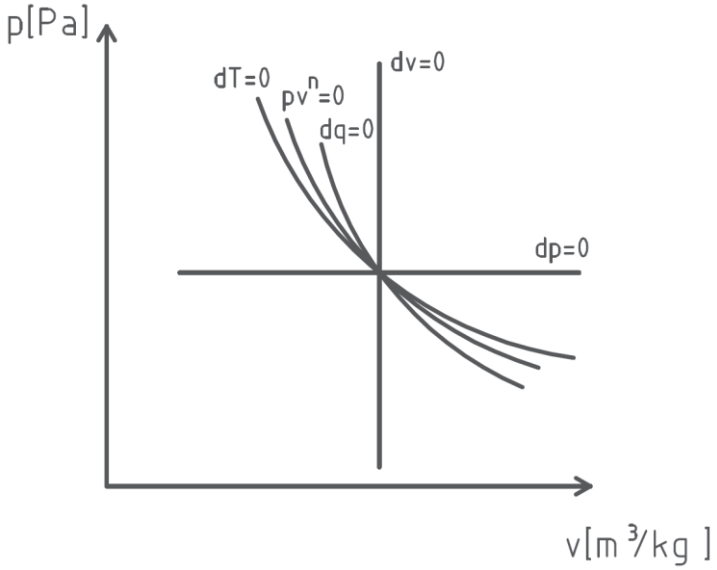

Isobaric process
$n = 0 \rightarrow p \cdot v^0 = p = consant$

Isochoric process
$n = \infty \rightarrow p^{\frac{1}{\infty}} \cdot v = v = constant$

Isothermal process
$n = 1 \rightarrow p \cdot v^1 = constant$

Adiabatic process
$n = \kappa \rightarrow p \cdot v^\kappa = constant$

Polytrophic process
$n \in (1; \kappa) \rightarrow p \cdot v^n = constant$

Figure 1.2 Comparing of ideal thermodynamic processes

These five processes are reversible. Hence they can run in both directions. The system returns to initial state if reverse process is undergone.

The theory of ideal gas also assumes constant-pressure heat capacity c_p and constant-volume heat capacity c_v. This simplifications enable to count specific enthalpy and specific internal energy without using of graphs or tables, how is expressed in following equations. [5]

$$\Delta h = c_v \cdot (T_2 - T_1) = (h_2 - h_1) \tag{1.14}$$

$$\Delta u = c_p \cdot (T_2 - T_1) = (u_2 - u_1) \tag{1.15}$$

h is specific enthalpy, *u* is internal energy of a system.

For thermodynamic calculation of any compressor, refrigerant tables and charts are usually used. It helps to accurate determination of gas states. Different refrigerants have different characteristic and these are captured in particular refrigerant charts.

1.1 ENERGY

Energy is an ability doing work. The total energy of a system is sum of internal energy *U*, kinetic energy and potential energy. In a case of refrigeration, changes in internal energy of a system are mostly considered. [5]

HEAT

Heat *Q* is the form of energy which can be transformed to other energy forms. Heat transfer occurs, where temperature equilibrium is not presented. A medium with higher temperature passes heat to a medium of lower temperature. The transfer is described by following equation.

$$Q = m \cdot (h_2 - h_1) \tag{1.16}$$

or

$$Q = m \cdot c \cdot (T_2 - T_1) \tag{1.17}$$

WORK

Work as form of energy has the same unit (joule) as heat but marked by W.

$$W = m \cdot \Delta h \tag{1.18}$$

$$\delta W = pdV \tag{1.19}$$

δ represents inexact differential, hence integration path dependency.

Both of these two energy forms, heat and work, are frequently used in refrigeration. In case of any thermodynamic circuit, enthalpies of different states are easy to read in circuit diagrams, thereby work and heat transfer can be determined.

LAWS OF THERMODYNAMICS

One of the most necessary knowledge for thermodynamic circuit solving are laws of thermodynamics. The first law of thermodynamics discusses energy conservation. It considers enclosed system with given volume, where a change of the system internal energy depends on heat inlet and work done by the system.

$$dU = \delta Q - \delta W \tag{1.20}$$

The second law of thermodynamics introduces the concept of entropy S, which is a measure of disorder.

$$dS = \frac{\delta Q}{T} \tag{1.21}$$

1.2 THERMODYNAMIC CYCLE

A thermodynamic cycle consists of several subsequent thermodynamic processes, after their performing the system comes back to initial state. Cycles can be of various types. There are distinguished clockwise and counter clockwise cycles, and opened, closed cycles. Clockwise cycles are applied in processes of work generation; counter clockwise cycles depict processes of cooling facilities and heat pumps. Reversible cycles consist of reversible processes, while irreversible cycles contain at least one irreversible process.

As an example of counter clockwise reversible cycle the Carnot cycle is shown (Figure 1.3). It is idealized cycle, which is based between two reservoirs of constant temperatures T_H and T_L. The cycle can be used for comparing cycles of refrigerant facilities and heat pumps since it has the biggest theoretically reachable efficiency.

One of the most frequently required characteristic of evaluating thermodynamic cycles is efficiency. It is defined as ratio of useful value (output) and value incoming in the system (input).

$$\eta = \frac{output}{input} \tag{1.22}$$

In the case of a general refrigerator, the required output is Q_L, thus the amount of energy absorbed from the cooled system for the goal of cooling the system. Its amount is counted as

area under the curve 4-1 (Figure 1.3). Q_H is a heat rejected as useless energy and is calculated as area under the curve 2-3. Unlike the Carnot heat engine, the reverse Carnot cycle require the work W as the input, which is defined as difference between Q_H and Q_L. The efficiency of reverse cycle is called Coefficient of Performance (COP).

$$COP_R = \frac{Q_L}{W} = \frac{Q_L}{Q_H - Q_L} \tag{1.23}$$

$$COP_R = \frac{T_L}{T_H - T_L} \tag{1.24}$$

COP for a general heat pump is counted differently since the required output is Q_H. Heating is wanted, not cooling.

$$COP_{HP} = \frac{Q_H}{W} = \frac{Q_H}{Q_H - Q_L} \tag{1.25}$$

$$COP_{HP} = \frac{T_H}{T_H - T_L} \tag{1.26}$$

The simplification of the Carnot cycles equations (1.24,(1.26) results from the Carnot cycle definition, when the processes 2-3, 4-1 are isothermal and the processes 1-2, 3-4 are isentropic.

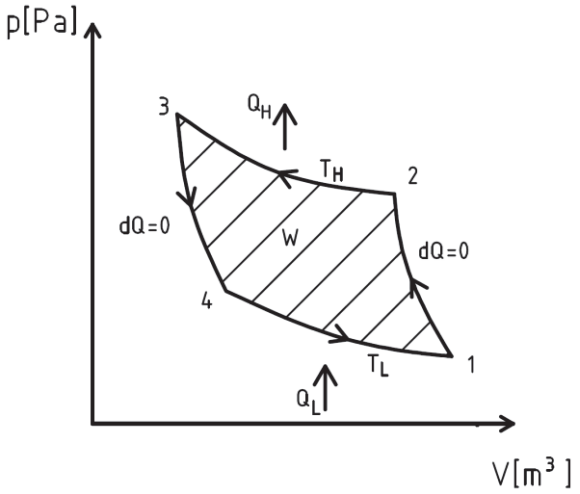

Figure 1.3 Carnot cycle

1.3 COOLING CYCLE

The need for cooling appeared thousands year ago. In distant history, only nature cooling by ice, evaporation and later molten salts were applied. The beginnings of mechanical cooling are dated in 18th century.

Process of cooling takes an advantage of phase change from liquid to vapour. One of the main components is compressor or absorption (adsorption) system, which maintain pressure difference. This is used for managing temperatures of evaporating and liquefaction.

An idealized cooling circuit consists of four processes. The first one is an evaporation process, an isobaric and isothermal process, during which a refrigerant absorbs heat from cooled environment and change its phase to vapour. This undergoes in an evaporator. The

next step is taken in compressor, where vapour of refrigerant is compressed up to required pressure. Following step is condensation, in case of subcritical cycle, when refrigerant heat is passed to heated environment. The condensing is isobaric and isothermal process. If there is not any requirement for heating, the heat is only passed to less warm surrounding without any purpose. A throttling device (expansion valve or capillary tube) reduces pressure back to suction pressure. The expansion is isenthalpic and compression can be adiabatic, isothermal. Cooling circuit is often divided by compressor and expansion device into high pressure and low pressure side.

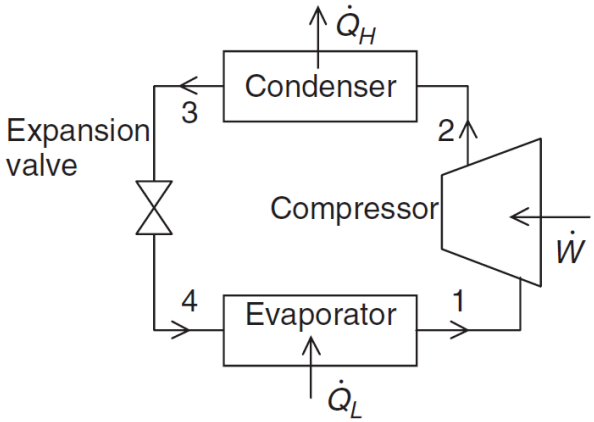

Figure 1.4 Cooling circuit

Cooling circuit can be modified depends on requirements. However, it is necessary to keep in mind that together with temperature (pressure) changes, efficiency and cooling capacity of the particular system also changes. This dependence is seen in the (Figure 1.5). If a temperature increases in condenser, condensing pressure also increase. Unfortunately, it results in lower amount of absorbed heat in evaporator. By simple visual comparing, it is unequivocal, that compressor work is raised.

Another example would be the need for lower temperature at the low pressure side. This can lead, depends on refrigerant, to lower cooling capacity, thus to decrease in amount of absorbed heat. The point 2'', after the compression, shows that the refrigerant reaches higher temperature, which can have a negative impact on materials and especially on quality of lubricating oil.

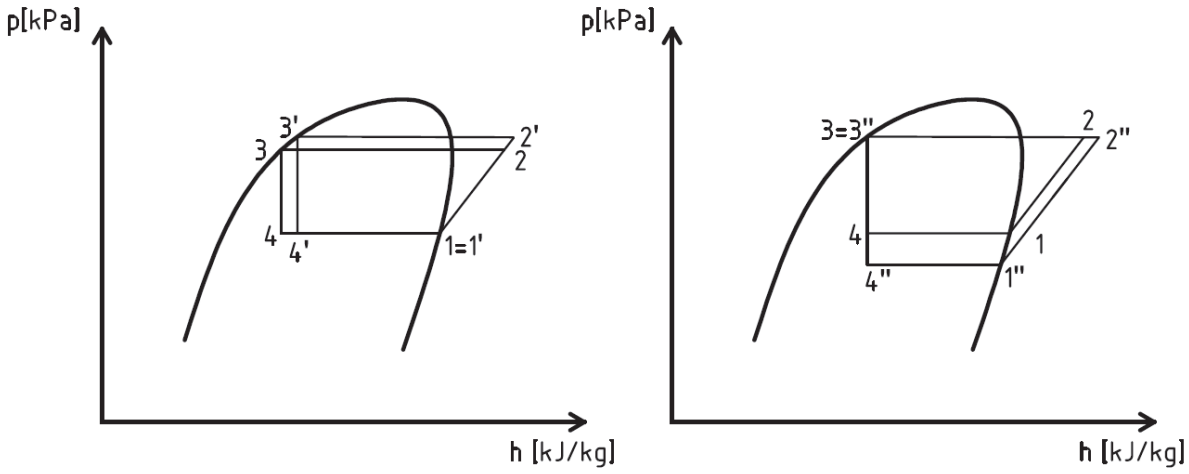

Figure 1.5 Influence of thermodynamic changes on a thermodynamic cycle

In addition, superheating and subcooling (Figure 1.6) are often proposed. Subcooling, isobaric cooling below bubble point temperature, is usually suggested for reducing of refrigerant flashing when passes through expansion valve (capillary). Flashing is a process of evaporation when a refrigerant enters to low pressure environment. Unfortunately, liquid takes energy from the system, when it evaporates. This is considered as energy loos or reduction of refrigerant capacity, which has to be substitute by energy provided as compression work. If refrigerant is subcooled, less liquid evaporates during expansion and temperature difference becomes lower, hence less energy loos occur. Subcooling also enlarge refrigerant capacity and prevent gas from entering into expansion device. Gas bubbles obstruct liquid flow and thereby negatively influence right function of throttling device.

Superheating is an isobaric heating above a dew point temperature. One of the main purposes of this action is to prevent liquid from entering into compressor. Additional benefit is an enlarging of refrigerant capacity in case of superheating in evaporator. On other side it is necessary to count with higher temperature at compressor discharge and increase of specific volume, which leads to reducing of mass flow rate since volume of compressor is constant. The reduced mass flow results in lower refrigerant capacity. [5]

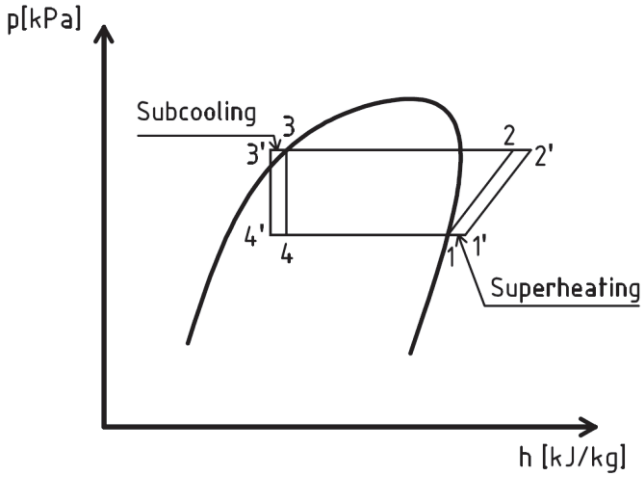

Figure 1.6 Subcooling and superheating

2 COMPRESSORS

Compressors have two basic functions driving and pressurizing gas medium, both of them are very tied together. Devices on those principles have been used for many years by people and even for longer time by nature. People has been using their lungs to drive air onto a fire since the time when a fire begun to be used.[1]

One of the first efforts to control mass of air started because of metallurgy, when higher temperatures of fire were required to melt metals. Hence people developed bellows in 1500 BC. This tool was used for next few thousand years till the time of blast furnaces, when a blowing cylinder powered by water wheel was developed in 1762.[1][2]

Big step in this branch was made in 1776, when John Wilkinson developed a device, which is a base for current mechanical compressors. These compressors started to be used for different purposes like mining, tunnel building and its ventilation. Hand in hand with growing industry compressors were spread all over the world and begun to be used for various utilizations. [1]

In today's world, compressors can be found on daily basis all around us. These devices are indispensable for cooling circuits in fridges, hence it helps us to transport and storage food. It is used for air-conditioning of buildings and industry objects. Units for keeping pressure range in gas pipeline transport are used. Compressors are also used for gas liquefying and vacuum creating. Last but not least energy storage should not be forgotten. Potential of compressors usage is very wide.

COMPRESSOR TYPES

A compressor is a base component of cooling circuit with steam circulation. Its construction depends on a refrigerant and its danger to the environment. High requirement is especially on tightness. It is necessary to avoid leakage of the refrigerant not only because of pollution but also because of a correct device operation. A lack of a cooling medium can lead to destruction of a compressor. [3]

Compressors can be sorted by its manufacturing design to:

- Hermetic compressors
- Semihermetic compressors
- Open types of compressors

According to working principle to:

- Displacement compressors
- Dynamic compressors

In the Figure 2.1, basic types of compressors are illustrated. Choosing of a required compressor depends on working conditions. We have to consider size, noise, efficiency, pressure ratio, price, mass flow, displacement, refrigeration capacity etc. When bigger mass flow is needed, positive displacement unit is usually replaced by turbine or centrifugal compressor. Dynamic compressors also include ejectors. [5]

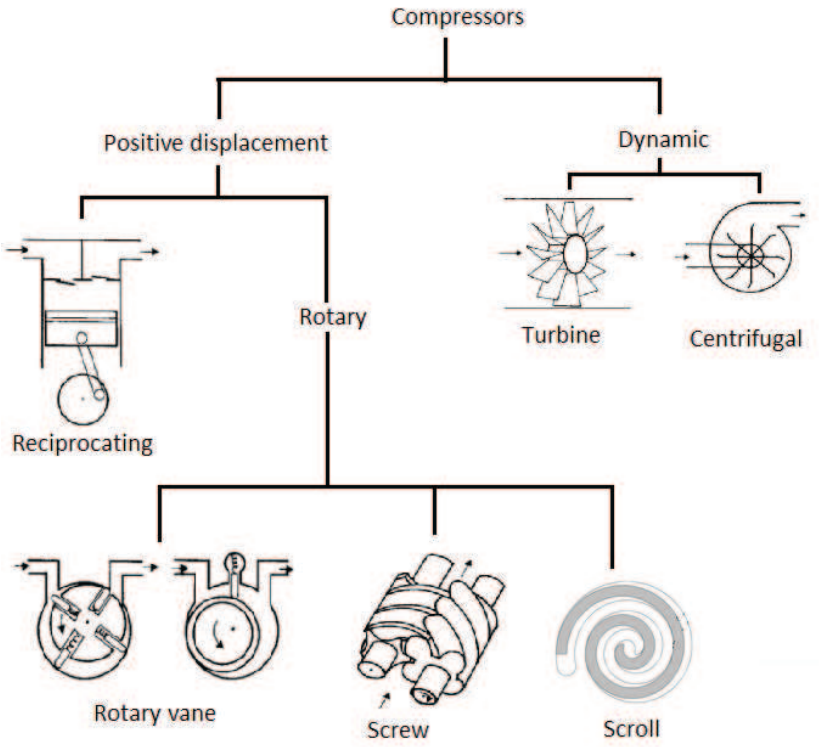

Figure 2.1 Types of compressors [4] [5]

Compressors need to be applied in defined working conditions for reaching an optimal performance. This is partially ensured by own lubricating and cooling. The device can be cooled either by sucked refrigerant, usually in a case of lower discharge temperatures, or by other medium as water. Lubricating systems employ different oils. Their type depends on its thermodynamic properties and reactivity with other materials used in the compressor.

2.1 HERMETIC COMPRESSORS

Hermetic sealed compressors are widely used in smaller application where the cost is critical, thus they are utilized especially in households in freezers and air conditioning. This type of unit is very compact and easy to transport since a motor and the compressor, joined by a shaft, are mounted in a single welded housing. Lubricating and refrigerant systems are also situated in the casing and both pass through body and the electric motor. Due to their constructional solution refrigerant leakage do not occurs and they are maintenance-free; hence there is not access to spare parts. An important component of the device is a thermistor, which measures motor temperature and is part of overload protection. [5] [6] [7]

A disadvantage of the unit is its sensitivity to voltage variation, which can cause a motor igniting. If the motor winding is destroyed, the entire compressor becomes contaminated and the whole compressor has to be replaced. [5] [6] [7]

One of the most frequently used hermetically sealed compressor type is reciprocating compressor, which was utilized in this manner as the first type. Nowadays, vane rotary compressors and scrolls are also very popular for their advantages resulted from design. The both types are often less noisy, have lower energy intensity and can have longer durability. All of these properties are given by smaller amount of frictional parts.[6]

2.2 SEMIHERMETIC COMPRESSORS

Semihermetic compressors are similar to hermetic ones. The main difference is that the casing can be unbolted. Hence the maintenance of inner device parts, such as a motor, is feasible. These devices are applied for bigger displacement values, which leads to bigger motors and theoretical overall efficiency over 70 %. [5]

Semihermetic compressors were developed as replacement for hermetic compressors and thus the goal was to avoid their deficiencies. Despite a possibility of the unit maintenance, any refrigerant leakage problems are not common. The cost of semihermetic compressors is usually higher than the cost of hermetic compressor. [5]

2.3 OPEN COMPRESSORS

An external electric motor joined to a compressor by a shaft is a typical design of this compressor type. Where the shaft goes through a casing of the compressor, suitable seals must be used to avoid refrigerant leaking out or air leaking in. In case of open compressors frequently usage is expected. If the unit is not used often enough, risk of leakage increases because of lubricant evaporating and subsequent seal degradation. [7]

3 RECIPROCATING COMPRESSORS

These compressors are used for its large-capacity range. The base is an electromotor, shaft and a cylinder with a piston. The motor propels the shaft which moves with the piston. The piston compresses a sucked refrigerant in the cylinder. Units are produced with different number of cylinders, located in different positions. Therefore V, W, line or radial cylinder positions are distinguished. [5]

The shaft is drove direct or indirect. In the first case, the power is distributed directly by motor. For the indirect way a belt or gear box is utilized. [5]

3.1 PARTS

The Figure 3.1 shows a cutaway through semihermetic reciprocating compressor, and so main parts can be easily seen.

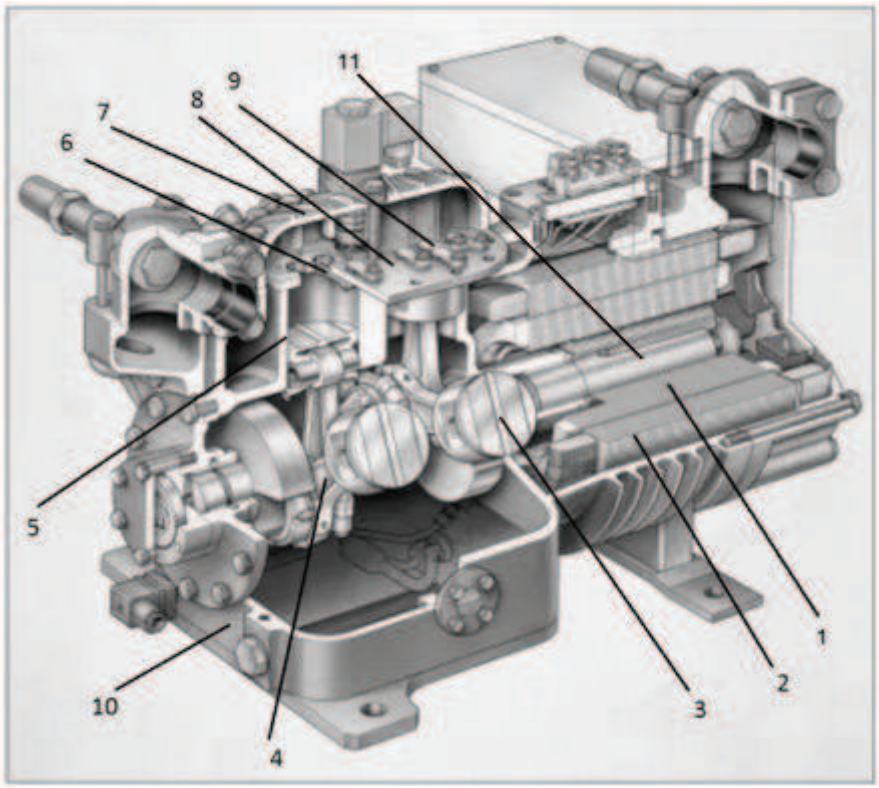

1. Motor rotor
2. Motor stator
3. Piston
4. Piston rod
5. Cylinder
6. Suction valve
7. Cylinder head
8. Valve plate
9. Discharge valve
10. Body
11. Shaft

Figure 3.1 Cutaway of a semihermetic reciprocating compressor [17]

The biggest part is the body, which cover all moving parts and lubricant. The body is usually casted from grey cast iron and subsequently individual elements are milled.

The motor converts electrical energy to mechanical energy. Especially in case of hermetic compressors motor can be sensitive for high voltage since wires of winding are very thin and overheating can occurs.

The main parts from point of thermodynamic view are cylinders, pistons and valves. Cylinder bores has to be preciously machined, as final operation honing is often applied. [11]

PISTON

Pistons are fitted with piston rings whereby gas leakage, from a cylinder space to a space around the crank mechanism, is prevented. Rings material depends on lubricant, basically has to be softer than the cylinder and the piston, and cannot react with lubricant or refrigerant. The most often used are soft metals, bronze and polytetrafluoroethylene. Pistons are often casted and then milled. Decreasing of clearance volume can be reached by milling of suction valve shape in the piston top. The piston is than connected to connecting rod by a pin. The piston low weight is important. [11][18]

VALVE

Valves are self-acting, driven by pressure difference. Their stiffness is influenced by their properties and springs. When a valve is opened, it hits counterpart. In case of a suction valve, the counterpart is usually the body, and a discharge valve is stopped by a pat called stopper (retainer). A designer should develop such a valve, of which properties fulfil criteria of lifetime, optimal stiffness, low drag and tightness. Valves can be classified into five groups:

- **Poppet valves** (Figure 3.4) are suitable for low compression ratio devices (up to 15 MPa) and are used in cases when rotor speed reaches up to 600 rpm. Flow characteristic can be similar to ring valve, however, bigger number of elements increase failure likelihood. [26] [32]
- **Ring valves** (Figure 3.5) are for devices with pressure difference up to 30 MPa and 600 rpm. This valve type is similar to a plate valve. It differs by function, when each ring can move independently on the other one. The valve rings are not connected to each other in compare to the plate valve, where rings are connected by radial ribs. The advantage is small energy loose, because of more efficient gas flow across valve (Figure 3.9). The disadvantage is a higher demand for valve seat accuracy. Also the valve sealing is usually plastic, which does not allow using in combination with some gases and high temperatures. [26] [32]
- **Plate valve** (Figure 3.6) suits for pressure difference up to 20 MPa and 1800 rpm. The valve can be either plastic or metallic. A different number of plate springs (dampers) is exploited. Despite larger flow areas bigger energy looses occur. These are cause by insufficient flow trajectory (Figure 3.9) [26] [32]
- **Discus valves** (Figure 3.8) have very good efficiency. Discharge valves fills discharge holes in valve plate, hence low clearance volume is reached. Very convenient is an arrangement of suction and discharge chambers, when sucked gas flows inside the valve plate, while the discharge chamber takes place above the cylinder. The design also ensures minimal heating of suction gas and large flow area.

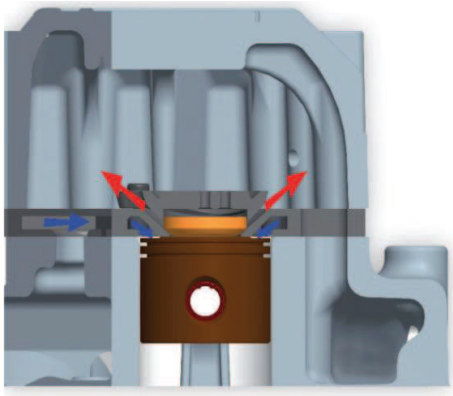

Figure 3.2 Flow through a discus valve [33]

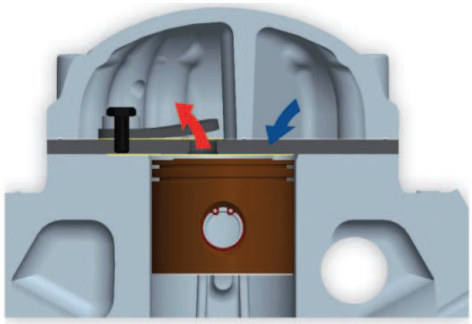

Figure 3.3 Flow through a reed valve [33]

- The **reed valve** (Figure 3.7) compressor is cheaper alternative to the discus valve compressor, however, efficiency is lower. The suction valve does not allow to the piston to come to the valve plate, thereby an additional clearance volume is created. This influence can be reduced by milling of the suction valve shape into the piston. A negative impact on the clearance volume has also an impossibility of discharge channels filling by discharge valves. [26] [33]

Figure 3.4 Poppet valve[27]

Figure 3.5 Ring valve[28]

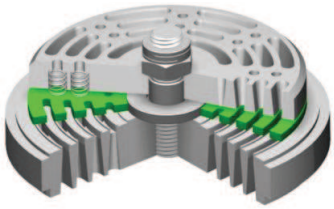

Figure 3.6 Plate valve[29]

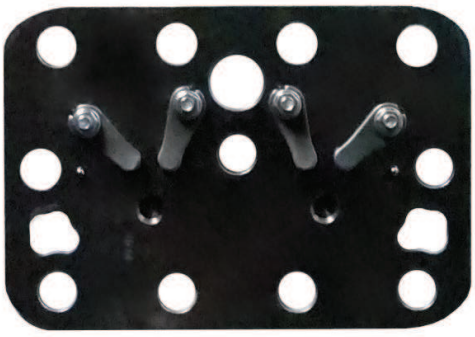

Figure 3.7 Flapper

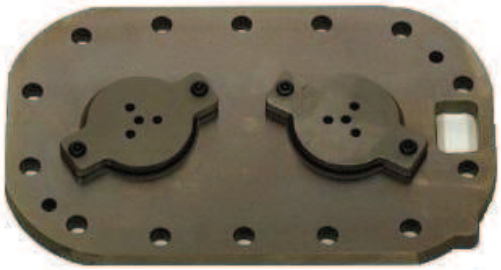

Figure 3.8 Discuss valve [30]

There are number of factors influencing valve performance:

- Stiffness of a valve and a spring affects the point of time when the valve opens or closes. Valves should react instantly for pressure differences. If they do not, power looses occur. When the valve is too stiff, valve opens too late or closes to early, also fluttering can occur. Too light valve can lead to late closing. [31]
- A valve plate assembly should have the right number of suction (discharge) valves and suction (discharge) holes with an optimal flow cross sectional area, and so allow sufficient filling and emptying of a cylinder. It is convenient to realize that sucked gas has another density than discharged gas. On the one hand, too small holes do not ensure sufficient filling or emptying. On the other hand, too big holes can cause equalization of pressure around valve, and so repetitive valve opening and closing during one suction (discharge) period. This may results in significant valve life time decrease. [26]

- A selection of a valve assembly materials and lubricant should be made with an attention to gas. This helps to avoid corrosion or other problems with reactivity of individual compounds. [26]
- The lubricant also affects valves opening. It is a reason why valves tend to stick in a seat. This can again cause opening delay, hence energy looses. [26]
- Other necessity is removing of dirt, which can have bad impact on valves function and their durability.
- An adverse effect on valve function, and so on compressor efficiency, can also have pulsations in an outlet and inlet gas pipes. [26]
- The valve lift is another factor affecting the efficiency of a compressor. The higher the valve lift, the higher valve velocity, hence the strain of the valve is raising and durability decreases. Conversely, if the lift is higher, cross sectional flow area is bigger and pressure drop decreases, hence less power is needed. [31]
- Shapes of valves also play its role. Examples are seen in the Figure 3.9. The flat plate valve causes gas to make two 90-degree turns compare to ring valve, where gas undergoes easier path. These shapes are the most important because of impurities, which follows same path as gas. The rounded shape has longer live time since impurities do not strike perpendicularly to the valve. In case of flat valve plate, premature failure can be developed. [26]

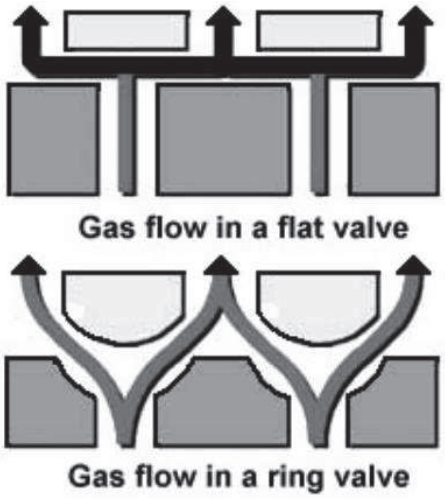

Figure 3.9 Gas flow through a valve [26]

CRANK MECHANISM

The crank mechanism transmits torque of a rotor to linear motion of a piston, and vice versa (in case of combustion motor). The whole crank mechanism assembly consists of a crankshaft, crank bearing, piston rod, wrist bearing, piston, and a pin. In case of an eccentric shaft, eccentric sheave, eccentric rod and an eccentric strap are the main parts putting the crank mechanism together.

VALVE PLATE

There are different types of valve plates depending mainly on a gas flow trajectory or type of valve used. Any valve plate has to withstand pressure differences especially between the cylinder and discharge chamber. When a valve plate is designed, it is important to focus on suction and discharge holes. These holes should influence the gas flow as least as possible; hence energy dissipation should be minimized. To fulfil this requirement CFD analysis is a necessity. Except an impact on the gas flow stability a size of discharge holes must be considered. The volume of discharge hole has a negative impact on a clearance volume.

3.2 DESCRIPTION OF A COMPRESSOR CYCLE

Every compressor circuit is put together by four processes compression, discharge, expansion and intake. A designer makes an effort to reach an ideal circuit, although is unreachable by physic law.

3.2.1 IDEALIZED THERMODYNAMIC CYCLE

A p-V diagram (Figure 3.10) describes the whole working cycle. The process 1-2 depicts compression, 2-3 represents discharge, 3-4 shows expansion and the last one is an intake. The two horizontal processes are isobaric. The remaining processes can be isothermal, polytrophic or isentropic.

The isothermal process describes maximum heat transfer, hence maximum cooling. It is not reachable, the process would take long time for sufficient heat transfer and it does not correspond with need of reasonable output. Apart from the isothermal process, the adiabatic (isentropic) process does not take into consideration any cooling. The polytrophic process represents only some cooling, hence it is the most realistic process.

The expansion process 3-4 results from expansion of the compressor clearance volume.

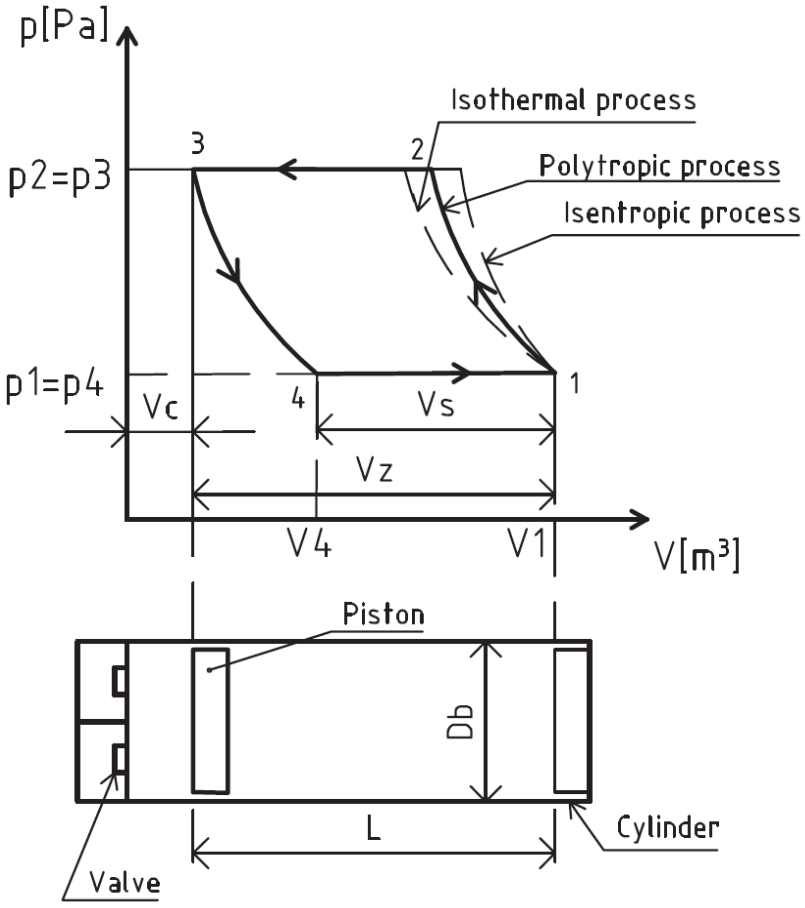

Figure 3.10 Idealized p-V compressor cycle

3.2.2 REAL THERMODYNAMIC CYCLE

The real thermodynamic cycle of a reciprocating compressor has few important differences (Figure 3.10). Apart from the idealized compressor, none of undergoing processes is reversible. It is seen that pressure inside the cylinder is during whole suction process below suction pressure and during whole discharge process above required discharge pressure. These pressure differences are necessary for valves opening. However, the shaded areas represent pressure looses, the bigger these areas, the bigger looses. Also higher (lower) pressure peaks can be noticed on the discharge (suction) beginnings in the cylinder. These peaks are caused by valves resistance. Thus, higher pressure differences are needed for the initial opening. This effect is mainly result of oil particles, which tend to stick valves to their seats. [40]

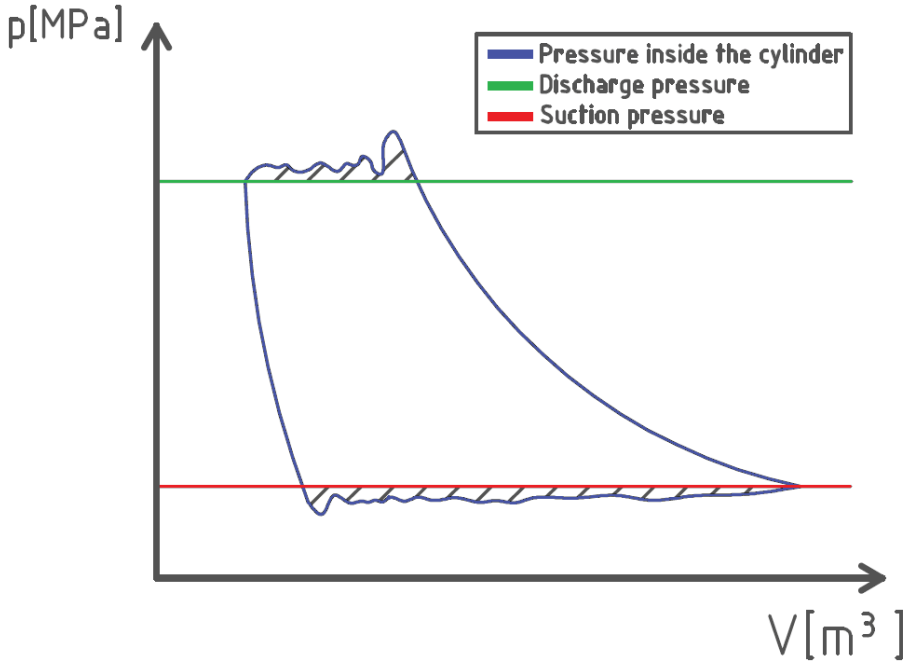

Figure 3.11 Real p-V compressor cycle

4 REFRIGERANTS

Only nature refrigerants substances were employed in the early years of cooling systems usage. One of them was ethyl ether (R610) because of its low evaporation temperature. Other useful refrigerants were carbon dioxide (R744), ammonia (R717), sulphur dioxide (R764) and many others. [5]

The period of change, in the refrigeration industry, begun in early 1930s when chlorofluorocarbons (CFCs) were introduced. One of the main claims for their applying was safety and environmental friendliness. Despite that, many accidents have happened in the course of time. CFCs can cause suffocation and later was found that they are originators of stratospheric ozone layer destruction processes and contribute tremendously to global climate change. Therefore, CFCs subject to regulations and prohibitions. [5]

The worldwide banning of CFCs is counted from the end of 1980s when the Montreal Protocol was agreed. The initial reason of this Protocol was the CFCs destructive influence on the ozone layer. The document has been instantly adjusted and amended. This helps to control new chemical substances and creates support in a sense of economical mechanisms for developing countries, which ratified the Protocol. [8]

A basic mechanism of ozone layer depletion can be introduced by an example of Dichlorodifluoromethan (R12). The reaction (4.1) shows a separation of Cl atom, a required condition for realization is electromagnetic radiation. Subsequently the chlorine atom reacts with ozone molecule and creates a chlorine monoxide and a molecule of oxygen (4.2). Chlorine monoxide reacts with an oxygen atom (4.3). Chlorine atom becomes free and can react with ozone molecule again. This reaction sequence makes an unwanted loop. Chlorine stays in atmosphere for decades.

$$CCl_2F_2 \rightarrow CClF_2 + Cl \quad (4.1)$$

$$Cl + O_3 \rightarrow ClO + O_2 \quad (4.2)$$

$$ClO + O \rightarrow Cl + O_2 \quad (4.3)$$

Because of an effort to phase out CFCs a replacement has been needed to be developed, and so nature refrigerants, even despites its drawbacks, have been begun to be used again.

4.1 CATEGORIZING OF REFRIGERANTS

- Hydrocarbons
- Halocarbons
- Zeotropic mixtures
- Azeotropic mixtures
- Inorganic compounds

4.1.1 HYDROCARBONS (HCS)

Carbon and hydrogen are basic components of these organic compounds. This group contains, for example, common well-known refrigerants as methane (R50), ethane (R170), propane (R290), butane (R600) and other. They are used for their properties and the environment impact, such as low influence to global climate change and zero ODP (ozone depletion potential). Their disadvantages are high flammability and explosiveness. Halocarbons are often replaced by HCs. [5]

4.1.2 HALOCARBONS

Halocarbons are compounds where one or more halogens (chlorine, bromine and fluorine) are linked to carbon atoms. They are used in refrigerants and air conditioning. CFCs like perfluorocarbons, carbon tetrachlorides and halons are contained in this group. [5]

CFCs have higher density in compare with air, are not toxic and are odourless. Being in a space with high concentration of CFCs can cause suffocation. By burning CFCs arise poisons which should not be breathed in. [5]

Halons are used for fire extinguishers but their production is also band in many countries, due to its depletion effect on ozone layer. Carbon tetrachloride manufacturing also stopped but because of its influence on creation and rising of carcinoma. Perfluorocarbons have not a harmful effect on ozone layer but, on other hand, have tremendously high global warming potential, 5,000 to 10,000 times higher than carbon dioxide, and their atmospheric lifetime is in thousands of years. [5] [9]

4.1.3 ZEOTROPIC MIXTURES

Zeotropic refrigerants also called nonazeotropic refrigerants are mixtures of various chemicals of different volatility. The compositions have significant temperature variation during constant pressure phase change. Thus, it comes about proportional composition changes during evaporation and condensation. An interest in those mixtures rose simultaneously with heat pumps developing but it is also applied in refrigeration for many years. [5]

Figure 4.1 shows a diagram of zeotropic mixture of 2-Butanol and 2-Propanol. The diagram is measured at constant normal pressure. On the left side is pure 2-Butanol and to the right side of the diagram, percentage of 2-Propanol is rising and representation of 2-Butanol is decreasing. Y-axis shows range of temperature value in Kelvin.

If the mixture is heated to temperature T_2, a vapour with composition of x_3, y_3 and a liquid at composition of x_2, y_2 arises. It tells that liquid is richer for 2-Propanol at the temperature T_2. However, by further heating temperature T_5 is reached and the proportion of 2-propanol in the mixture decreases. The liquid is even richer for 2-Butanol. At the temperature T_6 the compound with initial ratio of components is presented. [11]

It is important to mix properly all components to avoid diffusion processes in evaporator. If this requirement is not fulfilled, an efficiency of the whole system is lowered. The mixing has also influence on temperature variation during phase change. A replenishing problem occurs in case of leakage. The entire amount of refrigerant has to be replaced because of components proportion unknowingness. [11]

4.1.4 AZEOTROPIC MIXTURES

The azeotropic mixtures are compounds composed of two or more different chemicals. The mixtures behave as a single substance, although the mixed constitutes are various. The vapour and the liquid have constant proportion of components and temperature is not changing during the phase change at specified composition mixture. It means that chemicals are inseparable by heating processes as distillation. [5][11]

Figure 4.2 represents diagram of azeotropic compound. X-axis shows compositions and y-axis is temperature. The diagram describes situation at constant pressure. The bottom curve is bubble point curve. The top trace illustrates dew point curve.

If the letters are followed, condensing and evaporation, thus separation by distillation, can be described. This process tells that it is not reachable to get distillate of higher proportion of constituent *X* than in the azeotropic point. Analogical process can be done from right side of azeotropic point.

As an example of azeotropic mixture, compound of 95 % ethanol and 5 % water (volume percentage), can be mentioned. Boiling point of this mixture is at 78.2 °C.

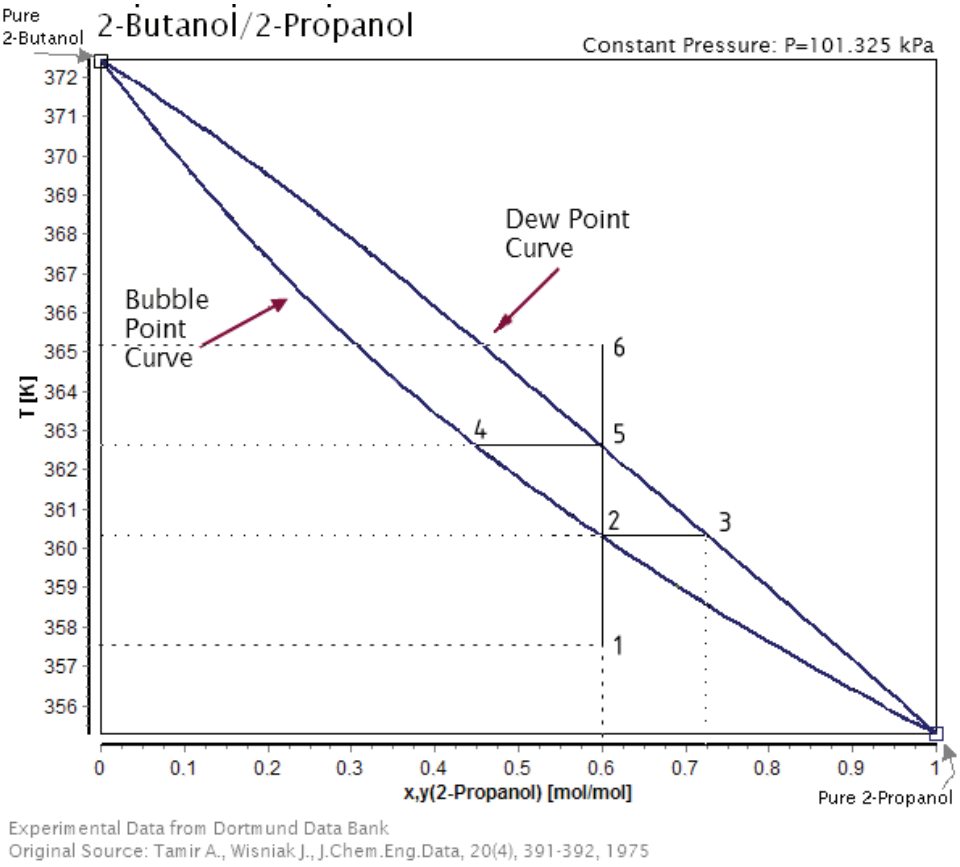

Figure 4.1 Zeotropic mixture [10]

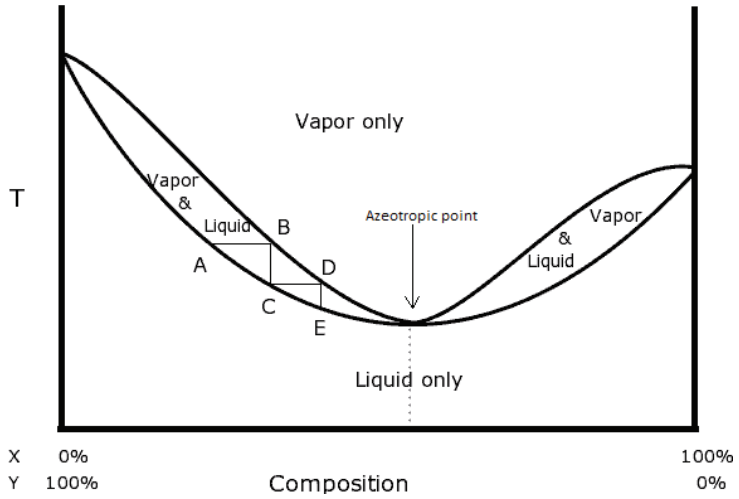

Figure 4.2 Azeotropic mixture [12]

4.1.5 INORGANIC COMPOUNDS

This class of refrigerants have been already used for refrigeration, heat pumps and air conditioning for many years. Two representatives are going to be introduced, namely ammonia and carbon dioxide. Carbon dioxide is getting an attention in recent years and a growth of his role in refrigeration industry is expected. [5]

AMMONIA (R717)

Ammonia has been employed as refrigerant since 1876. Its properties are good valuated, especially for its acceptable pressures in wide range of temperatures and high thermal capability of cooling. The evaporation temperature is at -33°C at atmospheric pressure. It has strong odour, thereby can be recognized by man sense at low concentration, and does not have any colour. [5]

Ammonia has also few disadvantages. It can irritate when it is in a contact with a mucous membrane. It can also cause serious health problems, specifically eyes damage and respiratory tract damage. A contact with skin can lead to chemical burns. The compound is flammable and explosive in mixture with air at specific concentration (16 % - 25 %).

CARBON DIOXIDE (CO_2)

This compound of carbon and oxygen was together with ammonia one of the first common used refrigerant. Unfortunately, they were replaced by Freons when these were developed. One of the main purposes of the replacement was toxicity of ammonia and high operation pressures of CO_2. However, CO_2 is a hot topic in refrigeration in last decades, since Freons have devastating impact on ozone layer and high global warming potential (GWP). [34]

Refrigerant	Critical temperature [°C]	Critical pressure [bar]	ODP	GWP	Flammable
R134a	101.1	40.7	0	1200	No
Ammonia (R717)	132.2	113.5	0	0	Yes
CO_2 (R744)	31	73.8	0	1	No

Table 4.1 Characteristics of chosen refrigerants [36]

Carbon dioxide has acid taste, is nontoxic, nonexplosive, nonflammable, has high heat transfer coefficient and is odourless at low concentration. Its density, in gaseous form, is 1.5 higher than a density of air, hence it gathers at ground level. In a compound with water, constitutes carbonic acid, which causes corrosion of metal and other materials. It does not react with common construction materials and lubricants as a pure compound. It forms "dry ice" at -78.4°C, which has two times bigger cooling capacity than common ice. [5] [36]

The price of R744 is very low, since it is abundant natural gas, which arises in a nature or as a product of combustion and other industrial processes. Its concentration in the earth atmosphere was around 397 ppm (according Mauna Loa Observatory) in December 2013. Carbon dioxide has GWP equal to one (CO_2 is the reference gas for GWP) and does not have any ozone depletion characteristics. [35] [36]

Its thermodynamic characteristics differ from most of other refrigerants. The critical pressure 73.8 bar is very high and the critical temperature 31.0 °C is very low, which results in significant consequences on its exploiting in refrigeration. The low critical temperature and high triple-point temperature are the main disadvantages of R744. The triple-point at 5.2 bar leads to higher operation pressures in compare to other refrigerants. It is necessary to avoid creation of solid phase. [36]

The CO_2 refrigerant can be employed either in subcritical or in transcritical cycle. A limitation of the subcritical cycle is an outside temperature which should be under 15 °C for direct heat releasing to the atmosphere. Because of the thermodynamic properties of R744 it is seen that the used devices have to be designed for high pressures, which has, obviously beside other affects, impact on lubrication and materials used. [44]

When transcritical cycle is used, condensing process does not exist, and so the temperature of refrigerant changes in a gas cooler. It enables to keep low temperature difference of heated fluid and refrigerant, which is suitable attribute for heat pumps. This means that R744 is convenient for simultaneous heating and air cooling.

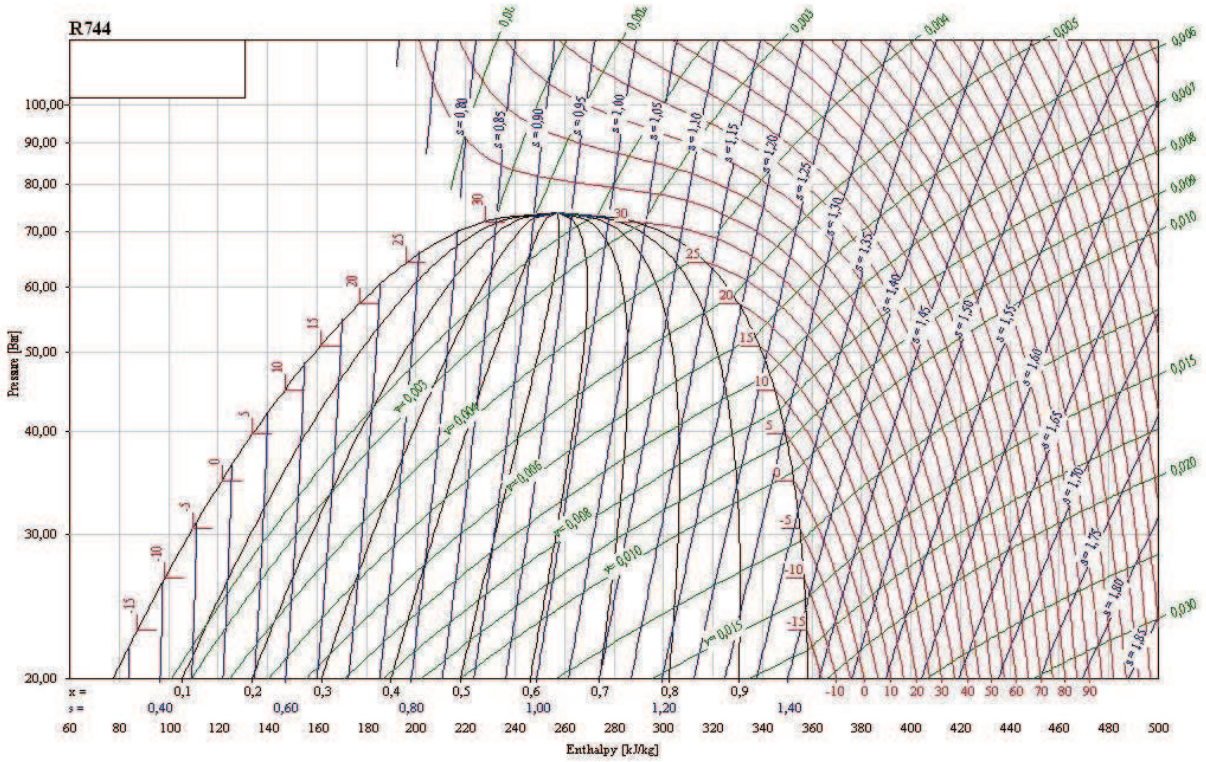

Figure 4.3 Carbon Dioxide p-h diagram [37]

5 ANSYS WORKBENCH

ANSYS is simulation software, which enables to simulate wide range of physical problems. Engineers use this software for structural and thermal analysis as well as for fluid dynamics, electrical and electromagnetic analysis. ANSYS is a finite element tool, which means that each analysed component or design consists of elements, which are described by equations with finite number of unknown quantities. Behaviour of the whole design is therefore given by behaviour of each element. Base on this information it is unequivocal, that FEA simplify real physical systems, which have infinite number of unknowns. The quality of the approximation depends, as a general rule, on engineer who cares about simulation setting.

ANSYS Workbench is going to be used, in this paper, for purposes of static structural analysis and modal analysis of the new suction valve, and for CFD analysis in the suction channels.

Before anybody proceeds to ANSYS session it is necessary to judge the simulated system. Objectives of analysis should be defined. Questions, whether are needed von-Mises stress, deformation, temperature or other data, should be answered. Neglecting details like radiuses should be weight. It obvious that it is necessary to know where is a critical place, and so where the best mesh quality is needed. A thought of geometry simplification should be also considered. Answers for these questions can decrease computational time significantly. However, the accuracy of simulation cannot be forgotten. [19]

5.1 TIME DEPENDENT SYSTEMS

Three basic time dependent problems can be mentioned. The first occurs when time varying forces are applied. The second appears when a body changes its phase. The last one comes up, when initial temperature distribution is defined. [20]

5.2 NONLINEAR SYSTEMS

Most of processes in our surroundings are considered as nonlinear. Fortunately, these physical processes can be often assumed to be linear, whereas results are sufficient. On the other hand, the nonlinearity cannot be avoided by some problems. As nonlinear structural cases following problems can be mentioned: a change of boundary conditions, material and geometric nonlinearity and a change of structural integrity. [20]

GEOMETRIC NONLINEARITY

Examples of geometric nonlinearity are a stress stiffening, rotation and a large deflection. The large deflection stands for process when a deflection of a component is large in compare to smallest dimension of the component, thus a force direction changes considerably. The rotation is analogical. [20]

Stress stiffening describes phenomenon, by which stiffness in one direction is influenced by stress in other direction. [20]

MATERIAL NONLINEARITY

The phenomena like a hyper-elasticity, viscoelasticity, nonlinear elasticity, creep and plasticity are placed in this group. The hyperelastic materials have similar behaviour to a rubber. Viscoelastic materials exhibit time dependent deformation when constant load is applied. However, after unloading do not have permanent deformations. Nonlinear elastic materials recover itself to initial state after unloading and its stress-strain curve is not linear. [20]

5.3 MID-SURFACE

The mid-surface feature gives an option to create a surface body from a solid body. From the original solid body two opposite faces are chosen, and then the mid-surface is made in the middle of the faces distance. It is convenient to pay attention to order of the faces choosing. According to the order, loading and connections are later defined.

The surface body is a body type, which has an area of a surface but does not have a volume. However, to any surface body thickness can be assigned, hence the impact of the volume can be considered. The thickness is calculated from original solid body or can be assigned manually. The surface body thickness is seen when meshing is performed. [45]

5.4 SYMMETRY

Applying of a symmetry condition is very suitable way how to reduce computational time. The symmetry condition can even lead to more accurate results, since the simulated section of the system can be more detailed than the entire system. The condition reduces number of DOF at symmetry region. Nevertheless, the tested system has to fulfil requirements of symmetry of loading, material, geometry and constrains. [20]

The symmetry can be classified into few types: Repetitive or translation symmetry, planar or reflective symmetry, cyclic symmetry and axisymmetry. [20]

5.5 MESH

Meshing is very complex and critical step in FEA. Many types of elements can be used as well as types of meshing methods. In general, bigger number of elements increases the accuracy of a result, however, an exception can come up. The higher number of elements can also raise round-off error. The necessity is to model appropriate mesh over whole system; hence the special attention should be paid in places of interest or in locations where problems are expected. Mesh should be usually finer there. Unfortunately, there is not any rule how fine mesh should be, this is derived from specific simulated system. [20]

When element type is selected, two basic options are offered: linear, and quadratic. These elements are depicted in the Figure 5.1

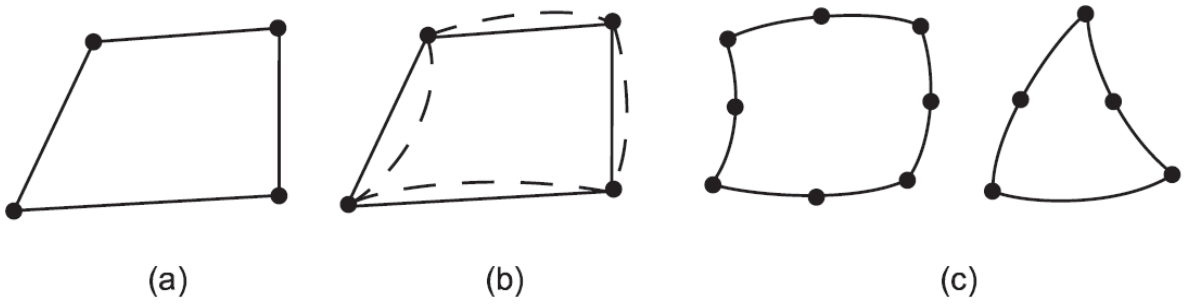

Figure 5.1 a) Linear isoparametric, b) Linear isoparametric with extra shapes, c) Quadratic [21]

When linear elements without mid node on each side (Figure 5.1 a, b) are used, it is necessary to avoid an element shape deformation in the critical location. The fine mesh of these elements can bring better quality of results in case of nonlinear structural analysis than when quadratic elements of comparable sizes are used. On the contrary, quadratic elements provide more accurate results when linear structure simulation with deformed element shape (3D

tetrahedral or wedge elements, 2D triangular elements) is performed. These deformations are usually called as element degradation. [22]

For further description of elements and meshing types, wide knowledge is needed. Meshing has three basic types: meshing by elements, meshing by an algorithm and part/body meshing or entire assembly meshing. [22]

Meshing by elements consists of many meshing submethods as Tet meshing (derived from tetrahedron), Hex meshing, Hybrid meshing, Cartesian meshing, Quad meshing and Triangle meshing. [22]

If a decision to use part meshing is made, specified parts are meshed individually. On the other hand, if it is decided to use assembly meshing, the whole assembly is meshed at once, this can reduce meshing time. The assembly meshing creates conformal mesh between all affected bodies. [22]

Meshing by algorithm covers techniques called patch independent and patch conforming. The patch independent does not strictly respect all faces and boundaries, if any boundary condition or load is not presented. It is usually applied in cases when elements of same sizes are required or details need to be excluded. The patch confirming technique is opposite to the patch independent. All boundaries are respected and defeaturing is applied only when meshing difficulties arise. [22]

5.6 CONTACTS

When any assembly needs to be analysed in ANSYS, a defining of contacts is necessary. The contact is set when surfaces of specified components touch each other initially or during simulation. [23]

CONTACT TYPES

Six contacts types can be set in Workbench Mechanical: *frictional*, *frictionless*, *rough*, *no-separation*, *bonded* and *force frictional sliding*. Choosing of the appropriate type is critical for right behaviour of a contact. [45]

The *bonded contact* does not allow any motion of contact bodies. When any gap is presented, the software closes it. If the gap closing needs to be avoided, pinball region has to be specified. This contact is linear and computationally the cheapest. [24] [45]

The *no-separation contact* is very similar to *bonded type*. The difference is that this type is applicable to edges of 2D solids and to faces of 3D solids. [45]

The *frictionless* type allows body motions, however, friction coefficient is set to 0. The contact type is nonlinear, since the contact area between contact bodies can change as a result of loading. [45]

The *rough contact* type is similar to frictionless but friction coefficient is equal to infinity. Hence a sliding cannot occur. [45]

The *frictional contact* type supports the option of defining friction coefficient. Hence share stress value, at which sliding starts, is defined. The type allows opening and closing of the particular contact. [45]

The *forced friction sliding contact* type is similar to the *frictional contact*. The difference is that share stress value for beginning of sliding is not used. At each contact point a tangential resistance force is defined. [45]

FORMULATIONS

To model the contact behaviour realistically a contact region of components must be specified. A correct establishing of the contact region defines exact amount of interpenetration, which is solved by contact formulations. When nonlinear contact is simulated, *Augmented Lagrange* or *Pure Penalty* formulation is used. Next available choices are *Normal Lagrange* and *MPC* (multi-point constraint). These all formulations have different way of contact detection, hence different conception of interpenetration evaluation. The *MPC* is suitable only for the bonded and the no-separation contact. The other contact region method can be used for any contact behaviour. *Augmented Lagrange* formulation is often used for *large deflection*. [23]

OTHER USED FEATURES

An important parameter for successful convergence is *normal stiffness*. In case when bending is dominated, a *normal stiffness* suppose to be set to 0.1 – 0.01, for bulk-dominated suppose to be set to 1. The higher the *normal stiffness*, the better accuracy is reached. Unfortunately, the higher value can cause convergence problem. Because of an influence of *normal stiffness* value, sensitivity analysis can be performed. [23]

Pinball region is a spherical region, which encloses each contact detection point. If a node on a *target* surface is inside the region, ANSYS considers the *target* body as the contact body and performs calculations, which determine reciprocal position of contact components during loading. The size of the *pinball* region results in different calculation time. The bigger region, the bigger amount of time is needed for calculation. [23] [24]

Symmetric and *asymmetric* behaviour is next option, which can be set in contact setting menu. This option is tied to right specification of *contact* and *target* surface. When the *symmetric* behaviour is set, the both *target* and *contact* surfaces are prevented from penetration each other. It means that designer does not have to distinguish between the surface types. Unfortunately, this option brings bigger requirement for computational time. When the *asymmetric* behaviour is used, entirely the *contact* surface is prevented from penetrating the *target* surface. Hence a designer should be careful about specifying the right surfaces types. The *asymmetric* behaviour decreases the computational time. In case of stiffness behaviour defined as *rigid*, only *asymmetric* behaviour can be used, the *rigid* body is always the one with the *target* surface. [23]

5.7 SUPPORTS

Workbench Mechanical offers wide range of boundary conditions, which include a few types such as supports, loads and conditions. We focus only on description of selected supports.

The *fixed support boundary* conditions prevents from deformation and moving of particular geometry. [45]

The *displacement boundary* allows setting of displacement by vector in global or local coordinate system. [45]

The *remotes displacement* is similar to the *displacement boundary* except that, a rotation of selected geometry can be specified. The support is applicable in rigid dynamics analysis. [45]

6 FATIGUE

Material properties are important indicators for designing and evaluating of new components, therefore they are tested in laboratories. Most of experiments, relevant to deformation and stress, are performed by an applying of gentle increasing load till material damage. These tests are executed many times at same conditions with different specimens of the same type. Afterwards, results are evaluated and statistical conclusions are made. [13]

Excluding static loading, individual components are influenced also by time dependent strain, in praxis. An example can be a bicycle pedal. A biker creates a force on the pedal approximately in the same time during each pedal cycle. It was observed that the cyclic loading can results in structural damage, even when resulted maximum stresses are far from ultimate tensile strength. The main characteristic of this damage is repeatable loading during long time and sudden damage. This process is called as fatigue of material. [13]

Static forces compare to cyclic forces are usually less dangerous. The damage due to static forces is, as a rule, coupled with big deformation and exceeding of material yield strength. The permanent deformation notifies us of the danger and urges component replacement. The fatigue fracture is immediate and much less predictable. [13]

A few methods are applied for evaluation of fatigue life. The methods enable to predict a number of cycles N_f to fracture during defined loading. Depends on cycle quantity N_f two regions are distinguished. The region $1 \leq N_f \leq 10^3$ is called low-cycle fatigue and $N_f > 10^4$ is a region of high-cycle fatigue (Figure 6.1). [13]

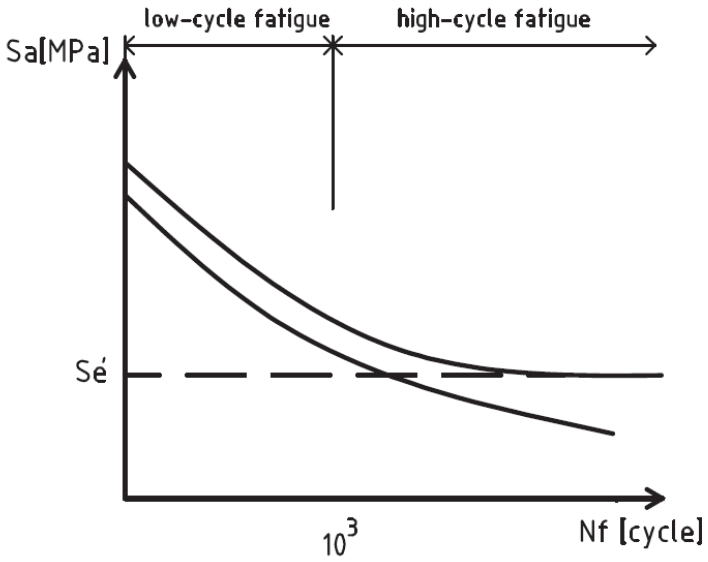

Figure 6.1 Cycles to failure (Wohler curve)

The first method called Nominal stress-life method represented by S-N diagram (Wohler curve) is rated as the least accurate, especially for the low-cycle fatigue. However, many experiment data are accessible for this method and using in the high-cycle fatigue can be sufficient. The appraisal of a fatigue life is made by using of stress amplitude S_a and the number of cycles to failure N_f. Wohler curve can be made for real components or only for experiment specimens. However, results of these two procedures can differ significantly. An important point of the curve is the one, which is marked as fatigue limit or endurance limit S_e'. Behind this turning point it does not matter how much cycles are performed, fatigue failure

does not appear. Some materials (eg. aluminium) do not have such significant fatigue limit, thus fatigue strength of these material is defined by total number of cycles, usually $N = 10^8$, which are endured at given stress. [13]

The second method, local strain-life method, is suitable for low-cycle fatigue. Unfortunately, necessary simplifications for obtaining results lead to uncertainty and also, detailed plastic deformation analyses are needed in places of interest. This method together with a fatigue crack growth method is not further used for solving diploma thesis, hence are also not described. [13]

6.1 FATIGUE LIMIT

Fatigue limit can be obtained by fatigue laboratory experiments, which is common but time expensive process. It is useful to have an estimation method for prototypes designing. According to Mischke, who analysed results of many mechanical experiments (bending during rotation), fatigue limit can be tied with ultimate tensile strength. An example of this relation for steel says that if $S_{ut} \leq 1460$ MPa the fatigue limit is equal to 0.504 S_{ut} MPa and if $S_{ut} > 1460$ MPa the fatigue limit is 740 MPa. [13]

When the fatigue limit is searched, it is necessary to have in mind that the data are only statistical and can vary according to steel or generally according to material, ambient conditions as well as according to loading conditions. [13]

Because of differences in components fatigue limit tested in laboratory, where materials are not tested in exact conditions, corrected fatigue limit S_e was implemented. Same conditions in laboratory and on a place of a component usage are not expected. [13]

INFLUENCE ON FATIGUE LIMIT

The fatigue limit is influenced by six basic factors. If these factors are multiply with fatigue limit, the wanted corrected fatigue limit is determined. [13]

$$S_e = k_a \cdot k_b \cdot k_c \cdot k_d \cdot k_e \cdot k_f \cdot S'_e \tag{6.1}$$

The first factor k_a, surface finish factor, depends on ultimate tensile strength and machined surface quality. [13]

$$k_a = a \cdot S_u^b \tag{6.2}$$

where a, b are constants depending on manner of machining.

The factor k_b, size factor, expresses influence of size, specifically an impact of shape and size of entire cross section. In case of axial loading $k_b = 1$, thus the influence is not considered. [13]

The factor k_c, loading factor, takes into consideration manner of loading. Rotating bending (shaft loading), reversed bending, reversed axial loading, reversed torsional loading are distinguished. Average values of the factor are following: [13]

$k_c = 1$ Bending
$k_c = 0.85$ Axial loading
$k_c = 0.59$ Torsional loading

The factor k_d, temperature factor, quantifies influence of temperature. When ambient temperature is under room temperature, probability of brittle fracture is rising. In case of higher temperature than room temperature, yield strength S_y decreases and plastic deformation can occurs. Creep can arise at high temperature and the fatigue limit does not have to be noticeable. It was observed that, fatigue strength of steel is increasing with rising temperature, however, between 200 and 350°C is decreasing. The factor for steel can be quantified by an equation, which depicts its relation to temperature. The equation is based again on statistic results and its trend is defined by fourth degree polynomial. The equation is valid for temperatures form 20 to 550°C. [13][14]

$$k_d = 0.987 + 0.613 \cdot 10^2 \cdot t - 0.302 \cdot 10^{-5} \cdot t^2 + 0.442 \cdot 10^{-8} \cdot t^3 - 0.518 \cdot 10^{-11} \cdot t^4 \quad (6.3)$$

The factor k_e, reliability factor, is based on an idea that every component is designed for specific reliability. It means that component withstand a stress at specified conditions with given probability. If the standard deviation of endurance strength is considered smaller than 8 %, k_e is defined by following equation: [13][14]

$$k_e = 1 - 0.08 \cdot z \quad (6.4)$$

where z is standardized random variable, of which value can be found in a literature (Table 6.1).

Reliability [%]	Standardized random value z	Reliability factor k_e [-]
50	0	1.000
90	1.288	0.897
95	1.645	0.868
99	2.326	0.814
99.9	3.091	0.753
99.99	3.719	0.702
99.999	4.265	0.659

Table 6.1 Reliability factor [13]

Factor k_f, miscellaneous factor, consider rest influences. The factor includes an impact of corrosion, cyclic frequency, electroplating, fretting, radiation, metal spraying. These impacts are often very difficult to quantify, but still can have big influence. For example, the electroplating by nickel or chromium can lead to 50 % fatigue limit decrease.

It is important to avoid or minimize factors, which affect fatigue life. Influencing factors are static stress, cyclic stress, electrolytes, properties of materials, temperature, cyclic frequency, speed of flow near component and notches. [13][14]

NOTCHES SENSITIVITY

A stress concentration caused by a shape irregularity is next very important factor to consider. These irregularities lead to significant stress increase in its close proximity. Maximum stress in the notches is counted by an equation (6.5). [13]

$$\sigma_{max} = K_f \cdot \sigma_0 \tag{6.5}$$

where σ_0 is nominal stress and K_f is reduced value of concentration factor K_t. The concentration factor can be found in tables and graphs intended to this purpose. The nominal stress is meant as a stress, which arises without stress concentrator. It is good to check conditions, at which the concentration factor was determined. [13]

If the reduced concentration factor K_f is required, the concentration factor K_t is found. Subsequently, the notches sensitivity q is looked up according material. Finally, the reduced concentration factor is reckoned for example from an equation (6.6). [13]

$$K_f = 1 + q \cdot (K_t - 1) \tag{6.6}$$

6.2 FLUCTUATING LOADING

Many mechanical parts are loaded by fluctuating forces. The caused stress is then often depicted by a sinusoid. This stress is expressed in relation with time and its type can differ. Basically, sinusoidal and nonsinusoidal cycles are distinguished, also sinusoidal with high frequency ripple can occur. Cycles also differ by position to zero level stress as completely reversed stress, repeated stress and fluctuating stress. [13]

The sinusoidal fluctuating stress is depicted in the Figure 6.2. It is seen that maximum σ_{max} and minimum σ_{min} stresses are periodically repeated. Mean stress σ_m, amplitude stress σ_a and range stress σ_r are identifiable, too. Static stress σ_s is often mentioned, however, it is usually independent of the cyclic stress and differs from the mean stress. It is defined as a permanent working stress. [13]

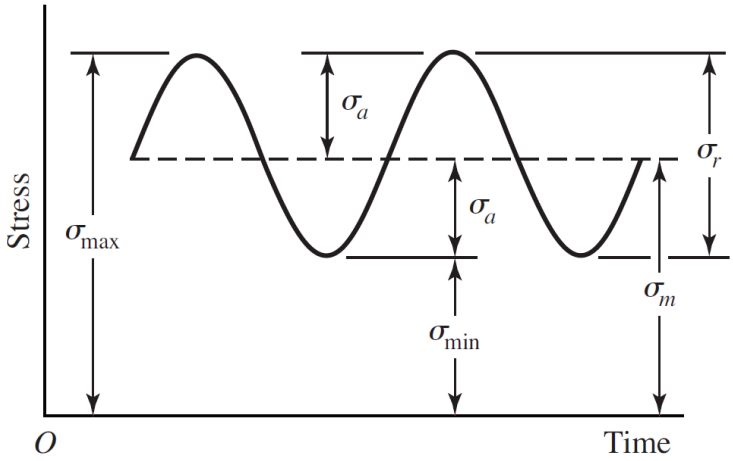

Figure 6.2 Sinusoidal fluctuating stress

$$\sigma_m = \frac{\sigma_{max} + \sigma_{min}}{2} \tag{6.7}$$

$$\sigma_a = \frac{\sigma_{max} - \sigma_{min}}{2} \tag{6.8}$$

6.3 HAIGH DIAGRAM

The Haigh diagram together with the Smith diagram and other methods are used for evaluating the fluctuating stresses. However, only Haigh diagram particularly Modified Goodman criterion and Lager criterion are addressed in this work. Despite that these criteria differ from each other, they can be depicted in one Hiagh diagram (Figure 6.3). [13]

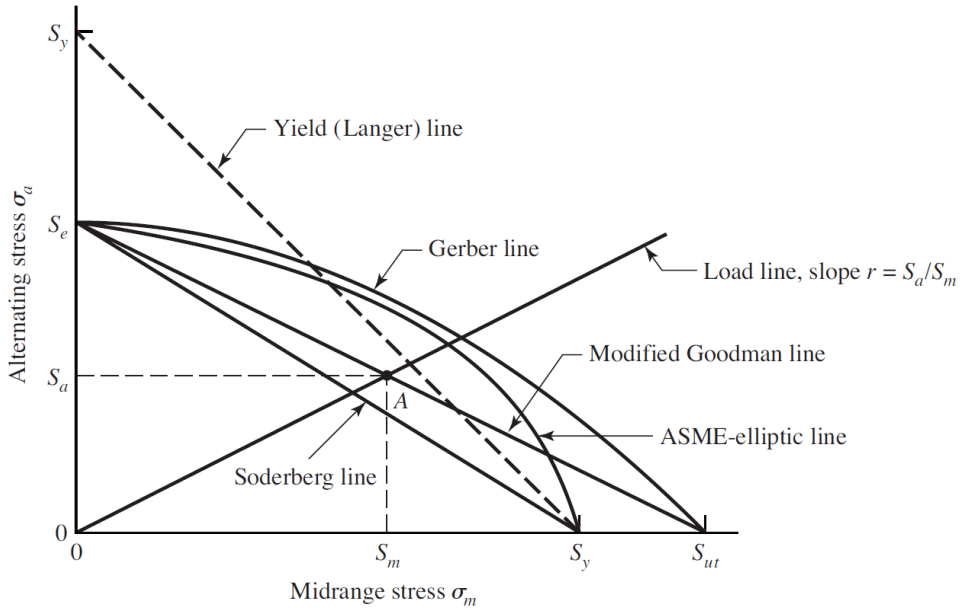

Figure 6.3 Hiagh diagram [13]

The Hiagh diagram is often used, since its construction is not exacting and is easy to read. A material and load characteristics are needed for its applying. Criteria, geometric figure, represent different view on safety. If the point of loading lies on criteria line, the fatigue safety factor n_f is equal to one. If a distance to coordinate origin is shorten, the fatigue safety factor grows. It is seen that Soderberg criterion is the most conservative and Gerber line is the complete opposite. The goal of using this diagram is to evaluate whether applied stresses are safe for specified probability of fatigue failure or not. [13]

Modified Goodman line starts in corrected endurance limit on vertical axes and ends in ultimate tensile strength on horizontal axes. Highlighting of yield strength is also very useful. The line beginning in origin is called load line and is defined by slope *r***.**

$$r = \frac{\sigma_a}{\sigma_m} \tag{6.9}$$

The Modified Goodman line is express by equation (6.10).

$$\frac{\sigma_a}{S_e} + \frac{\sigma_m}{S_{ut}} = 1 \tag{6.10}$$

The Langer line, line of plastic deformation, has following form

$$\frac{\sigma_a}{S_e} + \frac{\sigma_m}{S_e} = 1 \tag{6.11}$$

Coordinates of the Modified Goodman line and the loading line intersection are counted in equations (6.12)(6.13).

$$\sigma_a = \frac{r \cdot S_e \cdot S_{ut}}{r \cdot S_{ut} + S_e} \tag{6.12}$$

$$\sigma_m = \frac{\sigma_a}{r} \tag{6.13}$$

Coordinates of the Langer criterion and loading line intersection have following expressions

$$\sigma_a = \frac{r \cdot S_e}{1 + r} \tag{6.14}$$

$$\sigma_m = \frac{S_e}{1 + r} \tag{6.15}$$

An equation of safety factor is in the following form

$$n_f = \frac{1}{\frac{\sigma_a}{S_e} + \frac{\sigma_m}{S_{ut}}} \tag{6.16}$$

7 MODAL ANALYSIS

Modal analysis is used for determining vibration modes when almost any new mechanical system is design. Every physical system can vibrate with own natural frequency and modal shape. Modes are influenced by boundary conditions and material properties. For each mode can be determined modal parameters, namely modal shape, frequency and a modal damping. [25]

Vibration systems are usually described with a help of a particular component, damping element and a spring (Figure 7.1). Where the component has specified mass *m*, the damping element is defined by a damping coefficient *c* and the spring by a stiffness *k*. Then a differential equation, which states sum of all forces acting on the mass, can be written (7.1). The variable *x(t)* represents position of the mass. Capital letters in the equation means matrices, which are necessary to use in case of multiple degrees of freedom (MDOF) system. [25]

$$M\ddot{x}(t) + C\dot{x}(t) + Kx(t) = f(t) \tag{7.1}$$

Although the equation for MDOF system was mentioned, a simple degree of freedom (SDOF) system is often considered. Most of MDOF systems can be broken down to SDOF systems and counted as their linear superposition. [25]

If harmonic force acts at an undamped system and its frequency is equal to natural frequency of the system, thus $\omega = \omega_n$, a damage or life time decreasing of the system occur. However, all real systems are influenced by damping element. Unfortunately, it does not mean that we do not have to determine the natural frequency. The damping only decreases magnitude of natural frequency amplitude. Any employment of a damped system at the natural frequency is also unacceptable and must be avoided. The case when $\omega = \omega_n$ is called resonance (Figure 7.2). [25]

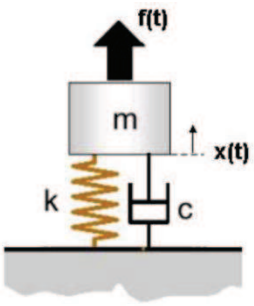

Figure 7.1 Model of a vibration system [25]

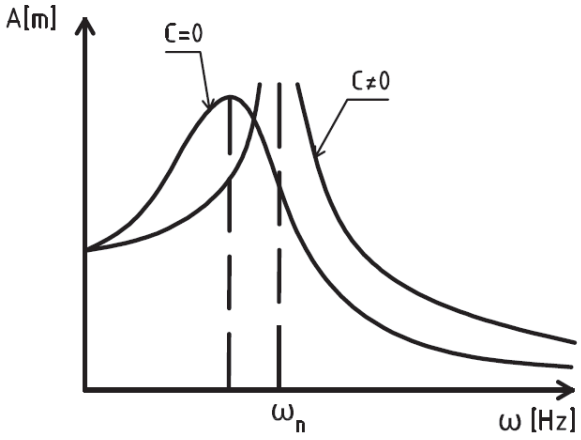

Figure 7.2 Resonance

7.1 USING OF ANSYS WB

The modal analysis is often first stage of other analysis as a dynamic analysis, harmonic response analysis, spectrum analysis or a transient dynamic analysis. [45]

The important information is that the modal analysis is a linear analysis, hence nonlinearities are not considered. For example, if any contact gap is set up, software ignores it automatically. For successful solution, a defining of correct material stiffness and mass is critical, this can be set by Poisson's ration, Young's modulus and density. [45]

A setting of a modal analysis is similar to static structural analysis. However, differences are also presented. From contacts point of view, joints can be used for degree of freedom restrictions. A damping is also taken in consideration if specified. Very important is to define number of required frequencies; the default settings solve only first six of them. Any zero value or nearly zero value frequency stand for tested component degree of freedom, hence if a component has six degree of freedom, the first six natural frequencies have the value around zero Hz and the mode shapes show the component translation (rotation) in the degree of freedom directions. In a case of modal analysis prestress effect can be applied, which means that the modal structure analysis is linked to a static structural analysis; hence initial conditions from the static structural analysis are used. Significant differences can be found for loads and supports. A remote displacement, velocity boundary conditions and a non-zero displacement are not available in compare with structural supports. A stand-alone model has only one loading option, which is rotational velocity load. [45]

During a result evaluation it is important to have in mind that actual magnitude of strains, stresses, and the deformations cannot be taken into consideration, they are meaningless. Only relative values of these mentioned quantities are useful. This fact is common for eigenvalues based analyses, so for modal analysis, too. [45]

8 COMPRESSOR TESTING METHOD

The compressor testing is governed by EN 13771-1, where the used method is marked as D2. According the standard, the method places the refrigerant flow meter in discharge line and refrigerant circuit consist of a compressor, expansion device and means for removing surplus heat. [38]

In the Figure 8.3, a testing circuit used in Emerson Climate Technologies laboratory can be seen. This laboratory solution complies with all requirements defined by the EN 13771-1.

The main control devices are: two expansion valve and water control valve. The first control valve sets inlet pressure *P1*. The more suction control valve is opened, the higher pressure *P1*. The second control valve sets outlet pressure *P2*. The more discharge control valve is opened, the lower pressure *P2*. The water control valve sets inlet temperature *T1*. The more water control valve is opened, the lower temperature *T1*. [38]

A compressor can be tested in in transcritical and subcritical circuit regime. These can be seen in the (Figure 8.1, Figure 8.2)

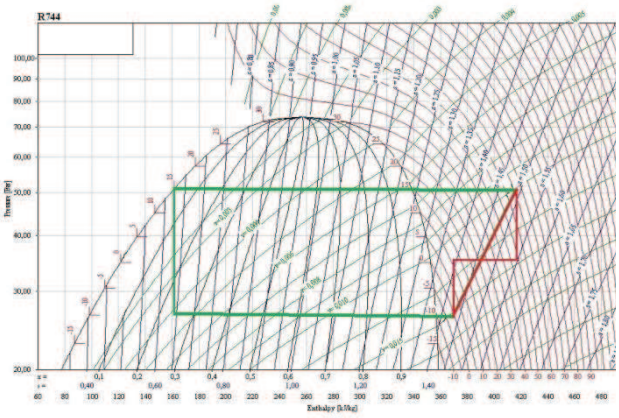

Figure 8.1 Subcritical refrigerant cycle [37]

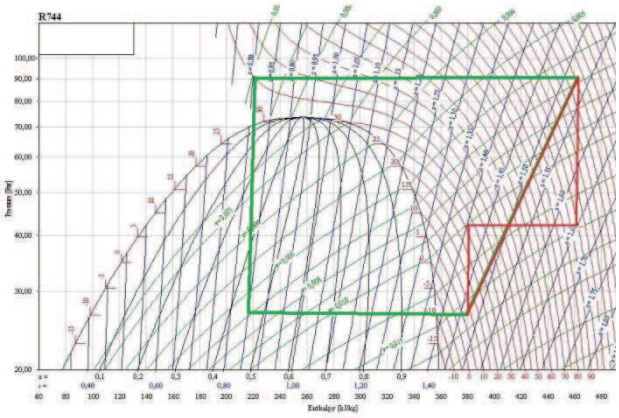

Figure 8.2 Transcritical refrigerant cycle [37]

The most important obtained result is *COP,* since it is the main criterion for comparing with original compressor design, as it is stated in the diploma thesis instructions. The EN 13771-1 tells that the coefficient of performance is calculated using the following equation:

$$COP = \frac{Q_L}{P_0} \tag{8.1}$$

where P_0 is electrical power input and Q_L is refrigerating capacity. Q_L is calculated by following equation

$$Q_L = \dot{m} \cdot (h_{g1} - h_{l2}) \tag{8.2}$$

where $\dot{m}$ is total refrigerant mass flow at compressor inlet, h_{g1} is specific enthalpy of refrigerant vapour at compressor suction, h_{l2} is specific enthalpy of saturated liquid refrigerant at outlet from condenser. In case of transcritical circuit, so in the circuit where saturation point at the outlet of condenser (gas cooler) is not reached, the specific enthalpy at the outlet of the

gas cooler is considered. Thus, the specific enthalpy $h_2 = h_{l2}$ is calculated from gas cooler outlet temperature and the compressor discharge pressure. The considered gas cooler outlet temperature is 35°C, which is governed by EN 12900. [38] [39]

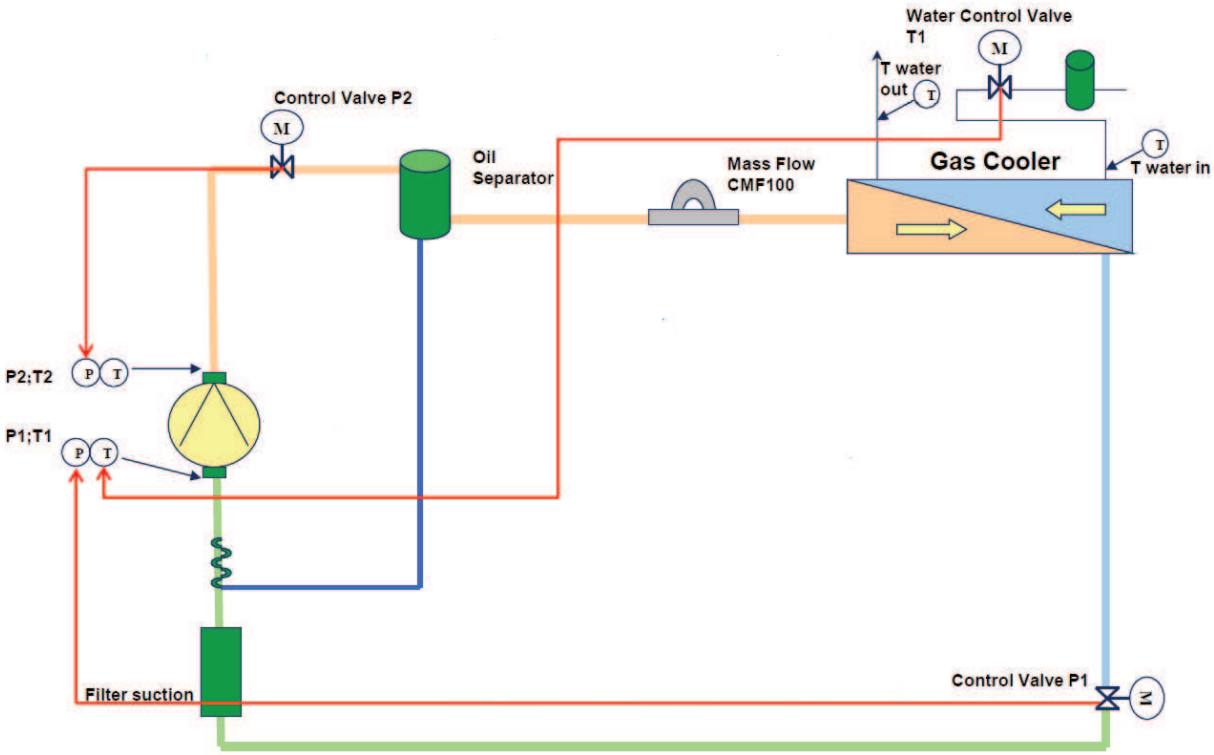

Figure 8.3 Laboratory cooling circuit

9 ORIGINAL COMPRESSOR

The original compressor is semihermetic reciprocating compressor for CO_2 refrigerant (Figure 9.2). It is powered by an electric motor and cooled by refrigerant passing through whole compressor body. Rotational move is transferred to linear by an eccentric mechanism and used valves are flappers. Lubrication is ensured by 1.6 l of RL68HB oil, this is splashed by a metal component in a shape of a plate mounted on the shaft. R744 is pressurized in four cylinders. It uses CoreSense^{TM} Diagnostics advance protection and diagnostic.

Nominal horse power [hp]	Displacement [m^3*h^{-1}]	Capacity [kW]	COP [-]	Oil quantity [l]	Weight [kg]
5	4.6	9.3	1.6	1.6	140

Table 9.1 The original compressor technical parameters. The tested conditions are stated by EN 12900 [42]

The Figure 9.1 shows transcritical conditions, for which the compressor is designed. The red squares depict conditions, in which the compressor is usually tested in Mikulov's laboratory.

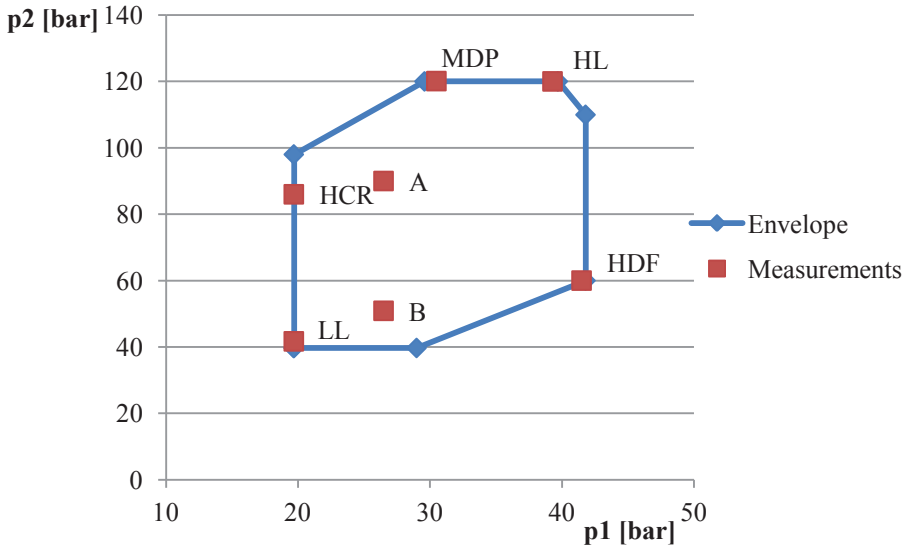

Figure 9.1 The original compressor working envelope and measurements conditions

Figure 9.2 The original compressor 4MTL-05X [42]

9.1 MATERIALS

Mentioned materials are solely materials of parts, which were used or modified in this diploma thesis.

Part	Material
Suction valve	7C27Mo2
Spring	7C27Mo2
Valve plate	11SMn30
Body	Cast Iron Grade 30

Table 9.2 Used materials

Material	Young's modulus [GPa]	Poisson's ratio [-]	Yield Strength [MPa]	Ultimate tensile strength [MPa]	Fatigue strength [MPa]	Density [kg·m^{-3}]
7C27Mo2	210	0.3	1300	1800	750	7700
Cast Iron Grade 30	89.655	0.24	144.86	220	NA	7200
11SMn30	190	0.27	415	540	NA	7700

Table 9.3 Materials' properties

7C27Mo2

Especially the material of valves has to be carefully chosen because the valves have to withstand very challenging condition. Therefore the 7C27Mo2 (flapper valve steel) is used. Its properties were taken from Sandvik website. Tensile strength, elasticity modulus and yield strength were measured at 20 °C. The tensile strength is for sheet thickness 0.03 – 1.00 mm, elasticity modulus for sheet thickness 0.03 – 2.50 mm and yield strength for thickness 0.03 – 0.50 mm. [15][16]

The fatigue strength for reversed bending (mean stress = 0 MPa), when maximum sheet thickness is 0.60 mm and 5 % of specimens withstand minimum cycles 2 x 10^6 load cycles, is 750 MPa. Unfortunately, exact data for our required conditions are not available. Hence, after discussion with Emerson Climate Technologies employee, the fatigue strength 750 MPa was used. The value was also used previously by the company. The fatigue strength is considered as the corrected value. The temperature of CO_2 during working process is changeable and the temperature of valve is not known, thus 20°C abundant temperature is considered. Changes in cross section of valve are neglect. The fatigue strength is statistic value provided by material producer, thus, the assumptions do not cause big mistake. These assumptions give possibility to depict all testing conditions in one Haigh diagram. This helps to better understanding and illustration. [15][16]

9.2 CALCULATION OF IDEAL COOLING CIRCUIT

Because of an objective assessment, the original idealized cooling circuit with specified values was calculated. A compression and expansion were assumed to be adiabatic and flow through throttling device was isenthalpic. R744 thermodynamic properties are taken from source [43] and quantities are in accordance with Figure 9.3 and Figure 9.4.

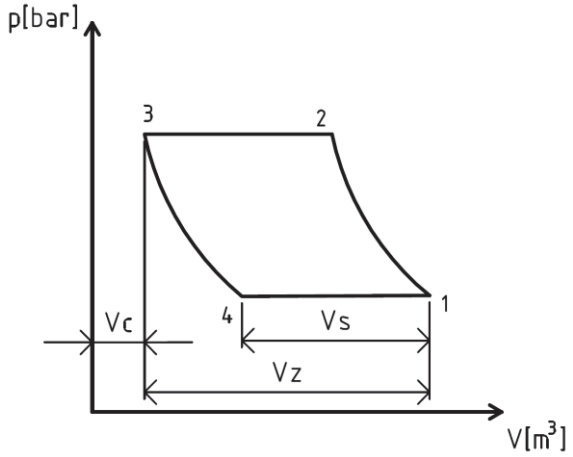

Figure 9.3 Compressor cycle – calculation

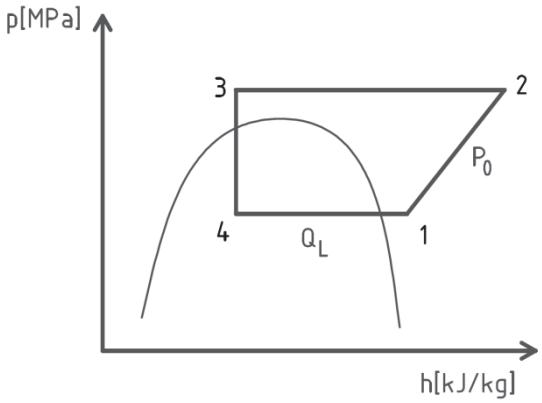

Figure 9.4 Cooling cycle – calculation

p_2 [bar]	p_1 [bar]	S_h [K]	D_b [mm]	$Vc=V_3$ [mm^3]	L [mm]	N [-]	F [Hz]	κ [-]	p_p [-]	t_3 [°C]
90	29	10	26	2,974	25	4	60	1.301	2	35

Table 9.4 Given calculated values

CALCULATION OF ORIGINAL COMPRESSOR

Number of shaft revolution per second *n*:

$$n_r = \frac{F}{p_p} = \frac{60}{2} = 30\ rps \tag{9.1}$$

Volume of all four cylinders (total swept volume) V_z:

$$V_z = \frac{\pi \cdot {D_b}^2}{4} \cdot L \cdot N = \frac{\pi \cdot 26^2}{4} \cdot 25 \cdot 4 = 53{,}092.9\ mm^3 \tag{9.2}$$

Total cylinders volume V_1 at the beginning of compression process:

$$V_1 = (V_z + V_c) = (53{,}092.9 + 2{,}974) = \ 56{,}066.9\ mm^3 \tag{9.3}$$

Volume V_4 at the beginning of compressor suction:

$$V_4 = \left(\frac{p_2 . {V_3}^{\kappa}}{p_1}\right)^{\frac{1}{\kappa}} = \left(\frac{90 \cdot 2{,}974^{1.301}}{29}\right)^{\frac{1}{1.301}} = 7{,}102.2\ mm^3 \tag{9.4}$$

Sucked volume V_s:

$$V_s = V_1 - V_4 = 56{,}066.9 - 7{,}102.2 = 48{,}964.7\ mm^3 \tag{9.5}$$

Volumetric efficiency η_v:

$$\eta_v = \frac{V_s}{V_z} = \frac{48{,}964.7}{53{,}092.9} = 0.92 \tag{9.6}$$

Transport efficiency assumption η_t:

$$\eta_t = \eta_v = 0.92 \tag{9.7}$$

Compressor displacement d:

$$d = V_z \cdot n \cdot \eta_t = 53{,}092.9 \cdot 30 \cdot 0.92 = 1{,}465.364 \cdot 10^3\ mm^3 \cdot s^{-1} \tag{9.8}$$

Compression ratio CR:

$$CR = \frac{V_1}{V_c} = \frac{56{,}066.9}{2{,}974} = 18.85 \tag{9.9}$$

Clearance volume V_c of the total volume V_1:

$$\frac{V_c}{V_1} \cdot 100 = \frac{2{,}974}{56{,}066.9} \cdot 100 = 5.30\ \% \tag{9.10}$$

COOLING CIRCUIT CALCULATION

Calculation is based on previous results.

Compressor power P_0:

$$P_0 = \frac{\kappa}{\kappa - 1} \cdot p_1 \cdot d \cdot \left(\left(\frac{p_2}{p_1} \right)^{\frac{\kappa - 1}{\kappa}} - 1 \right) =$$
$$= \frac{1.301}{1.301 - 1} \cdot 29 \cdot 10^5 \cdot 1{,}465.364 \cdot 10^{-6} \cdot \left(\left(\frac{90}{29} \right)^{\frac{1.301 - 1}{1.301}} - 1 \right) = 5{,}502\ W \tag{9.11}$$

Base on pressure p_1 and superheating 10 K

$$t_1 = 3.2\ °C \tag{9.12}$$

$$h_1(p_1; t_1) = 448.3\ kJ \cdot kg^{-1} \tag{9.13}$$

$$s_1(p_1; t_1) = 1.9353\ kJ \cdot kg^{-1} \cdot K^{-1} \tag{9.14}$$

Compression is adiabatic, hence

$$h_2(p_2; s_1) = 500.6\ kJ \cdot kg^{-1} \tag{9.15}$$

Mass flow rate $\dot{m}$:

$$\dot{m} = \frac{P_0}{h_2 - h_1} = \frac{5502}{(500.6 - 448.3) \cdot 10^3} = 0.105\ kg \cdot s^{-1} \tag{9.16}$$

The specific enthalpy on the condenser outlet h_3:

$$h_3(t_3; p_1) = 310\ kJ \cdot kg^{-1} \tag{9.17}$$

Since expansion in throttling device is considered to be isenthalpic

$$h_3 = h_4 = 310\ kJ \cdot kg^{-1} \tag{9.18}$$

Cooling capacity$\dot{Q}_L$:

$$\dot{Q}_L = \dot{m} \cdot (h_1 - h_4) = 0.105 \cdot (448.3 - 310) \cdot 10^3 = 14{,}521.5\ W \tag{9.19}$$

Coefficient of performance:

$$COP = \frac{\dot{Q}_L}{P_0} = \frac{14{,}521.5}{5{,}502} = 2.64 \tag{9.20}$$

	η_v [-]	$\dot{m}$ $[kg \cdot s^{-1}]$	$\dot{Q}_L$ [W]	P_0 [W]	COP [-]
Values based on measurements	0.74	0.082	12,211.5	6,754	1.81
Calculated values	0.92	0.105	14,521.5	5,502	2.64

Table 9.5 Comparison of calculated and measured data of the original compressor

10 NEW DESIGN

Base on previous analyses, it was decided to focus on a few main targets. These were increase of mass flow rate, decrease energy losses and achieve better cylinder filling. Therefore, following changes were suggested.

10.1 DESIGN CHANGES

During the analyses of the original compressor design, possibilities of changes of flow cross sectional areas of suction and discharge holes were observed. The original design has two discharge holes ($n_{OD} = 2$) with diameter ($D_{OD} = 4.70\ mm$), chamfers are not considered. Thus, the discharge cross sectional area S_{OD} is counted by following equation

$$S_{OD} = n_{OD} \cdot \frac{\pi \cdot D_{OD}^2}{4} = 2 \cdot \frac{\pi \cdot 4.70^2}{4} = 36.70\ mm^2 \tag{10.1}$$

The suction hole of the original valve is only one ($n_{OS} = 1$) with diameter ($D_{OS} = 8.00\ mm$), without chamfers. Thus, the suction cross sectional area S_{OS} is calculated by an equation (10.2).

$$S_{OS} = n_{OS} \cdot \frac{\pi \cdot D_{OS}^2}{4} = 1 \cdot \frac{\pi \cdot 8.00^2}{4} = 50.27\ mm^2 \tag{10.2}$$

The new valve plate design has discharge holes with same dimensions. However, the suction hole was changed significantly. Three suction holes into each cylinder were suggested. One is direct, normal to valve plate ($n_{NSD} = 1$), and two other holes are drilled at 65-degree angle to the valve plate ($n_{NSA} = 2$). A diameter D_{NSD}, of the direct hole without chamfers, is 5.00 mm. The angle holes create ellipses in the surface of the valve plate, hence the semi-minor axis b is equal to 2.30 mm and the semi-major axis a is equal to 2.54 mm (chamfers are not considered). Cross sectional area of suction holes S_{NS} is counted by following equation

$$\begin{aligned} S_{NS} &= n_{NSD} \cdot \frac{\pi \cdot D_{NSD}^2}{4} + n_{NSA} \cdot \pi \cdot a \cdot b = \\ &= 1 \cdot \frac{\pi \cdot 5^2}{4} + 2 \cdot \pi \cdot 2.54 \cdot 2.30 = 56.34\ mm^2 \end{aligned} \tag{10.3}$$

By comparison of the suction cross sectional areas can be seen that the new valve plate design has for 12.0 % larger suction cross sectional area than the original design.

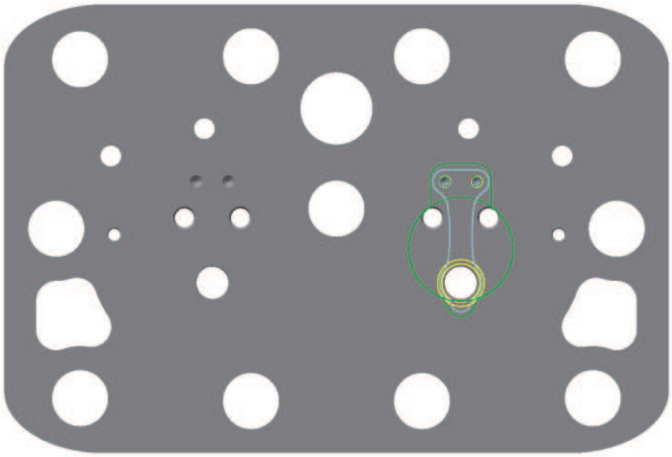

Figure 10.1 Original valve plate design

1. Suction valve; 2. Pins; 3. Discharge holes; 4. Cylinder bore; 5. Suction hole; 6. Suction valve seat; 7. Stopper

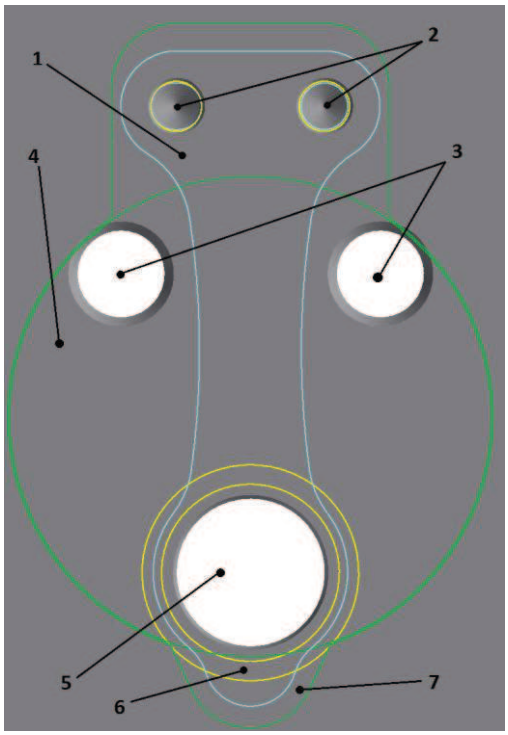

Figure 10.2 Detail of the original valve plate design

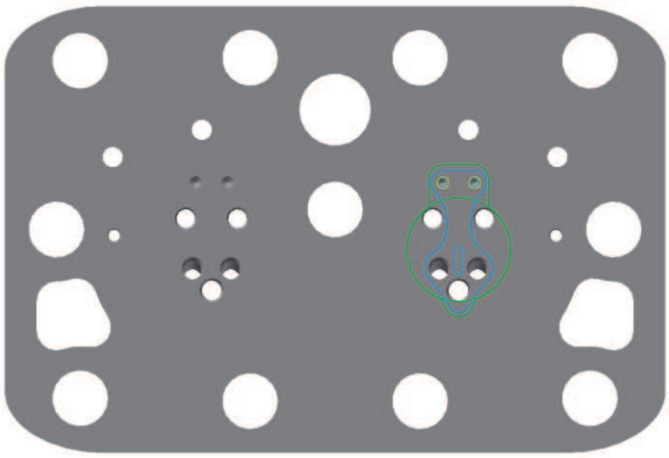

Figure 10.3 New valve plate design

1. Suction valve; 2. Pins; 3. Discharge holes; 4. Cylinder bore; 5. Suction hole; 6. Suction valve seat; 7. Stopper

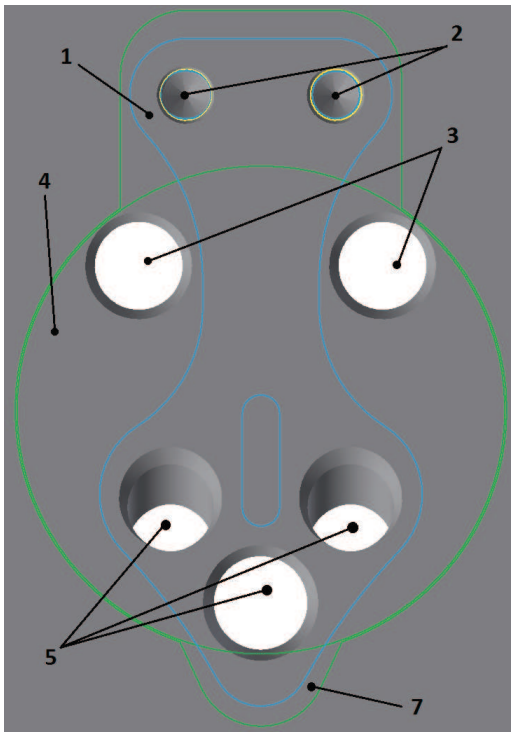

Figure 10.4 Detail of the new valve plate design

The other important design change is shifting of both discharge holes together with the whole discharge mechanism (stoppers, discharge valves and its attachment). Each of them was moved for 0.5 mm to the second one. Hence, the discharge holes are nearer for 1.0 mm to each other in compare to the original design. It was made to avoid an unwanted overlap of the compressor body over the discharge holes (Figure 10.2). A possible disadvantage of this adjustment is that the distance between the discharge valves was reduced to 3.81 mm at the narrowest point (Figure 10.5). The question is whether and how the two flows influence each other.

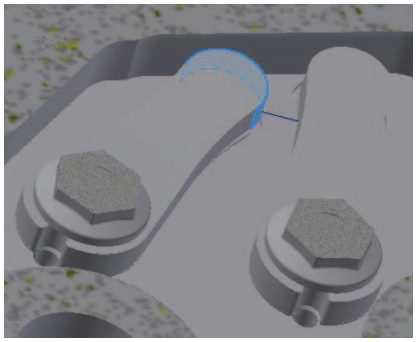

Figure 10.5 Detail of the discharge mechanism

The previous mentioned angle suction holes were made with the angle because of an effort to make cylinder filling more efficient. On the one hand, the direct hole is determined to fill mainly a space under the front part of suction valve, hence near to the stopper. On the other hand, angle holes should direct CO_2 flows to other side of the cylinder. In the Figure 10.6, can be seen the arrangement of all suction holes in valve plate in relation to the deflected suction valve (the depicted valve plate thickness is only 1 mm, the real designed valve plate thickness is 5.5 mm).

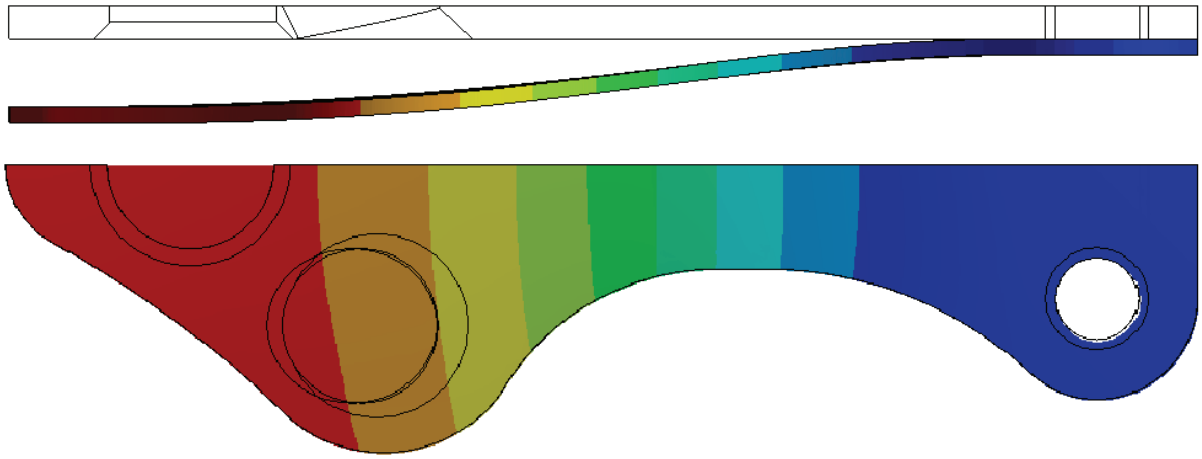

Figure 10.6 Relation between the suction holes and the deflected suction valve

For the efficient cylinder filling, shape of suction valve is also important. Base on this reason, two main suction valve designs were suggested. The first suction valve design is depicted in the Figure 10.7. The second valve design, the suction valve with a hole in between the suction channels, is illustrated in the Figure 10.8.

The hole of the second valve design increases cross sectional flowing area around the suction valve, hence smaller energy losses are expected. The smaller valve surface area also results in stress differences (chapter 10.2.2). When the original suction valve design was observed, a wear in edge regions, caused by refrigerant flow, was noticed. The new suggested valve plate design has larger cross sectional area of suction channels; therefore bigger mass flow is expected. The whole amount (bigger amount) of the gas has to pass around the valve, which could result in even increased wear in the edge regions. The suggested hole in the suction valve should redirect a specific amount of the gas from the edge regions to the middle of the

valve; hence the expected wear in the mentioned locations should be reduced. Finally, the hole in the suction valve creates another direction of flow.

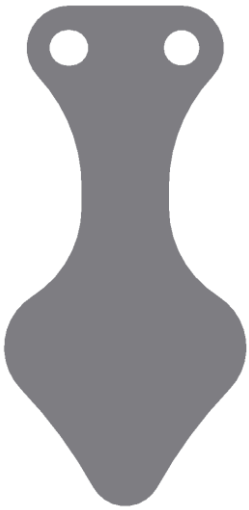

Figure 10.7 First suction valve design

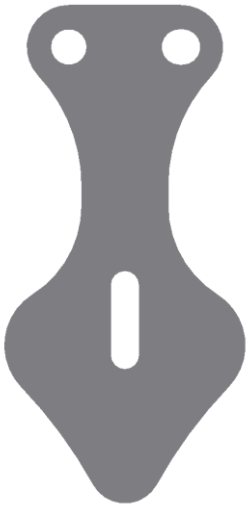

Figure 10.8 Second suction valve design

The second design has also some disadvantages. A possibility of vibration of edge regions because of stiffness reduction exists, this could be imagined as bird wings waving. If this occurs, the risk of significant valve life decreasing and leakages of pressurized gas to suction chamber would be possible. As another disadvantage, multiple valve opening and closing during one cycle can be mentioned. This can be caused by pressure equalization in cylinder (close to valve) and in suction chamber. The hole in suction valve increases this likelihood, because it enables faster passing of bigger mass flow around the valve. Thus, the piston motion does not have to create pressure difference fast enough. The last influence of the hole is increasing of clearance volume. If it is assumed that clearance volume of one cylinder of the original compressor design is same as clearance volume of the new compressor design with suction valve without hole (743.5 mm^3). It can be counted that the hole causes increase of "dead volume" for 0.9 %. The volume of the valve hole is 6.6 mm^3. Hence the clearance volume increase is very small and can be neglect.

Technical drawings of all modified parts, namely suction valve design one, suction valve design two, valve plate and piston are in annexes

10.2 FATIGUE LIFE

Final evaluation of fatigue life comes from static structure analysis performed in ANSYS Workbench. The objective of the simulation was to achieve a total deformation and equivalent stress during suction and discharge processes during the highest loading.

10.2.1 STATIC STRUCTURE ANALYSIS

For reaching of reasonable solving time the tested assembly was simplified by symmetry and also by a size reduction of the valve plate and the body. The valve plate was replaced by a solid body with size of contact surface between the valve plate and the suction valve. Instead of whole compressor body, two extracted solids made of contact surfaces of the body and the suction valve were used. All these decisions were considered to have not any impact on simulation results.

In the first step of simulation the defining of used materials was necessary. The materials properties are mentioned in chapter 9.1. Subsequently model assembly (Figure 10.9), made in Autodesk Inventor Professional, was loaded as tested geometry. The both suction valve designs were simulated for valve thickness 0.48 mm and 0.52 mm. The required manufacturing thickness was 0.50 ± 0.02 mm. The geometry was modified (divided) for purpose of better mesh quality and the suction valve was remodelled to a midsurface.

Prior to the structural simulation, a few assumptions were made. The assembly was modelled in such a way that production tolerance differences cause the highest stresses of the suction valve and the spring form was assumed to be squeezed into plane, hence was not bended. The next important decision was related to pressure or exactly to CO_2 flow and location, on which the carbon dioxide flow should be applied. This question could be solved by fluid flow simulation, however, in this case was assumed that the pressure made by CO_2 flow affects whole surface of the suction valve except areas around pins with size of the spring. This led to the highest force according to pressure definition. When pressure is constant and affected area increases the force has to also rise. These all assumptions were used for suction process as well as for discharge process.

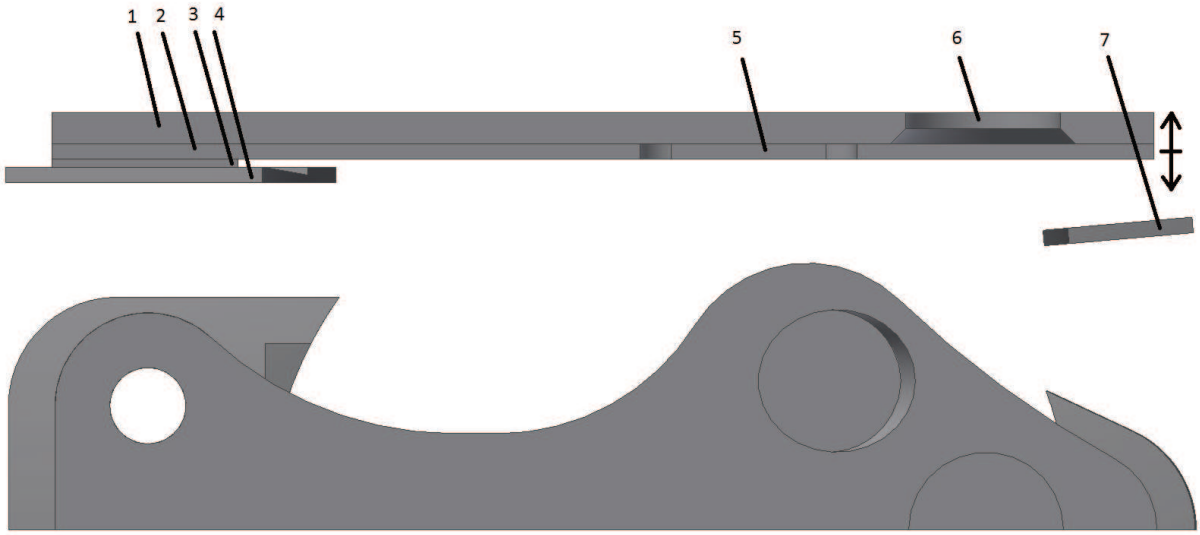

Figure 10.9 Model of the assembly

The next procedure was devoted to connections, parts properties, meshing and loading. Stiffness behaviour of the valve plate, the body and the stopper were defined as rigid. The suction valve and the spring were set to be flexible. Then materials were assigned to individual components and symmetry regions were defined.

CONNECTIONS

- Contact between the suction valve and the stopper.
  The contact type was frictional with friction coefficient 0.16. The contact body surface was a front part of the suction valve (marked by number 1) and a target consisted of two stopper faces (labeled by number 2). The shell thickness effect was defined. Behaviour was set to asymmetric, used formulation was Augmented Lagrange and normal stiffness was updated each iteration. 3.5 mm pinball radius was

used. Time step control was set up as Automatic Bisection. Offset 0 mm was applied with no ramping effect.

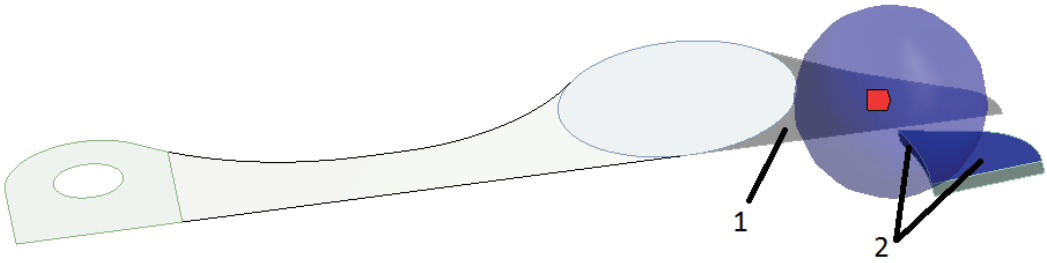

Figure 10.10 Contact between the suction valve and the stopper

- Contact between the suction valve and the spring.
  Contact was set up in same manner as the previous contact only behaviour was symmetric and pinball radius had value of 0.1 mm. The number one labels the contact part of the suction valve and the number two marks the spring.

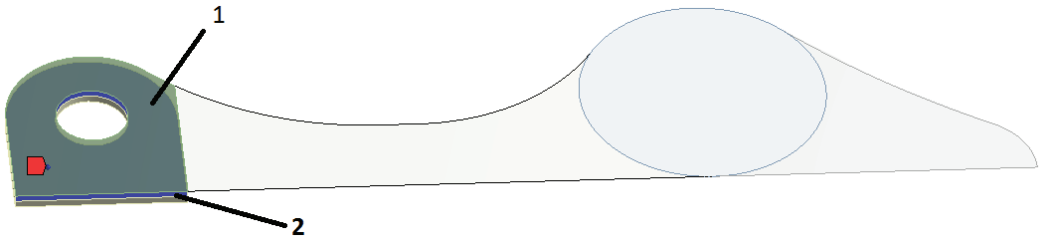

Figure 10.11 Contact between the suction valve and the spring

- Contact between the valve plate and the suction valve
  The contact was set identically to the first contact except pinball radius, which was equal to 0.3 mm. The number one labels the valve plate and the number two labels the suction valve.

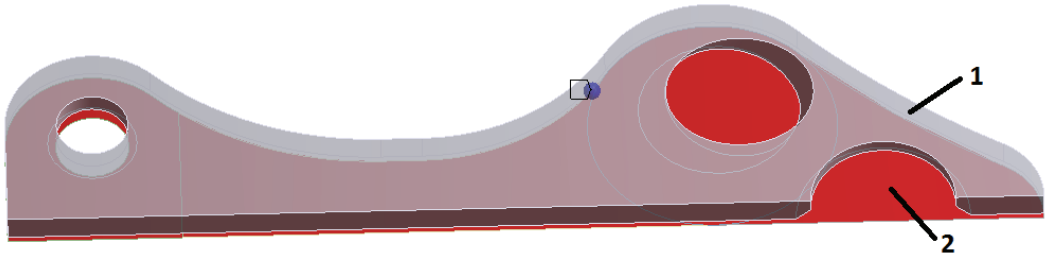

Figure 10.12 Contact between the valve plate and the suction valve

- Contact between the body and the spring
  The contact type was defined as the bonded contact with calculating formulation Augmented Lagrange and Pinball radius 0.1 mm. The body is labelled by the number one and spring by the number two.

Figure 10.13 Contact between the body and the spring

MESH

- The sizing of valve plate had value 0.15 mm, method used was Quadrilateral Dominant and free face mesh type were changed to All quad. Mesh had 1,597 elements and 5,176 nodes.

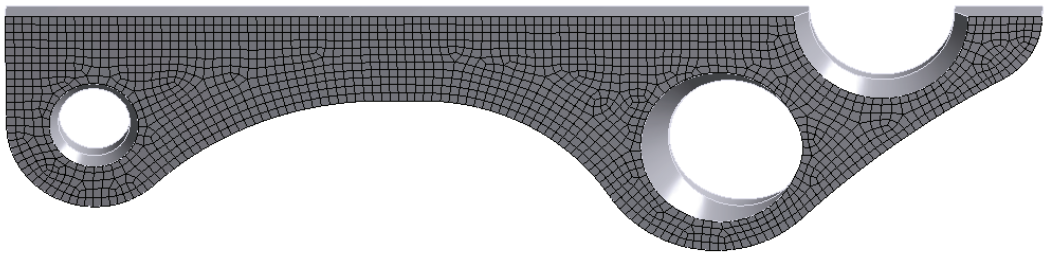

Figure 10.14 Mesh of the valve plate

- Stopper contact faces had size elements 0.2 mm with free face mesh type All quad. Other body contact area had size element 0.3 mm. All contact body surfaces together had 1,138 elements and 3,649 nodes.

Figure 10.15 Mesh of the body parts

- The mesh of the spring was performed again only on contact surfaces. The element size was 0.3 mm and meshing method was stated as automatic with all quadratic elements. The number of elements was 404 and the number of nodes 3,088.

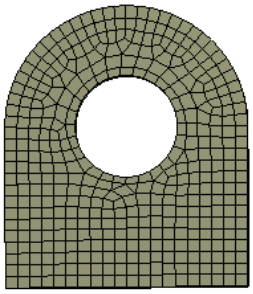

Figure 10.16 Mesh of the spring

- The most important part was valve plate, which also had the biggest number of nodes and elements, thus, the mesh was the most accurate. The component consists of 9,228 elements with 9,535 nodes. Average element quality was 94.05 %. The meshing method was Quadrilateral Dominant with all quadratic elements. The part was divided into three surfaces, which changed a way of element creating.

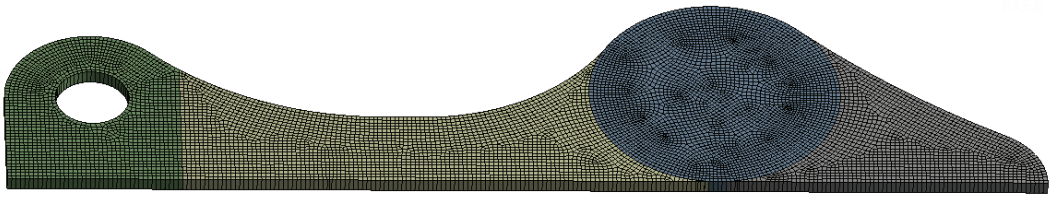

Figure 10.17 Mesh of the suction valve

Whole assembly had 21,448 nodes and 12,367 elements. The mesh quality is seen in the following figure.

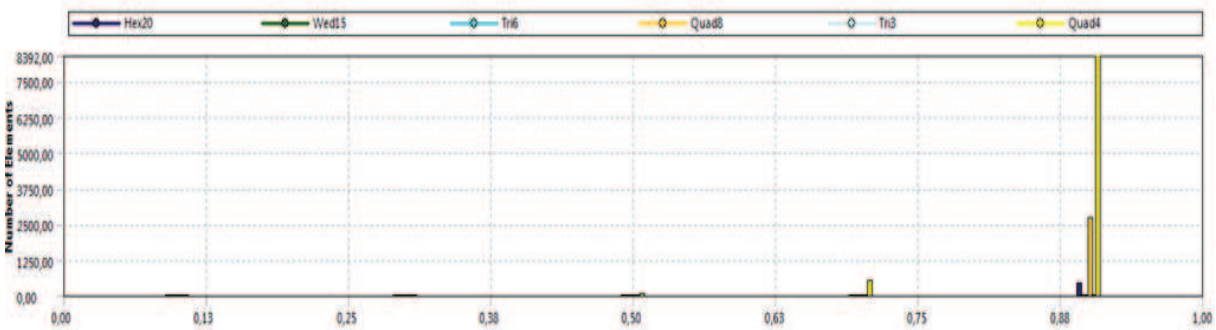

Figure 10.18 Mesh quality of the whole assembly

BOUNDARY CONDITIONS

The remote displacements without any DOF were applied at all rigid bodies.

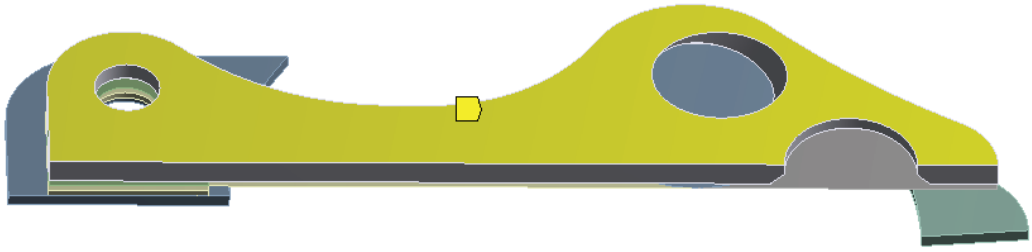

Figure 10.19 Remote displacement at the valve plate

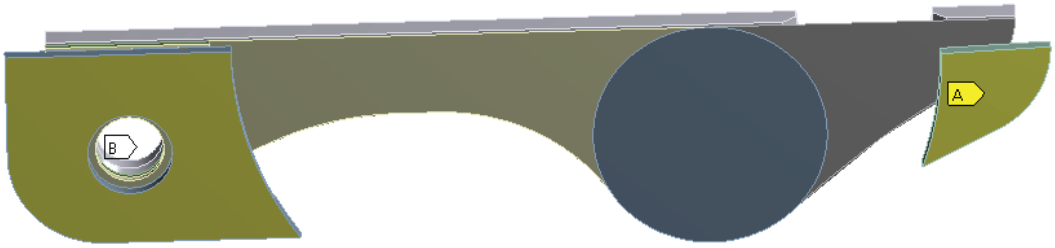

Figure 10.20 Remote displacement at the body parts

The fixed support was defined on suction valve in a place of pin.

Figure 10.21 Fixed support at the suction valve

LOADING CONDITIONS

Pressure differs depends on a process. During the suction process the maximum pressure, applied on suction valve from the side of valve plate, was 0.28269 MPa. In case of the discharge process the pressure maximum was 9.9491 MPa, this was applied in the opposite direction in compare with the suction process. Both these values were taken from measured data, which were provided by Emerson Climate Technologies.

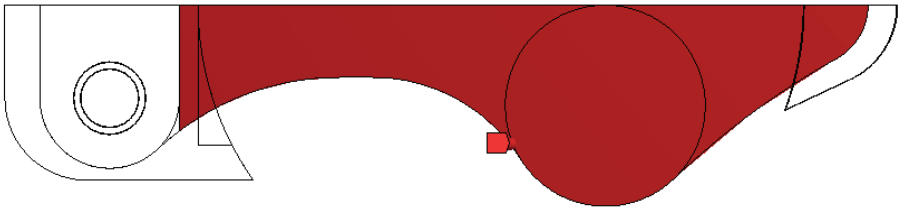

Figure 10.22 Loading condition

If it is spoken only about discharge process, the stopper was suppressed. Hence one contact was dropped out, number of elements and nodes decreased.

10.2.2 FATIGUE LIFE EVALUATION

This chapter is devoted to the static structure analysis data processing. The output of this chapter was critical for the prototype manufacturing, and so some of the simulations results with screenshots are depicted here.

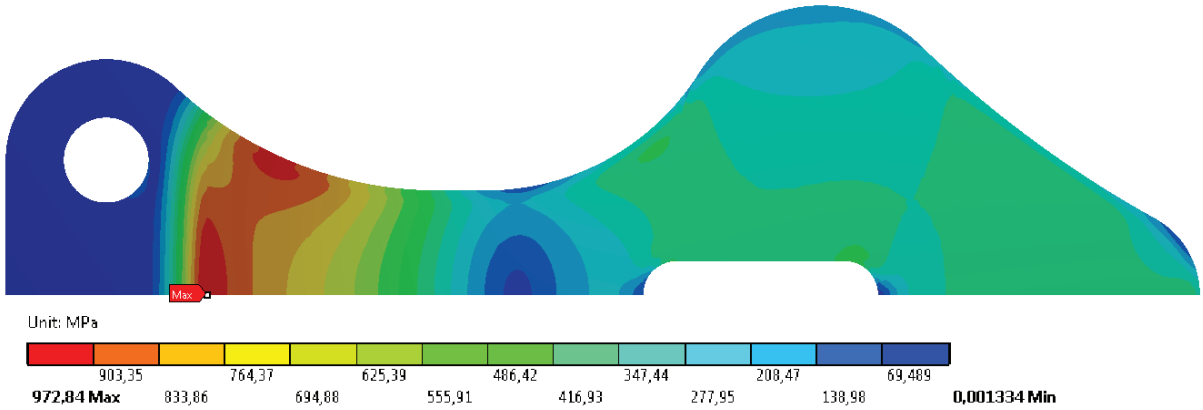

Figure 10.23 Equivalent stress of the second suction valve design during the suction process, thickness 0.48 mm (Case D)

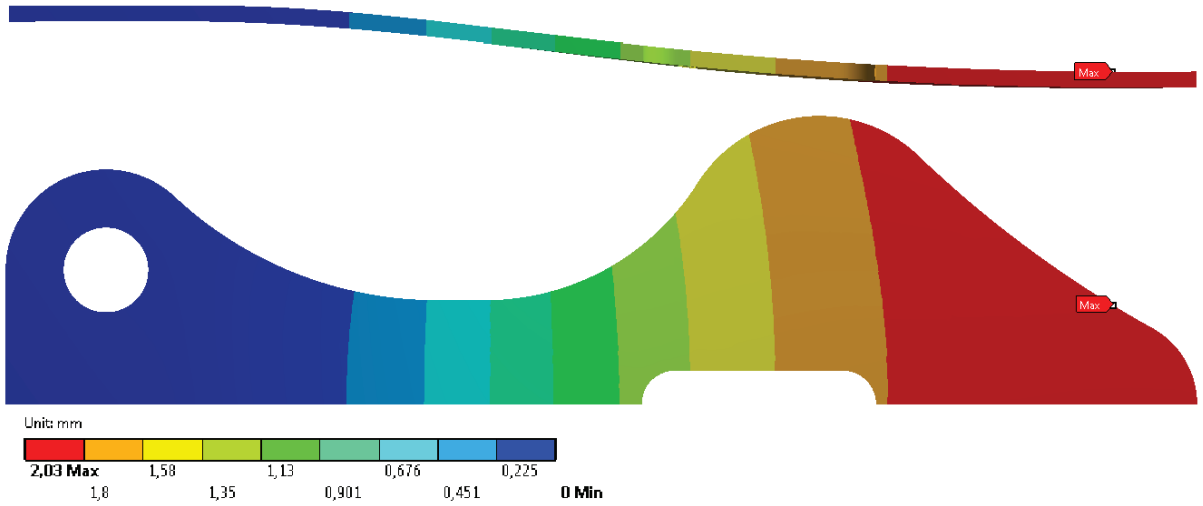

Figure 10.24 Deformation of the second suction valve design during the suction process, thickness 0.48 mm (Case D)

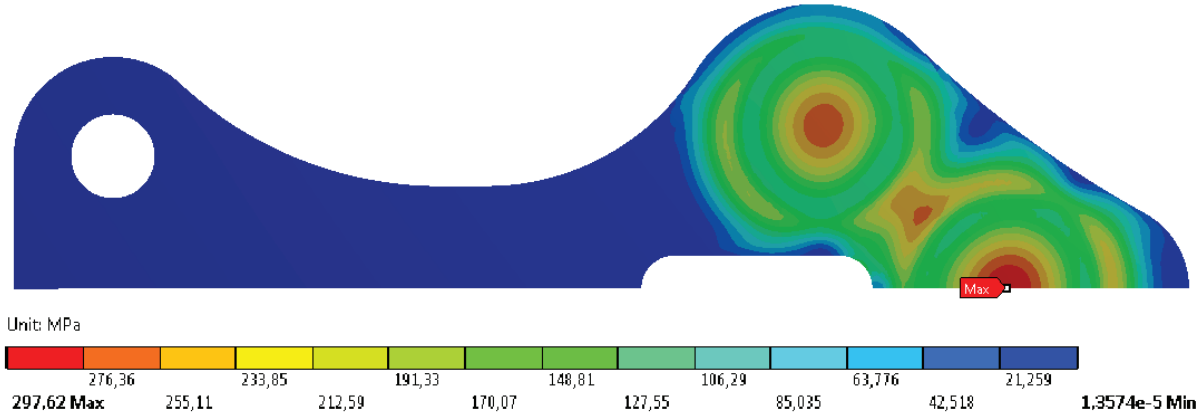

Figure 10.25 Equivalent stress of the second suction valve design during the discharge process, thickness 0.48 mm (Case D)

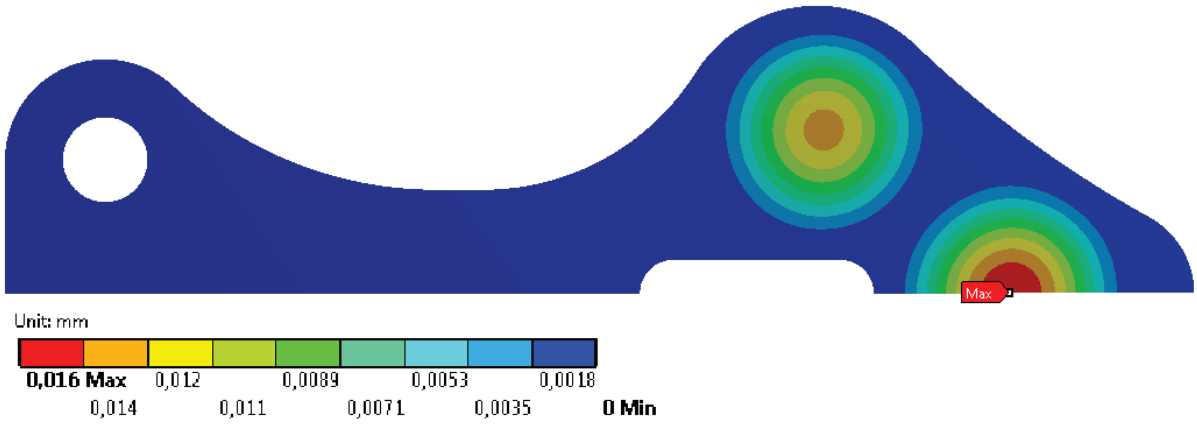

Figure 10.26 Deformation of the second suction valve design during the discharge process, thickness 0.48 mm (Case D)

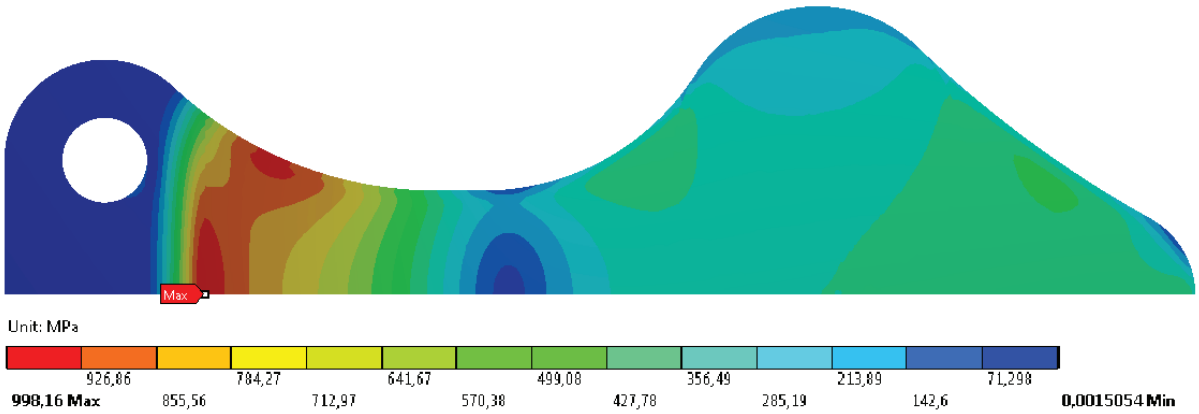

Figure 10.27 Equivalent stress of the first suction valve design during the suction process, thickness 0.48 mm (Case B)

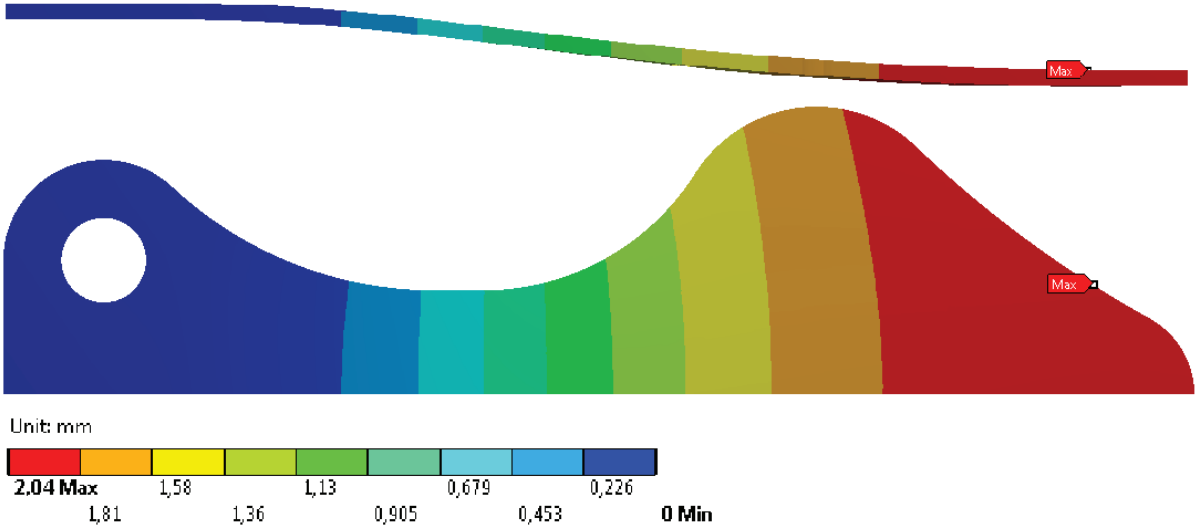

Figure 10.28 Deformation of the first suction valve design during the suction process, thickness 0.48 mm (Case B)

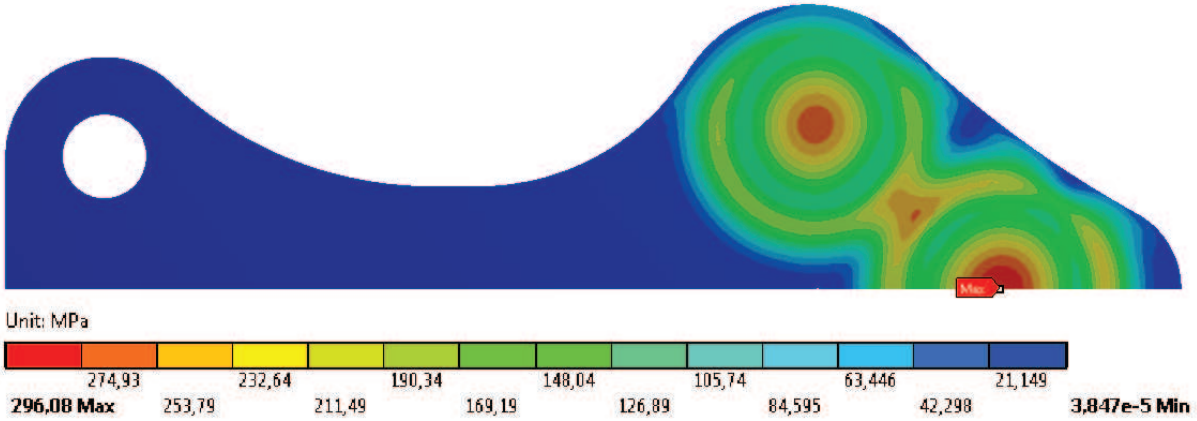

Figure 10.29 Equivalent stress of the first suction valve design during the discharge process, thickness 0.48 mm (Case B)

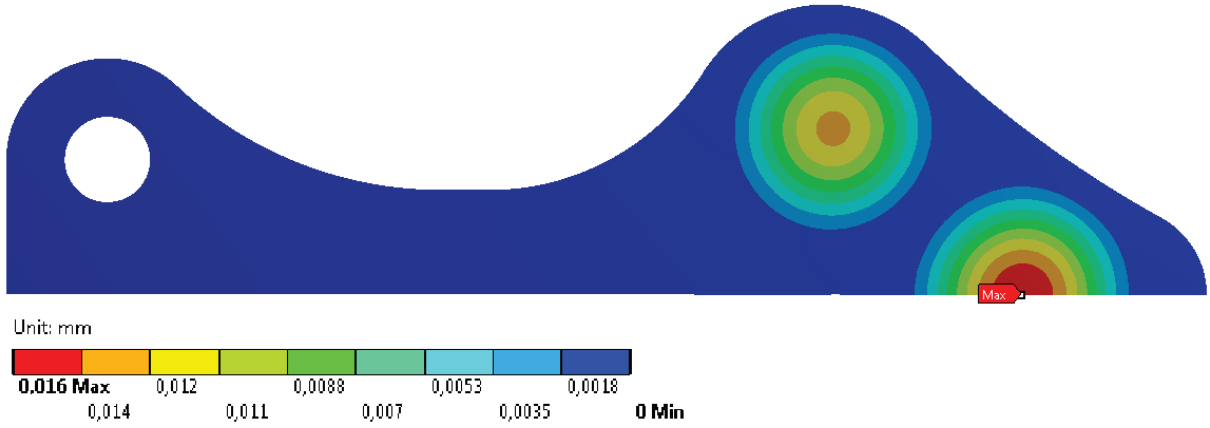

Figure 10.30 Deformation of the first suction valve design during the discharge process, thickness 0.48 mm (Case B)

The first step of data processing was taken in Matlab, where the equivalent stress values of each node during the suction and discharge process were loaded and paired together according its node number, therefore it was necessary to ensure that node numbers during the suction process are same as during the discharge process. From these values of von-Mises stress fatigue factor of safety n_f, according Goodman criterion, and yield factor of safety n_y were calculated (Figure 10.32). Used equations are mentioned in chapter 6. Both types of safety factors for each node were higher than 1. The lowest fatigue factor of safety had value 1.060 and the lowest safety factor to yield was 1.340. Both these numbers appeared in case B in location labelled with triangle (Figure 10.31). Overall, it is seen that the most prone location to fatigue damage and also to elastic deformation is the place labelled by the triangle. Stress differences caused by thickness and design can be observed from Table 10.1 to Table 10.4. The effect of thickness is, however, bigger than effect of the suction valve design. Von-Mises stress differences are about from 70 to 95 MPa when suction valve are compared by its thickness. Stress differences according suction valve type differ for about 20 MPa.

Observed locations are depicted in the Figure 10.31. The simulated equivalent stress values together with the safety factors describing the loading of the suction valves in these locations are in Table 10.1 up to Table 10.4. All locations were chosen according simulation result. The location labelled with triangle had the highest von-Mises stress during inlet process. The rhombus tags the location where the highest stress values of the original suction valve design were observed. The circle and square marked the locations where suction holes in the valve plate are situated. The highest von-Mises stress during the discharge process where observed in the location labelled with the square sign. The cross sign tags the location with the highest equivalent stress on the suction valve hole, the hole was presupposed as a place with potentially high notch equivalent stress.

Figure 10.31 Places of interest at the suction valve

Units	Loc. 1	Loc. 2	Loc. 3	Loc. 4	Loc. 5
Suction stress [MPa]	902.88	872.59	–	341.80	241.45
Discharge stress [MPa]	-2.12	-1.82	–	-257.90	-233.67
Sa [MPa]	452.50	437.20	–	299.85	237.56
Sm [MPa]	450.38	435.39	–	41.95	3.89
nf – fatigue factor of safety [-]	1.17	1.21	–	2.36	3.14
ny – yield factor of safety [-]	1.44	1.49	–	3.80	5.38

Table 10.1 Suction valve design one, thickness 0.52 (Case A)

Units	Loc. 1	Loc. 2	Loc. 3	Loc. 4	Loc. 5
Suction stress [MPa]	998.16	949.83	–	413.14	298.51
Discharge stress [MPa]	-2.32	-1.98	–	-296.08	-267.35
Sa [MPa]	500.24	475.91	–	354.61	282.93
Sm [MPa]	497.92	473.92	–	58.53	15.58
nf – fatigue factor of safety [-]	1.06	1.11	–	1.98	2.59
ny – yield factor of safety [-]	1.30	1.37	–	3.15	4.35

Table 10.2 Suction valve design one, thickness 0.48 (Case B)

Units	Loc. 1	Loc. 2	Loc. 3	Loc. 4	Loc. 5
Suction stress [MPa]	881.26	853.15	432.83	323.41	249.55
Discharge stress [MPa]	-2.17	-1.91	-83.78	-259.36	-238.12
Sa [MPa]	441.71	427.53	258.30	291.39	243.84
Sm [MPa]	439.55	425.62	174.53	32.03	5.72
nf – fatigue factor of safety [-]	1.20	1.24	2.27	2.46	3.05
ny – yield factor of safety [-]	1.48	1.52	3.00	4.02	5.21

Table 10.3 Suction valve design two, thickness 0.52 (Case C)

Units	Loc. 1	Loc. 2	Loc. 3	Loc. 4	Loc. 5
Suction stress [MPa]	972.84	927.93	530.77	389.13	308.00
Discharge stress [MPa]	-2.38	-1.53	-88.42	-297.62	-272.06
Sa [MPa]	487.61	464.73	309.60	343.38	290.03
Sm [MPa]	485.23	463.20	221.17	45.76	17.97
nf – fatigue factor of safety [-]	1.09	1.14	1.87	2.07	2.52
ny – yield factor of safety [-]	1.34	1.40	2.45	3.34	4.22

Table 10.4 Suction valve design two, thickness 0.48 (Case D)

These all data are also represented in graphic form (Figure 10.32). The data are compared with the Langer and the Modified Goodman criteria.

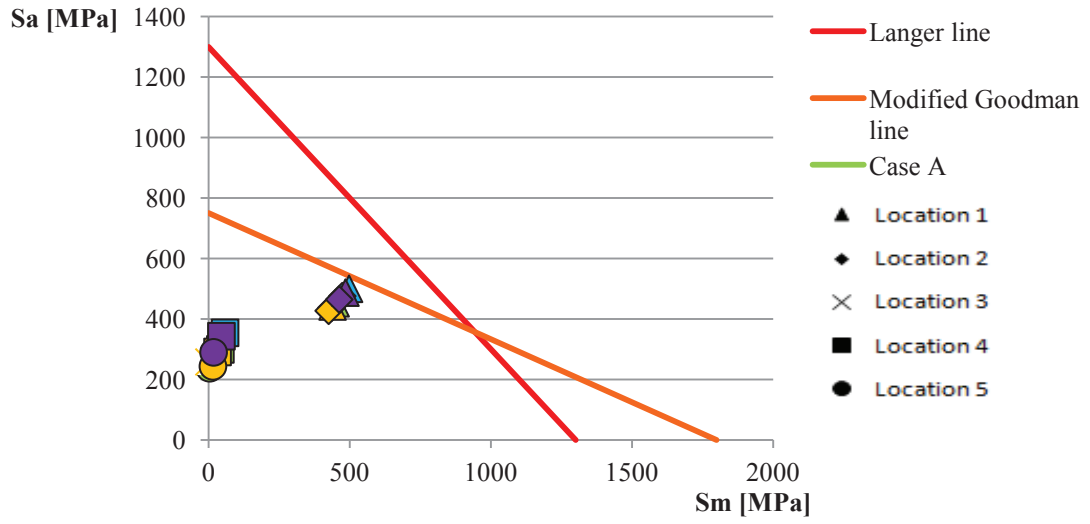

Figure 10.32 Haigh diagram the new suction valves

10.3 MODAL ANALYSIS

The modal analysis was performed for both types of designed suction valves and its thicknesses 0.48 mm and 0.52 mm in ANSYS WB.

It is not going to be described the valve mesh and the boundary conditions so deeply as in the case of previous mentioned static structural analysis. Neither symmetry nor mid-surface option was applied this time. The analysis was not computational expensive and non-use of symmetry allowed good depiction of mode shapes. The only uploaded component, into ANSYS WB, was the analyzed suction valve. Other components (spring, valve plate, stoppers, and pins) were not taken directly into account.

As the boundary conditions only the fix support was used at locations of the pins (Figure 10.33). A role of spring was neglect since its stiffness is very low. The mentioned fix support was evaluated as the suitable boundary condition for determining the natural frequencies of the valves.

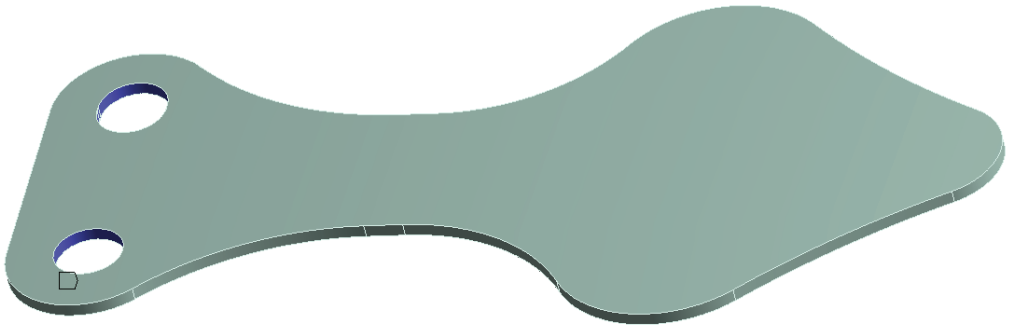

Figure 10.33 Boundary condition of the suction valve – fix support at the pins

Mode No.	Natural Frequency, Hz		Mode shape	Comment
	0.48 mm	0.52 mm		
1	375.37	406.18		In plane deformation
2	1,700.8	1,834.3		Out of plane deformation
3	2,820	3,047.8		Out of plane deformation

4	5,441.3	5,441.5		In plane deformation
5	7,607	8,217.5		Out of plane deformation
6	10,884	11,770		Out of plane deformation
7	13,523	14,614		Out of plane deformation
8	14,711	15,896		Out of plane deformation
9	18,633	20,096		Out of plane deformation
10	23,623	25,483		Out of plane deformation

Table 10.5 Natural frequencies of the suction valve design one

Mode No.	Natural Frequency, Hz		Mode shape	Comment
	0.48 mm	0.52 mm		
1	380.18	411.68		In plane deformation
2	1,663	1,797.1		Out of plane deformation
3	2,778.1	3,006		Out of plane deformation
4	5,380.5	5,380.6		In plane deformation
5	7,333.5	7,931.8		Out of plane deformation
6	10,275	11,112		Out of plane deformation
7	11,933	12,908		Out of plane deformation

8	14,306	15,471		Out of plane deformation
9	18,343	19,819		Out of plane deformation
10	23,405	25,298		Out of plane deformation

Table 10.6 Natural frequencies of the suction valve design two

The requirement was that the determined natural frequencies cannot be equal to compressor rotor speed. The compressor works in mains frequency range 25-70 Hz. The rotor frequency differs not only by dependence on the mains frequency but also by dependence on required power, thus on working point in a compressor envelope. For the frequency changes a variable-frequency drive is employed. The compressor is driven by asynchronous motor with four poles. It is also known that the compressor rotor speed is 1,450 rpm when mains frequency is 50 Hz. By using of equation (10.4) a stator electrical speed n_s is reckon.

$$n_s = \frac{F}{p_p} = \frac{50}{2} = 25\ rps => 1{,}500\ rpm \tag{10.4}$$

where F is mains frequency and p_p is number of pole pairs.
By an equation (10.5) is calculated a motor slip s_z.

$$s_z = \frac{n_s - n_r}{n_s} \cdot 100 = \frac{1{,}500 - 1{,}450}{1{,}500} \cdot 100 = 3.33\ \% \tag{10.5}$$

The slip is marked by s, n_r is mechanical rotor speed. The counted slip value was further used for calculation of a rotor speed according the whole used mains frequency range. Despite the reality, the slip differences were neglect.

Mechanical rotor speed for slip 3.33%			
Mains frequency [Hz]	25	50	70
Mechanical rotor speed [rps]	12.083	24.167	33.833
Mechanical rotor speed [rpm]	725	1450	2030

Table 10.7 Mechanical rotor speed

Values in Table 10.7 are calculated by applying equations (10.4 and (10.5). By comparing natural frequencies of valves (Table 10.5, Table 10.6) with mechanical rotor speed in rps (Table 10.7) it can be stated that the resonance is not going to occur.

10.4 CFD ANALYSIS

CFX was chosen for performing CFD simulation. The purpose of this analysis was to determine a refrigerant flow through suction channels. Only the refrigerant flow around the first suction valve design was simulated, since laboratory measurements of both designs were already known. The second suction valve design does not exhibit any improvements in compare to the suction valve without hole.

For the CFD simulation definition, it was decided to use results of the static structural simulation. Therefore positions of suction valve midline elements, after deformation by maximum pressure difference, were exported. According to these elements positions, 0.50 mm thick deformed suction valve was modelled. Then an assembly of the valve plate and the deformed suction valve was made in Inventor (Figure 10.34). It is necessary to mention that exact sizes of the cylinder were not used, only and solely sizes of valve plate, suction valve and a distance between suction holes and a partition separating suction and discharge chambers are exact.

The fluid body was defined as CO_2 ideal gas. The simulation is not time dependent and flow is isothermal at 25°C. Turbulence model was set to k-Epsilon. This model is suitable for $Re \geq$ 200,000, however, it is not recommended for flow along curvilinear bodies. [46]

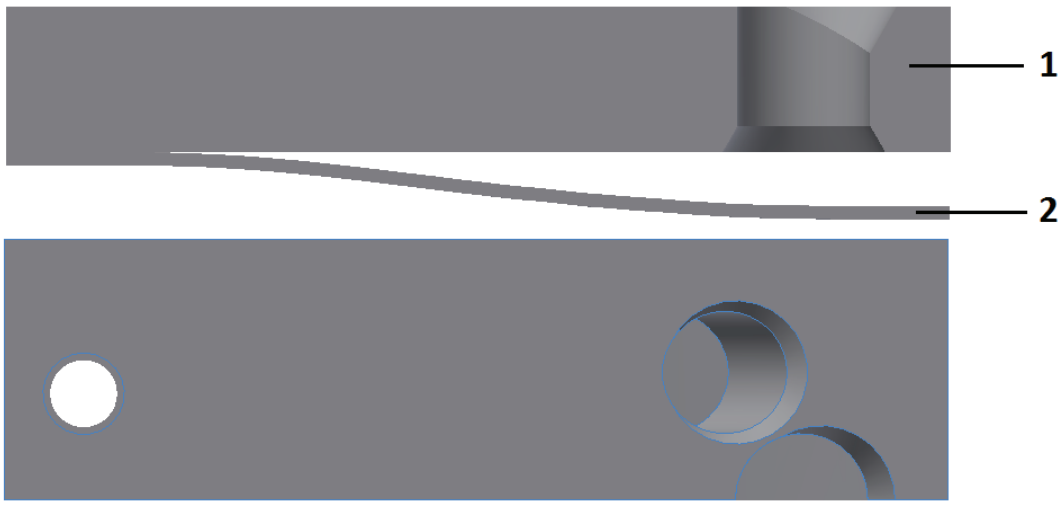

Figure 10.34 Assembly of the valve plate and the deformed suction valve

MESH

The assembly was imported into ANSYS WB and fluid body was created. During the CFD simulation preparation, model symmetry was used. The used mesh method was Hex Dominant, element size 0.4 mm (Figure 10.35).

Figure 10.35 Fluid body mesh

BOUNDARY CONDITIONS

An inlet marked by inlet arrows was set as subsonic flow regime with static pressure 2.551 MPa with zero gradient flow direction and turbulence zero gradient. An outlet marked by outlet arrows was set also to subsonic flow regime with static pressure 2.268 MPa. This pressure condition corresponds to the suction process simulated previously. The symmetry region is marked by red signs (Figure 10.36, Figure 10.37). The wall was set to be no slip wall, which means zero fluid velocity in an immediate near to a wall, and the wall roughness was assumed to be same around whole wall boundary condition. Sand grain roughness ε was set to 4.6904 μm. This was calculated from an equation (10.6). Ra0.8 is manufacturing roughness of suction holes. [41]

$$\varepsilon = 5.863 \cdot Ra = 5.863 \cdot 0.8 = 4.6904\ \mu m \tag{10.6}$$

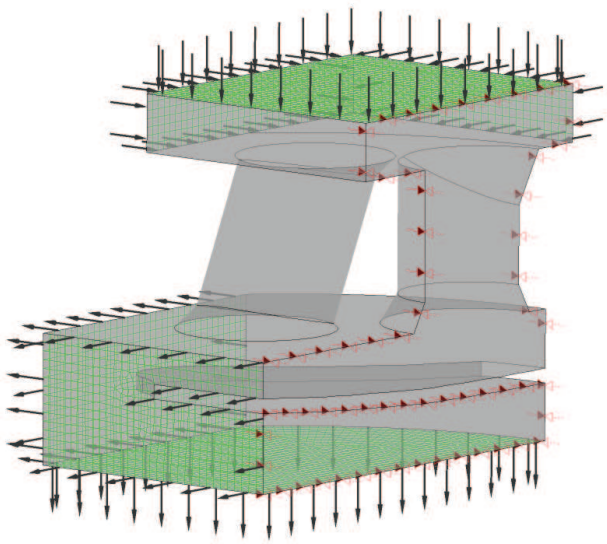

Figure 10.36 Inlet and outlet boundary conditions

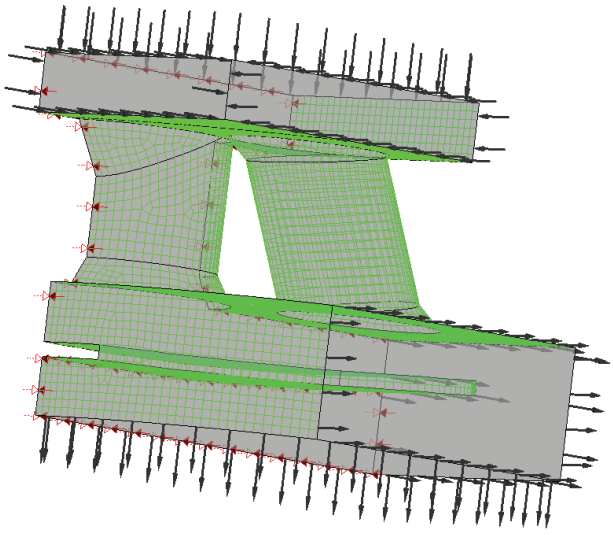

Figure 10.37 Wall boundary condition

SIMULATION RESULTS

The judged quantity is velocity, which is seen in the pictures (Figure 10.38 up to Figure 10.45). The velocity gives an option to observe flow direction as well as its magnitude, because of that, vortexes can be seen. Velocity also influences energy dissipation by friction and can be indicator of a wear. A coordinate system and a model miniature, for better orientation, are depicted in the following pictures.

Firstly, the angle hole was observed. It can be seen that the angle of the hole fulfils its expected function; hence it directs the refrigerant flow to the right side (Figure 10.38). However, the angle showed to have also some disadvantages. The flow tents to make vertex at the outlet left side of the hole (Figure 10.39). The direction has to be changed for more than 90° there, which leads to energy loose. Second disadvantage does not showed up much. On the right side of the hole, in the middle of the flow trajectory through the valve plate, decrease of velocity is observed. The decrease would be much higher, if the distance between the angle hole and the partition separating suction and discharge chamber would be bigger. The bigger the distance, the bigger area of velocity decrease occurs, and so smaller flow area. If the partition would be further than in our case, the flow at the inlet of the hole would go horizontally and would have to turn over 90°. The refrigerant flow goes vertically at the inlet of the hole in the presented case (Figure 10.38).

Despite that the modelled cylinder diameter is not exact, the cylinder wall would be nearer to the suction valve, a tendency to create vertex can be seen at a cylinder top corner (Figure 10.39). This decreases flow area around the suction valve. It can be expected that with exact diameter the flow area would be even smaller.

The influence of the direct hole to the angle hole can be observed in the Figure 10.40. A part of the refrigerant flow turns to the left at the left top corner. The Figure 10.43 shows that the flow is directed mainly to side of the cylinder, hence on the other side from direct hole.

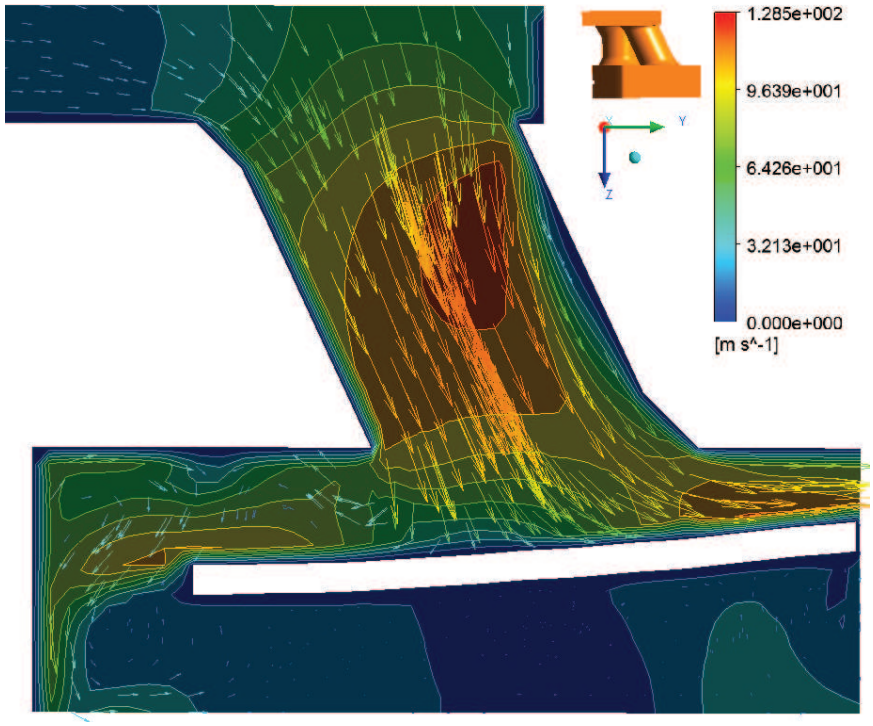

Figure 10.38 Flow velocity in the angle suction hole (YZ)

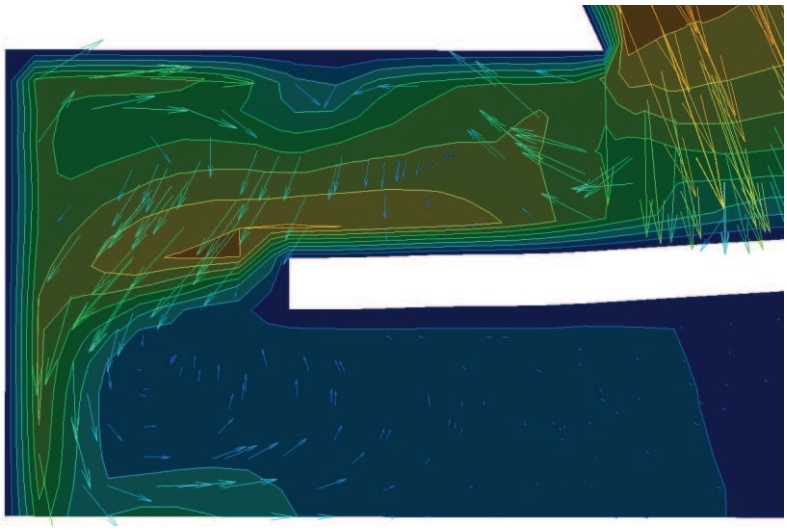

Figure 10.39 Flow velocity in the angle suction hole – detail1(YZ)

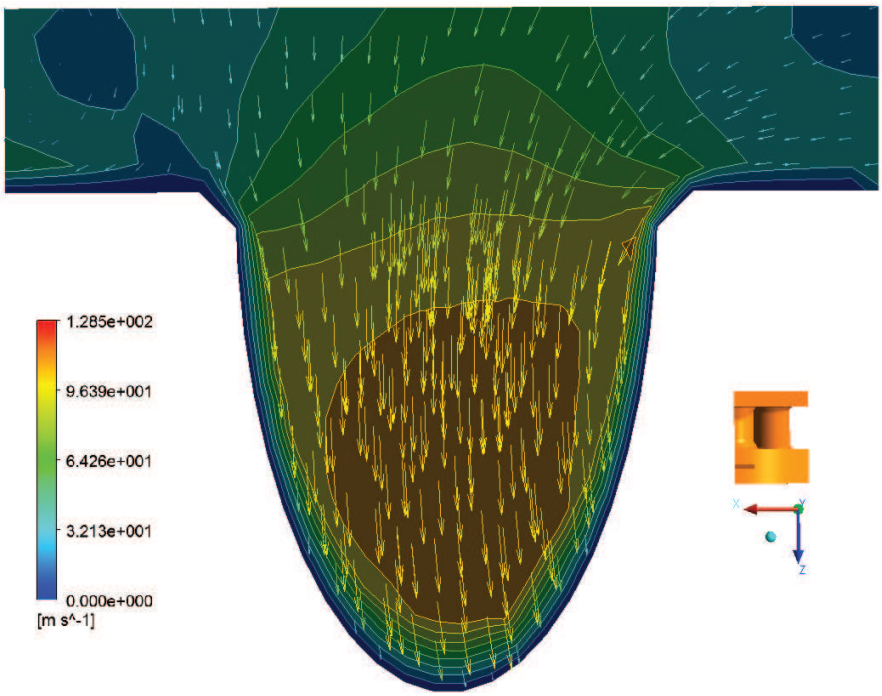

Figure 10.40 Flow velocity in the angle suction hole – inlet (XZ)

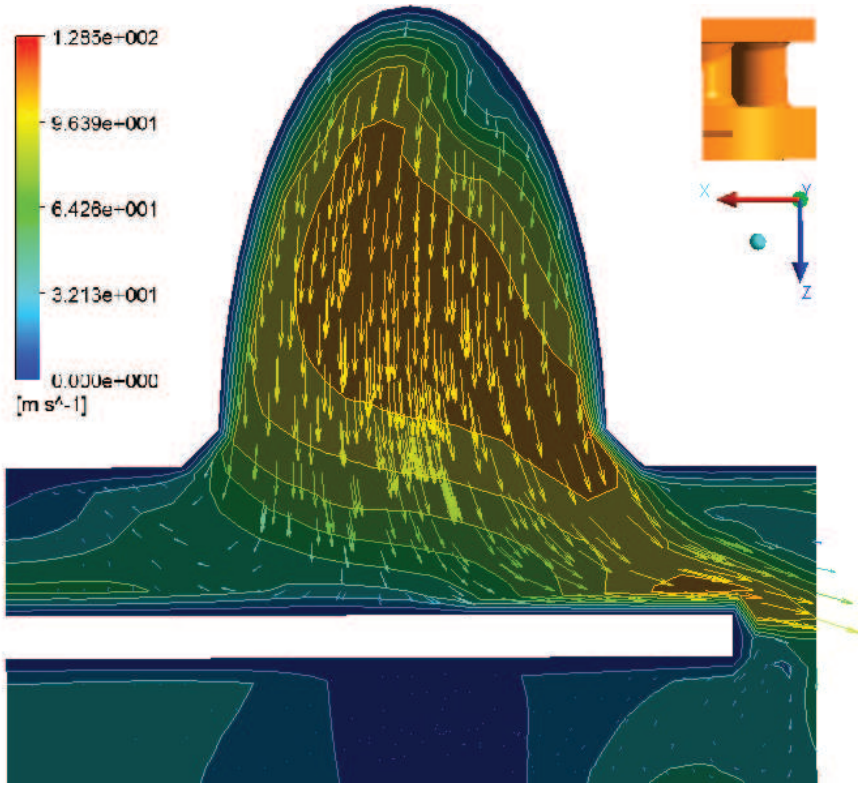

Figure 10.41 Flow velocity in the angle suction hole – outlet (XZ)

Secondly, the refrigerant flow in the direct hole was observed. The Figure 10.42 shows a difference between chamfered edge and not chamfered edge. Refrigerant flow is unsatisfactory at right side of the hole inlet. An inconvenient design of chamfer is also seen at the right side of the hole outlet, which leads to creation of a pocket (Figure 10.43), where velocity is equal to zero, hence the volume there is not used and cross-sectional flow area is decreased. At the other side of the hole outlet, vertexes appear (Figure 10.44). Despite that the stopper is not modelled in this location, similar flow behaviour could be expected in real. Figure 10.45 shows that CO_2 flows to a side of suction valve, which supports convenience of angle hole using, and so using of holes, which are not in a one row.

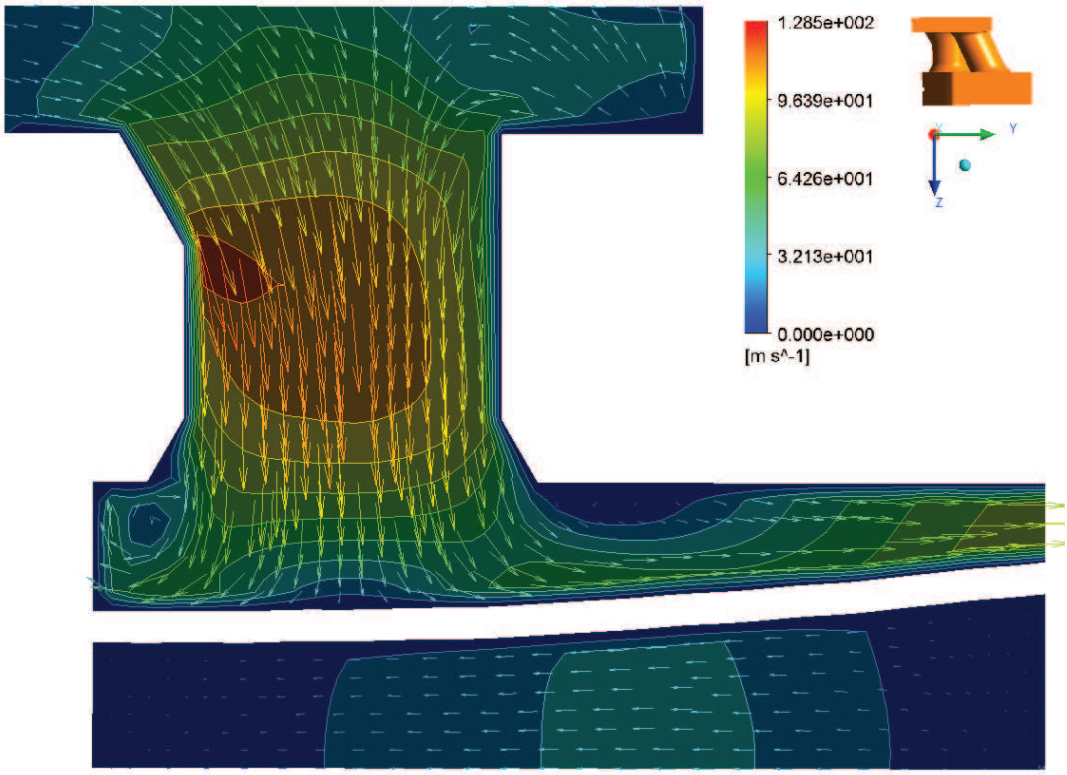

Figure 10.42 Flow velocity in the direct suction hole (YZ)

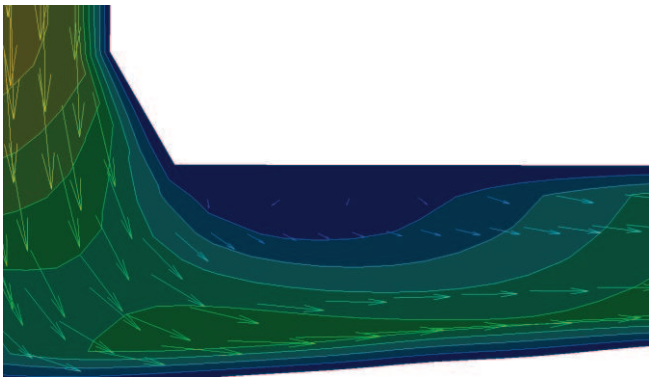

Figure 10.43 Flow velocity in the direct suction hole – detail1(YZ)

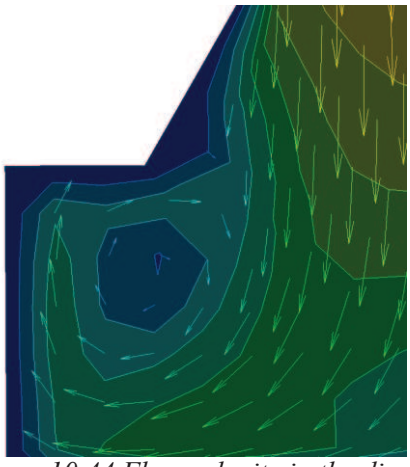

Figure 10.44 Flow velocity in the direct suction hole – detail2 (YZ)

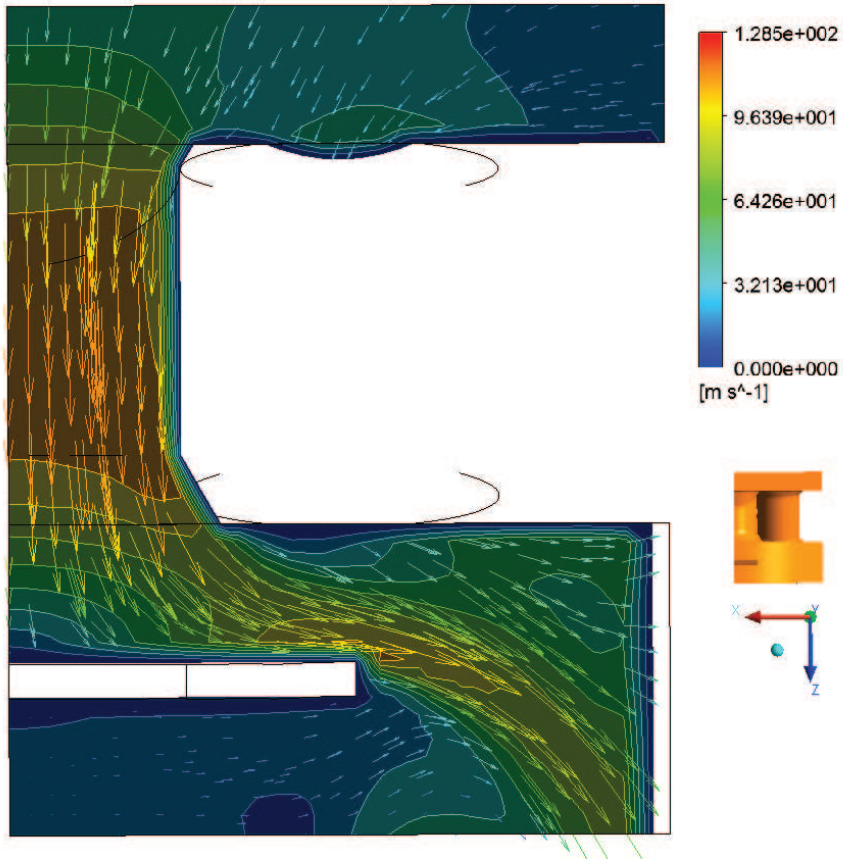

Figure 10.45 Flow velocity in the direct suction hole (XZ)

10.5 EVALUATION

The new designs where tested in laboratory of Emerson Climate Technologies in Mikulov. The method used is described in chapter 8.

Firstly, the original compressor design was tested in order to obtain comparative data. Then the new valve plate assemblies were installed in the same compressor. The first test ran with the first suction valves design (Table 10.8). By an examination of the data it can be seen that *COP* was increased differently according tested location in compressor working envelope. The second finding is that power tends to decrease but change in one percent is not significant and can be considered as a measurement error. According expectations, mass flow rate became also higher.

Tested conditions	m_f [%]	η_{vol} [%]	η_{is} [%]	P [%]	Q_0 [%]	COP [%]
A	2.54	3.5	3.6	-0.1	3.5	3.6
B	1.49	1.3	2.1	-0.6	1.3	2.1
HCR	4.66	3.9	3.7	0.1	3.9	3.7
MDP	2.22	2.4	2.8	-0.4	2.4	2.8
HL	3.76	1.7	2.5	-0.7	1.7	2.5
HDF	0.71	0.8	1.9	-1.0	0.8	1.9
LL	0.45	0.3	0.4	-0.1	0.3	0.4
A	2.45	1.8	1.3	0.5	1.8	1.3

Table 10.8 The original design versus the first design

The second test was performed in the same manner as the previous one. Only the valve plate assembly was changed for the one, which had the second suction valve design. Unfortunately, after an observing of measured data, it has to be stated that the design is not successful (Table 10.9). The *COP* changes were up to one percent in compare to the design number one, and so were considered as measurement errors.

Tested conditions	m_f [%]	η_{vol} [%]	η_{is} [%]	P [%]	Q_0 [%]	COP [%]
A	1.33	0.7	1.2	-0.4	0.7	1.2
B	-0.16	0.1	0.2	-0.1	0.1	0.2
HCR	-0.26	0.3	0.7	-0.3	0.3	0.7
MDP	0.74	0.9	0.9	0.0	0.9	0.9
HL	-0.72	0.5	0.6	-0.1	0.5	0.6
HDF	-0.27	0.2	-0.2	0.4	0.2	-0.2
LL	0.41	0.4	0.5	-0.1	0.4	0.5
A	0.75	1.1	0.8	0.3	1.1	0.8

Table 10.9 The second suction valve design versus the first suction valve design

11 RECOMMENDATIONS AND POSSIBILITIES OF FURTHER DEVELOPMENT

During compressor analyzes few development ideas arose and some design possibilities for adjustment were found. Some of them would be highly recommended to consider. Their application could raise an efficiency of the compressor.

- The first one relates to gas flow into the suction chamber. How it can be seen in the Figure 11.1, the cylinder head overlap a suction channel in valve plate. According to original design drawings 002-0441-00 (cylinder head) and 003-1562-00 (valve plate) the difference is 1.17 mm. The same difference can be calculated also from the new design of the valve plate K003-003-A107-00. From my point of view an adjustment of cylinder head is the most suitable way. If valve plate would be modified, the body would have to be also readjusted.

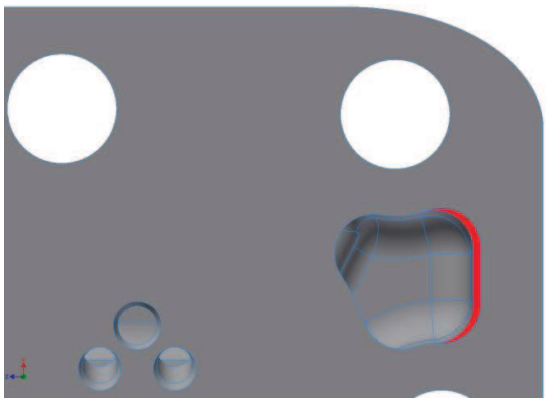

Figure 11.1 Overlap of the cylinder head over the valve plate

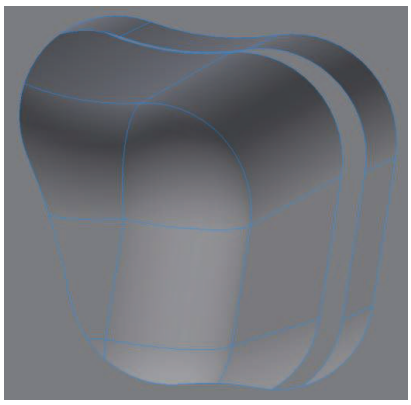

Figure 11.2 Overlap of the cylinder head over the valve plate – detail

- Two other suction valve designs and valve plate design were considered (Figure 11.3 up to Figure 11.6). These design solutions would allow greater variableness of suction holes positions and sizes. Also the direction of suction holes can be changed. Even a discharge cross sectional area would be increased if it would be needed. The depicted valve plate (Figure 11.3 and Figure 11.5, both valve plate are same) has the discharge cross sectional area for 7.88 % bigger and suction cross sectional are for 18.50 % bigger than the original valve plate design. However, the suitability of these designs would be dependent on further calculations and observations. The disadvantage would be that more compressor parts would have to be modified. Specifically the body, discharge valve, suction valve, retainer, valve plate, attachment of discharge system and probably also design of gaskets. The change in a number of discharge channels would lead to smaller discharge edge length, which can cause worse empting of a cylinder.

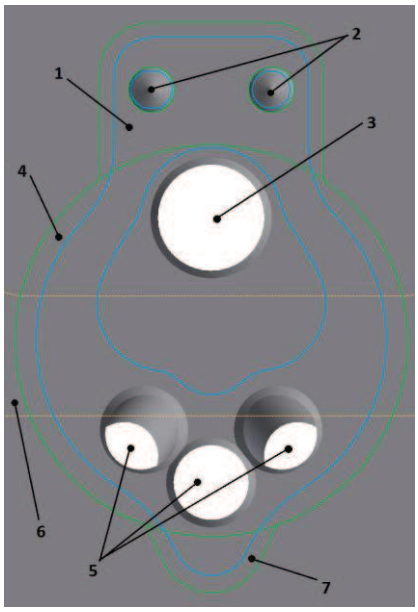

Figure 11.3 Suggestion number three

1. Suction valve; 2. Holes for pins; 3. Discharge hole; 4. Cylinder bore; 5. Suction holes; 6. Partition separating suction and discharge chamber; 7. Stopper of suction valve.

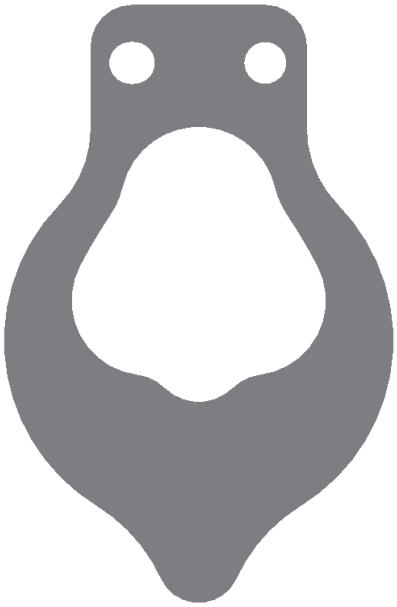

Figure 11.4 Third suction valve design

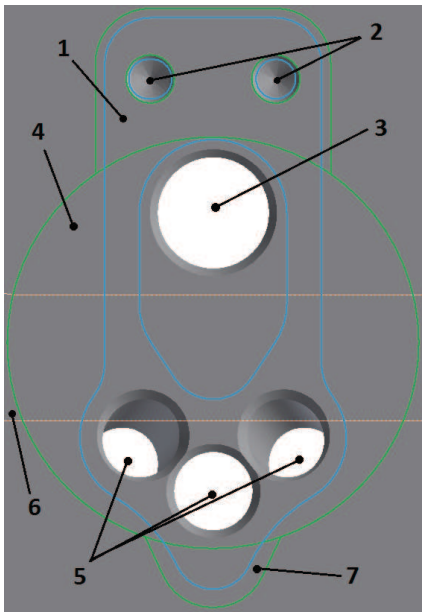

Figure 11.5 Suggestion number four

1. Suction valve; 2. Holes for pins; 3. Discharge hole; 4. Cylinder bore; 5. Suction holes; 6. Partition separating suction and discharge chamber; 7. Stopper of suction valve.

Figure 11.6 Fourth suction valve design

For a purpose of a possibility of further development of the fourth suction valve design static structural analysis in ANSYS WB was performed. The analysis had very similar setting to analysis in chapter (10.2.1). The analysed suction valve thickness was 0.48 mm and only maximum suction load was simulated. The simulation result was shown to be comparable to the previous simulation of the suction valves design one and design two (Figure 11.7). The maximum calculated equivalent stress was 942 MPa. Hence, any consideration of a further development of design four, and in my opinion of the other design (design number three), seems to be reasonable.

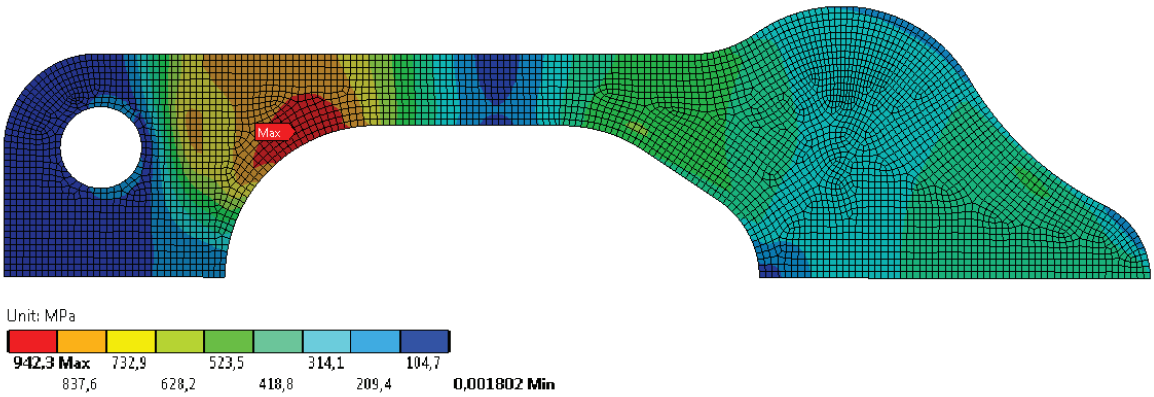

Figure 11.7 Static structural simulation of the fourth suction valve design

CONCLUSION

The aim of this diploma thesis was to increase *COP* of reciprocating compressor for R744 refrigerant from Emerson Climate Technologies. This should be achieved by modifying of valve plate assembly.

In a first step, an analysis of an original compressor design was preformed. Based on provided drawings, 3D model were made and analyzed. A reason of this action was to clarify compressor function, to find possibility for mechanism changes and to determine imperfections if any.

After data and the model analyzing, it was decided to focus on energy losses reduction, mass flow rate increase and improvement of a cylinder filling. This resulted in a few valves and valve plate designs, which were evaluated especially according to time requirements. Base on that time criteria two designs were chosen and their expected advantages and disadvantages were discussed. The chosen designs were focused solely on suction valve and suction channels modifying. The two chosen types differentiate form each other by suction valve design; the design number two has a hole in its body in compare to the design number one, which has not. All suggested designs were characteristic by increasing of suction holes flow area and by not perpendicular direction of suction holes. The designs, which were not chosen (design number three and four), however, were considered to have a potential for further development, are mentioned in the last chapter.

The designs, which were designated for a prototype manufacturing, were tested in ANSYS WB. Simplified models were subjected to a static structural analysis and then accordingly adjusted in the manner they fulfilled life requirements. A subsequent modal analysis provided suction valve natural frequencies, which were compared with a rotor speed, not any damage risk was determined. For a purpose of a flow understanding and possible further development, also very simplified CFD analysis was performed in ANSYS CFX. This simulation determined few unwanted vortices that would be appropriate to remove. Simulation boundary conditions were made base on compressor p-V diagrams, which were measured in a laboratory at the original compressor.

In the final step, design drawings were made and prototypes were manufactured. These were then tested in Emerson laboratory in Mikulov. The tests were performed base on standards EN 13771-1 and EN 12900. The obtained results were compared to the original design. *COP* of the first design increases, in compare to the original design, according to working compressor conditions from 0.4 % to 3.7 %. The second design, in compare to the first suggested design, had *COP* values from -0.2 % to 1.2 %, according compressor working condition. Base on the results it can be stated that the compressor development has been relatively successful and that the both designs have same effect on *COP*. The measured *COP* increase of the second design is considered to be in an interval of measurement error.

In my opinion this work can serve solid base for further development, which can be, however, still very time consuming. I would further recommend to elaborate possibilities of the design three and four and to make a FEA modelling of the whole compressor working process. The good results of the valve plate assembly development, and so this diploma thesis, is highlighted by the fact that Emerson Climate Technologies started process of considering patent protection for this submitted invention.

REFERENCES

[1] Ezine articles. In: JAKUBOWSKI, Nick. *Beginning of Air Compressors* [online]. 2012 [cit. 2014-10-18]. Dostupné z: http://ezinearticles.com/?Beginning-of-Air-Compressors&id=6836158

[2] Compressed Air History. *ECompressedair* [online]. © 2014 [cit. 2014-10-18]. Dostupné z: http://www.ecompressedair.com/library-pages/compressed-air-history.aspx

[3] SVAZ CHLADÍCÍ A KLIMATIZAČNÍ TECHNIKY. *Chladící a klimatizační technika*. 1. vyd. Praha, 2012, 181 s.

[4] Scroll Principles of Operation. *Air Squared* [online]. © 2006-2012 [cit. 2014-10-18]. Dostupné z: http://airsquared.com/scroll-technology/principles#!lightbox/0/

[5] DINÇER, İbrahim a Mehmet KANOGLU. *Refrigeration systems and applications*. 2nd ed. Chichester, West Sussex, U.K.: Wiley, 2010, xvi, 464 p. ISBN 04-707-4740-4.

[6] KHEMANI, Haresh. Hermetically Sealed Refrigeration Compressors. *Bright Hub Engineering* [online]. 2009, 10/12/2009 [cit. 2014-10-19]. Dostupné z: http://www.brighthubengineering.com/hvac/52198-hermetically-sealed-refrigeration-compressors/

[7] Gas compressor. In: *Wikipedia: the free encyclopedia* [online]. San Francisco (CA): Wikimedia Foundation, 2001-2014, 1 September 2014 [cit. 2014-10-19]. Dostupné z: http://en.wikipedia.org/wiki/Gas_compressor#Hermetically_sealed.2C_open.2C_or_semi-hermetic

[8] United Nations Environment Programme - Montreal Protocol. *The Montreal Protocol on Substances that Deplete the Ozone Layer* [online]. © 2010 - 2011 [cit. 2015-02-13]. Dostupné z: http://ozone.unep.org/new_site/en/montreal_protocol.php

[9] Swedish Environmental Protection Agency. *Swedish Pollutant Release and Transfer Register - Perfluorocarbons (PFCs)* [online]. 2009-10-16 [cit. 2015-02-13]. Dostupné z: http://utslappisiffror.naturvardsverket.se/en/substances/greenhouse-gases/perfluorocarbons/¨

[10] Zeotropic mixture. In: *Wikipedia: the free encyclopedia* [online]. San Francisco (CA): Wikimedia Foundation, 2001-, 19 June 2014 [cit. 2015-02-14]. Dostupné z: http://en.wikipedia.org/wiki/Zeotropic_mixture#mediaviewer/File:VLE_of_a_Zeotropic_Mixture.png

[11] TUHOVČÁK, J. CFD simulace proudění chladiva semihermetickým kompresorem. Brno: Vysoké učení technické v Brně,Fakultastrojního inženýrství, 2012. 88s.Vedoucí diplomovépráce doc. Ing. Jaroslav Katolický, Ph.D.

[12] Azeotrope. In: *Wikipedia: the free encyclopedia* [online]. San Francisco (CA): Wikimedia Foundation, 2001-, 28 January 2015 [cit. 2015-02-14]. Dostupné z: http://en.wikipedia.org/wiki/Azeotrope#mediaviewer/File:PositiveAzeotropePhaseDiagram.png

[13] SHIGLEY, Joseph Edward, Charles R MISCHKE a Richard G BUDYNAS. *Mechanical engineering design*. 7th ed. New York, NY: McGraw-Hill, 2004, xxv, 1030 p. ISBN 0072520361.

[14] *Metal Fatigue and Endurance* [online]. 2013, 06/03/2013 [cit. 2015-03-02]. Dostupné z: http://www.roymech.co.uk/Useful_Tables/Fatigue/FAT_Mod_factors.html

[15] Sandvik 7C27Mo2 flapper valve steel. *Sandvik* [online]. 2014, 2014-12-18 [cit. 2015-03-04]. Dostupné z: http://www.smt.sandvik.com/en/materials-center/material-datasheets/strip-steel/sandvik-7c27mo2-flapper-valve-steel/

[16] Sandvik Chromflex. *Sandvik* [online]. 2012, 2012-08-02 [cit. 2015-03-04]. Dostupné z: http://www.smt.sandvik.com/en/materials-center/material-datasheets/strip-steel/sandvik-chromflex/

[17] Piston compressors. *Wiki-ref.com* [online]. Copyright 2009 - 2013 [cit. 2015-03-08]. Dostupné z: http://www.ref-wiki.com/content/view/31467/28/

[18] Reciprocating Compressor Basics. *MACHINERY LUBRICATION* [online]. 2005 [cit. 2015-03-08]. Dostupné z: http://www.machinerylubrication.com/Read/775/reciprocating-compressor

[19] *2.FEA and Ansys* [online]. 3.12.2001 [cit. 2015-03-19]. Dostupné z: http://www.fem.unicamp.br/~lafer/im437/Cap01.pdf

[20] MADENCI, Erdogan a Ibrahim GUVEN. *The finite element method and applications in engineering using ANSYS* [online]. New York: Springer, c2006 [cit. 2015-03-19]. ISBN 0-387-28289-0. Dostupné z: http://www.springer.com/cda/content/document/cda_downloaddocument/9780387282893-c2.pdf?SGWID=0-0-45-418420-p74053407

[21] *ANSYS Modeling and Meshing Guide* [online]. 2005 [cit. 2015-03-20]. Dostupné z: http://www.ewp.rpi.edu/hartford/users/papers/engr/ernesto/hillb2/MEP/Other/Articles/MeshingGuide.pdf

[22] *ANSYS Meshing User's Guide* [online]. 2013 [cit. 2015-03-20]. Dostupné z: http://148.204.81.206/Ansys/150/ANSYS%20Meshing%20Users%20Guide.pdf

[23] *ANSYS Mechanical ANSYS Mechanical Structural Nonlinearities: Introduction to Contact* [online]. 2010 [cit. 2015-03-21]. Dostupné z: http://inside.mines.edu/~apetrell/ENME442/Labs/1301_ENME442_lab6_lecture.pdf

[24] Mechanical Engineering. *FEA* [online]. 2013 [cit. 2015-03-21]. Dostupné z: https://sites.google.com/site/mechanicalengineeringforlife/FEA

[25] GUILLAUME, Patrick. Vrije Universiteit Brussel. In: *MODAL ANALYSIS* [online]. 2012 [cit. 2015-03-30]. Dostupné z: http://mech.vub.ac.be/avrg/publications/ModalAnalysis.pdf

[26] [EDITORS, Cornelia A. *Recent advances in applied and theoretical mechanics: proceedings of the 5th WSEAS International Conference on Applied and Theoretical Mechanics (MECHANICS '09) : Puerto De La Cruz, Tenerife, Canary Islands, Spain,*

December 14-16, 2009. S.l.: WSEAS, 2009, 138 – 143. ISBN 9789604741403. Dostupné z: http://www.wseas.us/e-library/conferences/2009/tenerife/MECHANICS/MECHANICS-24.pdf

[27] *Direct Industry: Poppet valve / compressor* [online]. © 2015 [cit. 2015-04-04]. Dostupné z: http://www.directindustry.com/prod/dresser-rand/poppet-valve-compressor-13998-1160429.html

[28] *Hoerbiger* [online]. 2014 [cit. 2015-04-04]. Dostupné z: http://www.hoerbiger.com/en-8/pages/64#center

[29] *Indiamart* [online]. © 1996-2015 [cit. 2015-04-04]. Dostupné z: http://www.indiamart.com/arizonatechzeal/plate-valves.html

[30] *Dayton Refrigeration* [online]. © 1943-2015 [cit. 2015-04-04]. Dostupné z: http://daytonrefrigerationinc.com/Discus-Valve-Plate-Assembly-Copeland-Compressors-VP117.htm

[31] ALMASI, Amin. Pace process & control engineering. In: *Understand the technology behind reciprocating compressor capacity control* [online]. 2013 [cit. 2015-04-04]. Dostupné z: http://www.pacetoday.com.au/features/reciprocating-compressor-capacity-control

[32] *Compressor and Valves from the Same Source* [online]. 2002 [cit. 2015-04-04]. Dostupné z: https://www.sulzer.com/zh/-/media/Documents/Cross_Division/STR/2002/2002_01_10_samland_e.pdf

[33] *Emerson Climate Technologies* [online]. © 2008 [cit. 2015-04-05]. Dostupné z: http://emersonclimate.com/europe/ProductDocuments/CopelandLiterature/Discus_1008_E_0_1.pdf

[34] OHIO UNIVERSITY. *Chapter 9: Carbon Dioxide (R744) - The New Refrigerant* [online]. © 2010 [cit. 2015-04-06]. Dostupné z: http://www.ohio.edu/mechanical/thermo/Applied/Chapt.7_11/Chapter9.html

[35] *National Oceanic and Atmospheric Administration* [online]. 2015 [cit. 2015-04-06]. Dostupné z: http://www.esrl.noaa.gov/gmd/dv/data/index.php?site=mlo&parameter_name=Carbon%2BDioxide&frequency=Monthly%2BAverages

[36] CENTRE TECHNIQUE DES INDUSTRIES AÉRAULIQUES ET THERMIQUES. *Transcritical R744 (CO2) heat pumps* [online]. 2007 [cit. 2015-04-07]. Dostupné z: http://www.cetiat.fr/docs/newsdocs/166/doc/R744%20Technicians%20Manual%20CETIAT%20GRETH.pdf

[37] *Kaeltetechnik: R744* [online]. 2013 [cit. 2015-04-09]. Dostupné z: http://gunar.lima-city.de/kaelte/files/r744.jpg

[38] EN 13371-1. *Compressor and condensing units for refrigeration – Performance resting and tests methods*. London: British Standards Institution, 2003.

[39] DIN EN 12900. *Refrigerant compressors – Rating conditions, tolerances and presentation of manufacturer's performance data*. Berlin: Deutsches Institut für Normung, 2013.

[40] MA, Yuan, Zhilong HE, Xueyuan PENG a Ziwen XING. Experimental investigation of the discharge valve dynamics in a reciprocating compressor for trans-critical CO2 refrigeration cycle. In: *Applied Thermal Engineering* [online]. Elsevier, 2012 [cit. 2015-04-29]. ISSN 1359-4311. Dostupné z: http://www.sciencedirect.com/science/article/pii/S1359431111001542

[41] ADAMS, Thomas, Christopher GRANT a Heather WATSON. *A Simple Algorithm to Relate Measured Surface Roughness to Equivalent Sand-grain Roughness* [online]. [cit. 2015-05-05]. DOI: 10.11159/ijmem.2012.008. Dostupné také z: http://ijmem.avestia.com/2012/PDF/008.pdf

[42] Copeland™ Stream Compressors for R744 Refrigeration. 2014. *Emerson Climate Technologies* [online]. [cit. 2015-05-07]. Dostupné z: http://www.emersonclimate.com/europe/en-eu/About_Us/News/PublishingImages/doc/DSH120-Stream-For-CO2-EN.pdf

[43] WISCHNEWSKI, Berndt. *Peace Software* [online]. [cit. 2015-05-14]. Dostupné z: http://www.peacesoftware.de/einigewerte/co2_e.html

[44] GIROTTO, Sergio, Silvia MINETTO a Petter NEKSA. Commercial refrigeration system using CO2 as the refrigerant. *International Journal of Refrigeration* [online]. 2004 [cit. 2015-05-19]. ISSN 0140-7007. Dostupné z: http://www.sciencedirect.com/science/article/pii/S014070070400132X

[45] ANSYS. Ansys Workbench: Software help. 2013

[46] BLEJCHAŘ, Tomáš. *Turbulence modelového proudění - CFX: učební text*. Vyd. 1. Ostrava: Vysoká škola báňská - Technická univerzita Ostrava, 2012, 1 CD-ROM. ISBN 9788024826066. Dostupné také z: http://www.person.vsb.cz/archivcd/FS/Tur/Turbulence.pdf

LIST OF SYMBOLS

A	[m]	Amplitude
a	[mm]	semi-major axis – suction angle holes
b	[mm]	semi-minor axis – suction angle holes
C, c	[N·s·m^{-1}]	Damping coefficient
C_3H_8O		2-Propanol
$C_4H_{10}O$		2-Butanol
$CClF_2$		Monochlordifluoromethan
CFCs		Chlorofluorocarbons
CFD		Computational fluid dynamics
Cl		Chlorine atom
ClO		Chlorine monoxide
CO_2		Carbon dioxide
COP	[-]	Coefficient of performance
COP_{HP}	[-]	Coefficient of performance of heat pump
COP_R	[-]	Coefficient of performance of reverse cycle
c_p	[J·kg^{-1}·K^{-1}]	Specific heat capacity at constant pressure
CR	[-]	Compression ratio
c_v	[J·kg^{-1}·K^{-1}]	Specific heat capacity at constant volume
D	[m^3·h^{-1}]	Compressor displacement
D_b	[mm]	Bore diameter
D_{NSD}	[mm]	Diameter of suction direct holes
D_{OD}	[mm]	Diameter of discharge hole
D_{OS}	[mm]	Diameter of suction hole
E	[GPa]	Young's modulus
F	[Hz]	Mains frequency
GWP		Global-warming potential
$h_1 – h_4$	[kJ·kg^{-1}]	Specific enthalpy at specified point of thermodynamic circuit
HCs		Hydrocarbons
K,k	[N·m^{-1}]	Stiffness
k_a	[-]	Surface finish factor
k_b	[-]	Size factor
k_c	[-]	Loading factor

k_d	[-]	Temperature factor
k_e	[-]	Reliability factor
k_f	[-]	Miscellaneous factor
K_f	[-]	Reduced value of concentration factor K_t
L	[mm]	Cylinder length
M	[kg·mol^{-1}]	Molar mass
$\dot{m}$	[kg·s^{-1}]	Mass flow rate
M, m	[kg]	Mass
MDOF		Multiple degree of freedom
MPC		Multi-point constraint
n	[-]	Polytrophic exponent
N	[-]	Number of cylinders in compressor
N_f	[-]	Number of cycle to fracture
n_f	[-]	Fatigue factor of safety
n_{NSA}	[-]	Number of suction angle holes
n_{NSD}	[-]	Number of suction direct holes
n_{OD}	[-]	Number of discharge holes
n_{OS}	[-]	Number of suction holes
n_r	[rpm]	Rotor speed
n_s	[rpm]	Stator speed
n_y	[-]	Yield factor of safety
O_2		Molecule of oxygen
O_3		Ozone molecule
ODP		Ozone depletion potential
p	[Pa][bar]	Pressure
$p_1 – p_4$	[Pa][bar]	Pressure at specified point of thermodynamic circuit
P_C	[Pa]	Critical pressure
p_p	[-]	Number of pole pairs
P_R	[-]	Reduced pressure
Q	[J]	Heat
q	[-]	Notch sensitivity
Q_H	[J]	Heat at higher temperature
$\dot{Q}_H$	[W]	Rate of heat transferred at lower temperature

Q_L	[J]	Heat at lower temperature
$\dot{Q}_L$	[W]	Rate of heat transferred at higher temperature
R	[$J \cdot kg^{-1} \cdot K^{-1}$]	Specific gas constant
r	[-]	Loading slope
$\bar{R}$	[$J \cdot mol^{-1} \cdot K^{-1}$]	Universal gas constant
R12 (CCl_2F_2)		Dichlorodifluoromethan
R134a		1,1,1,2-Tetrafluoroethane
R170		Ethane
R290		Propane
R50		Methane
R600		Butane
R610		Ethyl-ether
R717		Ammonia
R744		Carbon dioxide
R764		Sulphur dioxide
RL68HB		Lubrication oil
S	[$J \cdot K^{-1}$]	Entropy
$s_1 - s_4$	[$kJ \cdot kg^{-1} \cdot K^{-1}$]	Specific entropy at specified point of thermodynamic circuit
S_a, σ_a	[MPa]	Amplitude stress
SDOF		Single degree of freedom
S_e	[MPa]	Endurance limit at critical location, corrected fatigue limit
S_e', $\sigma_{e'}$	[MPa]	Endurance limit
S_h	[K]	Superheating
S_{NS}	[mm^2]	Cross sectional area of suction holes
S_{OD}	[mm^2]	Discharge cross sectional area
S_{OS}	[mm^2]	Suction cross sectional area
s_s	[%]	Motor slip
S_{ut}, σ_{ut}	[MPa]	Ultimate tensile strength
S_y	[MPa]	Yield strength
T	[K]	Absolute temperature
t	[°C]	Temperature
$T_1 - T_4$	[K]	Temperature at specified point of thermodynamic circuit
T_C	[K]	Critical temperature

T_H	[K]	Absolute temperature at hotter side of thermodynamic cycle
T_L	[K]	Absolute temperature at cooler side of thermodynamic cycle
T_R	[-]	Reduced temperature
U	[J]	Internal energy
$u_1 – u_4$	[J·kg^{-1}]	Specific internal energy at specified point of thermodynamic circuit
v	[m^3·kg^{-1}]	Specific volume
V	[m^3][l]	Volume
$V_1 – V_4$	[m^3]	Volume at specified point of thermodynamic circuit
V_C	[m^3]	Critical volume
V_c	[mm^3]	Clearance volume of all four cylinders
V_R	[-]	Reduced volume
V_s	[mm^3]	Sucked volume
V_z	[mm^3]	Total swept volume
W	[J]	Work
$\dot{W}$, P_0	[W]	Compressor power input
WB		Workbench
x	[m]	Position
Z	[-]	Compressibility factor
ε	[μm]	Sand grain roughness
H	[-]	Efficiency
η_t	[-]	Transport efficiency
η_v	[-]	Volumetric efficiency
κ	[-]	Adiabatic exponent
μ	[-]	Poisson’s ratio
ρ	[kg·m^{-3}]	Density
σ_0	[MPa]	Nominal stress
σ_m, S_m	[MPa]	Mean stress
σ_{max}	[MPa]	Maximum stress
σ_{min}	[MPa]	Minimum stress
σ_r	[MPa]	Range stress
σ_s	[MPa]	Static stress
ω	[Hz]	Frequency
ω_n	[Hz]	Natural frequency

LIST OF FIGURES

LIST OF TABLES

ANNEXES

1.	Valve plate	K003-003-A107-00
2.	Piston machining	K003-004-A019-00
3.	Suction valve – design one	K003-056-A022-00
4.	Suction valve – design two	K003-056-A025-00